On large deformations of elastic circular arcs

-Bifurcation, stability and application as spring and gripper elements

Dissertation

zur Erlangung des akademischen Grades

Dr. rer. nat.

an der Technischen Universität Ilmenau

vorgelegt von

Xianjun Yin

Juli 2002

On large deformations of elastic circular arcs

-Bifurcation, stability and application as spring and gripper elements

D i s s e r t a t i o n

zur Erlangung des akademischen Grades

Dr. rer. nat.

vorgelegt von Master of Science Xianjun Yin

Contents

II

Acknowledgement

IV

Summary

The topic of this work comes from the practical gripper system, whose simplified essential part is composed of two elastic clamped-free circular rods. The motion of this system originates in the deformations of the elastic circular rods under the force load acting at the free end.

The elastic circular arcs can be of any form, from straight line to slitted entire ring and their deformations can be arbitrarily large.

After the mathematical model's being built, which finally resulted in a boundary value problem for a pendulum equation with three parameters representing the acting force and the geometric character of the undeformed elastic circular arc, the study was focused on the investigation of multiplicity and stability of the solutions of the pendulum equation and the corresponding configurations of the deformed arcs. In the study of the multiplicity, a powerful method, namely the manifold method, was developed, based on the discussion of the phase curves of the pendulum equation. Primarily, the manifold method yields qualitative insight to bifurcation. Quantitative results then by combination with numerics. Combining this manifold method with numerical calculations sketched in Section 3.1, the bifurcation diagrams of the pendulum equation were obtained for various possibilities of the parameters. The bifurcation indicated clearly the multiplicity and the change tendency of the solutions of pendulum equation and the configurations of deformed arcs. Using the manifold method and bifurcation diagrams the phenomenon of bifurcation was also investigated, for our model the turning point, bifurcation point of pitchfork and X-type and hysteresis were encountered and therefore were given a special attention. The theoretical study on the phase curves of the half ring was carried out and the result showed an exact coincidence with the result obtained with manifold method. For the stability study of the solutions, especially the non-trivial solutions, of the pendulum equation, a new concept about stability, namely "P-stability", which was based on the embedding of the pendulum equation into a parabolic partial differential equation and led to an eigenvalue problem, was defined. The stability study could be carried out by means of connecting the partial differential equation with the bifurcation function obtained by manifold method or other ways, such as Liapunov and Schmidt reduction. By turning the researches back to the original practical problem, some characters of elastic circular arcs used as spring and gripper element were given out, in particular the load-displacement character (spring behavior) was studied, exploiting this, the grasping forces at given opening width and friction coefficient was found for a gripper that consists of two such arcs in symmetric configuration.

The methods introduced in this work, especially manifold method and P-stability, will be potentially useful in the bifurcation and stability study of ordinary differential equations.

VI

Über große Deformationen elastischer Kreisbögen

-Bifurkation, Stabilität und Anwendung als Feder und Greiferelement

Zusammenfassung

Das Thema dieser Arbeit kommt von einem praktischen Greifersystem, dessen vereinfachter wesentlicher Teil aus zwei eingespannt-freien elastischen kreisförmigen Stäben besteht. Die Bewegung dieses Systems wird durch die Deformationen der elastischen kreisförmigen Stäbe unter der am freien Ende angreifenden Kraft erzeugt. Die Bögen können von jeder möglichen Form sein, von der Geraden bis zum gesamten geschlitzten Ring, und ihre Deformationen können beliebig groß sein.

Nach Aufstellung eines mathematischen Modells in Form eines Randwertproblems mit drei Parametern (Kraft, Bogengeometrie) für eine Pendelgleichung wurden Vielfachheit und Stabilität der Lösungen der Pendelgleichung und der entsprechenden Stabkonfigurationen untersucht. Dazu wurde eine leistungsfähige Methode, die "Mannigfaltigkeitsmethode", entwickelt, die auf der Diskussion der Phasenkurven der Pendelgleichung basiert. Mit dieser Methode, gekoppelt mit numerischen Rechnungen, wurden die Bifurkationsdiagramme der Pendelgleichung für verschiedene Kombinationen der Parameter erhalten. Die Bifurkationsdiagramme zeigten Vielfachheit und die Änderungstendenz der Lösungen der Pendelgleichung und der Konfigurationen der verformten Bögen an. Die Bifurkationsdiagramme zeigen für unser Modell turningpoint-, pitchfork- und X-Bifurkationen sowie Hysteresis. Die Kraftparameterebene wurde nach der Zahl der Lösungen in Gebiete unterteilt. Die theoretische Untersuchung des Halbringes mittels elliptischer Integrale wurde durchgeführt, und das Resultat zeigt eine genaue Übereinstimmung mit den Ergebnissen der Mannifaltigkeitsmethode. Für die Stabilitätsuntersuchung versagen klassische Methoden, da das Randwertproblem für die Pendelgleichung keine trivialen Lösungen besitzt. Deshalb wurde die Pendelgleichung in eine parabolische partielle Differentialgleichung eingebettet, die Liapunovstabilität der stationären Lösungen definiert die "P-Stabilität" der Konfiguration des elastischen Stabes. Stabilitätsaussagen werden mit Hilfe der Methode der ersten Näherung und unter Benutzung der Bifurkationsfunktion gewonnen. Zum ursprünglichen praktis-

chen Problem "Feder und Greifer" wurden als Ergebnisse Federcharakteristiken, insbesondere Kraft-Verschiebungs-Kennlinien für kreisbogenförmige Federn gefunden. Für Greifer, die aus zwei symmetrisch angeordneten elastischen Kreisbögen bestehen, wurden Zusammenhänge von Öffnungsweite, Haftreibungskoeffizient und Haltekraft gefunden.

Die Methoden, die in dieser Arbeit eingeführt werden, besonders die Mannifaltigkeitsmethode und P-Stabilität, können für die Untersuchung von Bifurkation und Stabilität bei allgemeinen gewöhnlichen Differentialgleichungen nützlich sein.

Chapter 1

Introduction

In mechanical and civil engineering and many other areas one often meets some problems related to grasping devices and spring systems, the simplification of the essential parts of which has something to do with the deformation of elastic rods [77], [85], [99], for instance, the manipulator of a robot, the front limb of a crab and the grasping part of a crane . The rod theory is probably one of the most attractive and active parts of the elasticity researches [25], [50], [56], [59], [60]. It has been always drawing interests of the scientists who work in the fields of mathematics, mechanics, engineering, material science, *etc*. Euler, Saalschuetz and Born represented their earlier work in [64], [11] more then 100 years ago. Euler discussed the deformation of the elastic straight rod and stability of disturbed equilibrium in about the year of 1744, Born represented the variation method for stability studies of the elastic rods in his dissertation. These early researches laid the foundation of study of elastic rods and are still of importance and used in the research of this area. In [7] and [82], one can find brief summaries of some earlier and recent results of stability studies of straight elastic rods and general introduction to the research methods, namely adjacent method, energy method and dynamical method. There are also plenty of other literature which partly or totally deals with the researches in this area [1], [6], [5],[8], [13], [22], [42], [52], [74], [88],[89], [93], [94], [95].

Concerning the object, the researches on the theory of elastic rods consist of two parts: the three-dimensional rod theory and one-dimensional rod theory. In the three-dimensional rod theory the rod is treated as an elastic body, so its spatial shape and physical features play an important role in the study. In one-dimensional rod theory, the elastic rod is considered as a curve along the center axis of it with or without mass. Of course sometimes we can not separate these two parts totally, because the study of the partial differential equations which describe the deformation of a three-dimensional rod is frequently turned to an ordinary differential system. So these two parts of theories are both of importance

in the theoretical study and in practical applications.

From the view of mathematics, the mathematical model used to describe the practical problem is normally parameterized by several parameters governing the practical problem, *e.g.*, bifurcation parameters, which could be acting force in mechanical system, temperature in physical system, density of solutions in chemical system and so on. For some values of them the uniqueness of the solutions could be invalid, that is, multiplicity phenomenon arises [16], [48], [70], [81], [87], [91]. This situation brings out two research directions: bifurcation discussion and stability investigation. The bifurcation theory deals with a common phenomenon in nature and many scientific and technological fields, this is sometimes connected with the concept of catastrophe [3]. As the qualitative structure may undergo an abrupt change at bifurcation points, so bifurcation theory deals with the critical values of parameters, the multiplicity of the solutions and classification of the configurations. About this theme some methods are developed both from mathematical discussion and engineering consideration. Jepson and Spence in their work [40], [41] studied the nonlinear problems of the form: $f(x, \lambda, \alpha) = 0$, where $x \in I\!R$ is the state variable, $\lambda \in I\!R$ is a bifurcation parameter and $\alpha \in I\!R$ represents a control parameter, f is a scalar function. They used singularity theory and hierarchy of singularities to develop a numerical approach such that they can calculate part of the α-parameter region in which the problem has equivalent bifurcation diagrams (or the discussed systems are qualitatively similar). Seydel did also some important work in the bifurcation discussion, he investigated the equilibrium of an equation in his series of papers [67], [68], [69]. He introduced the concept of extended system, that is, combining the original equation, the necessary condition for bifurcation and boundary conditions together to form a new system with more equations and new boundary conditions. He also defined a test function. In numeric calculation of the bifurcation point, the value obtained is normally an approximation value of bifurcation, he defined a function, namely test function, with which one can determine in certain circumstances whether the value obtained is a bifurcation value or not [90]. For boundary value problems (shorted as BVP)

$$y''(t) = f(t, y, \lambda), \quad r(y(a), y(b)) = 0,$$

here $a \leq t \leq b, \lambda \in I\!R, y, f, r$ are n-vectors. f, r are sufficiently smooth, by choosing two suitable values $1 \leq k \leq n$ and δ, two distinct solutions $y(t, \lambda), z(t, \lambda)$ of the BVP can be solved simultaneously from a new system

$$Y' := \begin{bmatrix} y \\ \lambda \\ z \end{bmatrix}' = F(t, Y) := \begin{bmatrix} f(t, y, \lambda) \\ 0 \\ f(t, y + d, \lambda) - f(t, y, \lambda) \end{bmatrix}$$

$$R(Y(a), Y(b)) = \begin{bmatrix} r(y(a), y(b)) \\ r(y(a) + d(a), y(b) + d(b)) \\ d_k(a) - \delta \end{bmatrix} = 0$$

with $d = z - y$. His another approach of handling the boundary value problem is: choosing a suitable k and $y_k(a)$, let $y_k(a, \lambda) = \eta$ and solving

$$\begin{bmatrix} y \\ \lambda \end{bmatrix}' = \begin{bmatrix} f(t, y, \lambda) \\ 0 \end{bmatrix}, \begin{bmatrix} r(y(a), y(b)) \\ y_k(a) - \eta \end{bmatrix} = 0.$$

Then two distinct solutions of BVP correspond to different values of η. For these two methods k could be chosen as

$$k = \min_{1 \le j \le n} \{j | y_j(a) \quad \text{not} \quad \text{fixed} \quad \text{by} \quad \text{an} \quad \text{initial} \quad \text{condition}\}.$$

Smoller and Wassermann [72] studied the solution of $u'' + f(u) = 0, -L < x < L$, they used a time-map method [66] to discuss the special case for $f(u) = (a-u)(u-b)(u-c), a < b < c$ and $u(L) = u(-L) = 0$ as well as $u'(L) = u'(-L) = 0$, the result they obtained is that the BVPs have at most three solutions for each L. Pönisch [61] and Ramachandra [63] did also some work on the computation of turning points. Of course the mentioned work is only a small part of the work done in bifurcation calculations.

In elasticity theory stability study is also a very important theme, because the phenomenon of loss of stability could occur in almost each area of science and technology [86], and sometimes it may bring some trouble or damage to the system, so many scientists manage to find more useful and efficient methods to detect or control a system in order that it maintains in a state of stability. Most of the available methods for stability study apply to the trivial equilibria, for non-trivial equilibria there is still a lot of work to do.

As we know the work done on elastic rod (one dimension) mainly dealt with the deformation of straight elastic rods or elastic rods with small imperfection(the curvature is relatively small and the both ends of them are usually not free or sometimes the symmetry of a descriptive system is needed)(see the literature cited before), so some well-known methods, for instance, approximate linearization, small perturbation, Liapunov-Schmidt reduction [6] (see Appendix 1) and time-map could be used. In [44], [77], [78] the authors presented their work on circular elastic rings and their application in micro-technology, in the works some transversing time expressions $T_i(\beta, k^2)$ are defined according to the different types of segments of the phase curves and treated numerically. In our work we mainly investigate the mechanical motion originated by deformations of circular elastic arcs with acting force on their free ends, the arcs can be of any form, from straight line to ring. After

a suitable transformation the mathematical model results in a boundary value problem for a pendulum equation. The results include mathematical modelling, bifurcation investigation through phase plane discussion and numerical calculation, stability of equilibrium and total system, deformed configuration and some useful characteristics of elastic arcs as spring and gripper elements. The methods introduced in this paper for bifurcation and stability study should be potentially useful in the study related to boundary value problem of differential equations.

We organized our work in the following parts: The first part is a brief introduction to the work, including the background and former related work and results. In the second part we put forward the practical problem originated in mechanical engineering and abstract the mathematical model by means of the balance equations of forces and moments at the cross section of the rod, after a suitable transformation the model results in a boundary value problem for a pendulum type equation with three parameters. The difficulty of solving this BVP is that some parameters enter the boundary conditions, and the non-uniqueness of the solutions. By turning BVP into an initial value problem we introduce a new unknown parameter indicating the initial rate of change of the angular formed by the tangent of deformed rod and the horizontal axis. As it is difficult and sometimes impossible to obtain the exact solution for the general equation, we try in part 3 to use numerical method. Except the frequently used method we introduce a very powerful method, namely a "manifold method", which is based on the phase curve consideration of BVP of pendulum equation. In the following part 4, we use this method to get the effect of the parameters on the multiplicity of the solutions and show the result by means of bifurcation diagrams. We also give a special consideration to the bifurcation behavior. In order to compare the results obtained by the manifold method with the direct theoretical discussion we take some special cases for example. In section 5 we study the stability of the solutions by means of partial differential equations of parabolic type, we pay attention also to the structural stability of the system. In section 6, we turn back from mathematical considerations to the original practical problem, we get some typical characteristics of the circular elastic arcs as spring and gripper elements, in which engineers are interested. In our study of bifurcation and stability we try to give a general explanation of our methods in order to make them useful for general BVP of ordinary differential equations.

Chapter 2

Mathematical modelling

The mechanical or biological structure of practical problems mentioned in the introduction is usually very complex. For simplicity and without loss of generality, we investigate mainly the essential part of the device shown in figure 2.1.
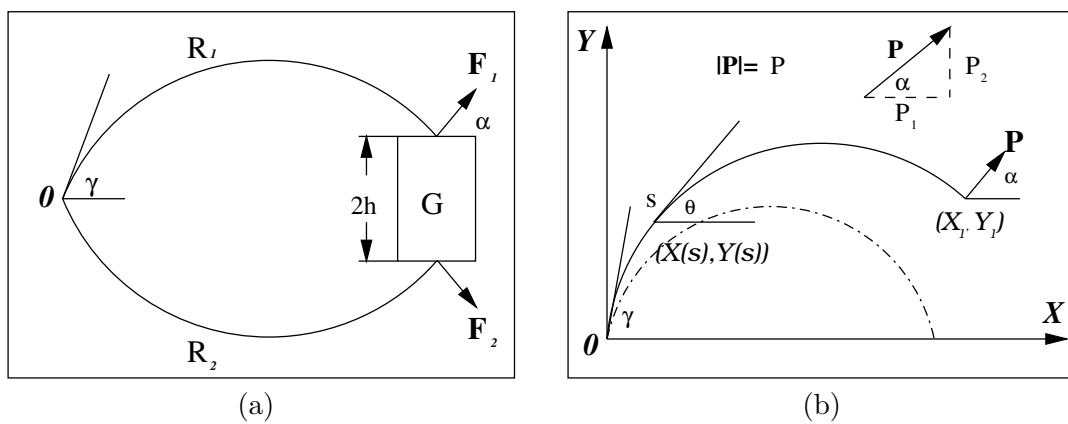

Figure 2.1: (a): The grasping device of two circular elastic arcs. (b): The simplified part of figure (a), the dash-dotted line represents the undeformed arc.
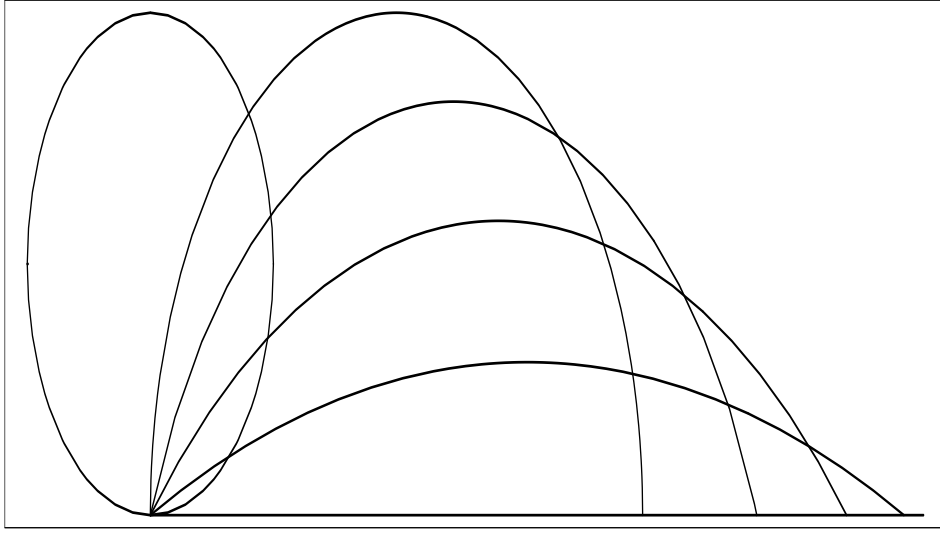
Figure 2.2: Samples of the undeformed arcs (note: the aspect ratio of the figure is not 1).

In figure 2.1(a) R_1 and R_2, whose undeformed shapes are circular arcs, whose left and right ends coincide, are deformed elastic inextensible circular arcs as gripper elements, clamped at their left ends 0, grasping a body of weight $\mathbf{G}$ (acting horizontally), $\mathbf{F_1}$ and $\mathbf{F_2}$ are forces acting on the device, which make R_1, R_2 open. h is the half opening of the gripper. By symmetry of the device, we need only to investigate half of it as shown in figure 2.1(b). Here $s \in [0, L]$ is the arc length and $s = 0$ at the left end, while $s = L$ at the right end. The planar coordinate system takes the left end of the arc as its origin. $\gamma \in [0, \pi]$ is the angle made by the tangent of the undeformed arc at its left end and the x-axis, so the undeformed elastic arc could be of any form, from straight line segment to a total circular ring (see figure 2.2). θ is the direction angle of the tangent of the rod at any point. (X_1, Y_1) is the coordinate of the free right end of the arc. $\mathbf{P}$ is the acting force with α as its direction angle, its magnitude is denoted by P. Based on the assumption that the arc is inextensible and undergoes pure bending, we can describe the practical problem in

the following mathematical model, according to mechanical laws [57], [76], [83], [96]:

$$
\begin{aligned}
\frac{dX}{ds} &= \cos\theta(s), \\
\frac{dY}{ds} &= \sin\theta(s), \\
\frac{d\theta}{ds} &= \frac{1}{EI}\{P_2[X_1 - X(s)] + P_1[Y(s) - Y_1]\} + \kappa, \\
X(0) &= 0, \\
Y(0) &= 0, \\
\theta(0) &= \gamma,
\end{aligned}
\tag{2.1}
$$

where P_1 and P_2 are the $X-$ and $Y-$ components of $\mathbf{P}$, I is the moment of inertia of the cross section, E is the elasticity modulus of the material, in our model both I and E are assumed to be constants. κ is the curvature of the undeformed circular rod, thus $0 > \kappa =$ constant. The first two equations of (2.1) are the geometrical description of the arc and the third equation is derived from the balance equations of forces and moments. System (2.1) is an initial value problem(IVP) with two unknown parameters, namely X_1 and Y_1, which depend obviously on the parameters P, γ and α and can not be given in advance provided that we take p, α, γ as parameters which can be given in advance in our model, therefore we can not solve (2.1) in a direct way as usual. If we in some cases need to determine the acting force which maintains an appointed form of the deformed rod, we should think of X_1, Y_1 as adjustable in advance. Differentiating the third equation of (2.1) with respect to s, we get

$$
\begin{aligned}
\frac{d^2\theta}{ds^2} &= \frac{1}{EI}(-P_2\cos\theta(s) + P_1\sin\theta(s)) \\
&= \frac{P}{EI}(\frac{-P2}{P}\cos\theta(s) + \frac{P_1}{P}\sin\theta(s)) \\
&= \frac{P}{EI}(-\sin\alpha\cos\theta(s) + \cos\alpha\sin\theta(s)) \\
&= \frac{P}{EI}\sin(\theta - \alpha),
\end{aligned}
$$

and then making the following transformation:

$$
\frac{L^2}{EI}P = p, s = L\sigma = \frac{L}{\sqrt{p}}t,
$$

$$
\theta(s) = \vartheta(\sigma) = \Psi(t) + \alpha - \pi,
$$

the essential part of system (2.1) is turned into a dimensionless boundary value problem for a pendulum equation with three parameters p, γ and α, which are included in the boundary

conditions:

$$
\begin{aligned}
\Psi'' &= -\sin\Psi, \\
\Psi(0) &= \pi + \gamma - \alpha, \\
\Psi'(\sqrt{p}) &= -\frac{2\gamma}{\sqrt{p}}.
\end{aligned}
\tag{2.2}
$$

Note: The advantage of equation (2.2) is: the parameters γ, α and p are not involved in the differential equation, they appear only in the boundary conditions, so they have no any influence on the qualitative phase portrait defined by the equation. It is especially beneficial for the study based on the discussion of phase curves of the equation.

Now we make the further transformation,

$$
X = Lx, Y = Ly,
$$

the original system (2.1) is then turned into an initial value problem with an unknown parameter ω_0:

$$
\begin{aligned}
x'(\sigma) &= \cos\vartheta(\sigma), \\
y'(\sigma) &= \sin\vartheta(\sigma), \\
\vartheta'(\sigma) &= p\left[y(\sigma)\cos\alpha - x(\sigma)\sin\alpha\right] + \omega_0\sqrt{p}, \\
x(0) &= 0, \\
y(0) &= 0, \\
\vartheta(0) &= \gamma,
\end{aligned}
\tag{2.3}
$$

where $\omega_0 := \Psi'(0)$, which depends on the parameters p, γ and α, essentially describes the curvature of the deformed arc at $\sigma = 0$ (the normalized length of the arc is 1).

In (2.2), $'$ represents the derivative of Ψ with respect to $t, t \in \left[0, \sqrt{p}\right]$, while $'$ in (2.3) represents the derivative with respect to $\sigma, \sigma \in [0,1]$. (2.3) will preferably be used to calculate the configurations of the deformed rod, which is described by $(x(\sigma), y(\sigma)), \sigma \in [0,1]$, and later will be used to get some mechanical characters. In order to solve equation (2.3) as an usual initial value problem we should find the value of the unknown parameter ω_0 first. This will be done by virtue of BVP (2.2), by solving (2.2), we could get the value of ω_0, substituting this value into (2.3), it becomes a normal initial value problem. Our approach to solve (2.3) is: solving equation (2.2) first to get the value of ω_0, then for each obtained ω_0 solving (2.3) to get its solution which describes the configuration of deformed elastic circular arc. In the context of (2.3), we have $\omega_0\sqrt{p} = L\kappa + p\left[x(1)\sin\alpha - y(1)\cos\alpha\right]$.

Note: 1. Study on pendulum equation is also an interesting theme, it is connected frequently with the study on vibration and oscillation [10], [65], [71]. 2. The existence of solutions for (2.2) is guaranteed by several criteria [30], [54]. 3. If we confine our discussion only to the small deformation of the arc from its original (or undeformed) form, we may probably find some existing methods. For example, for the originally straight arc, assuming the perturbed solution is of the form:

$$\Psi = \sum_{i=1}^{\infty} \Psi_i(t)\epsilon^i,$$

$$p = \frac{\pi^2}{4} + \sum_{i=1}^{n} b_i\epsilon^i,$$

where ϵ is the amplitude of small deflection, $\Psi_i(t), b_i$ are unknown parameters, they are to be determined by (2.2)[85]. Another similar idea is: supposing

$$\Psi(t) = a_0 + \sum_{i=1}^{\infty} (a_i \cos it + b_i \sin it)$$

be solution of (2.2), here a_i, b_i are unknown coefficients, they can be determined by substituting the series in (2.2) and comparing the coefficients of $\cos it, \sin it$ [88]. Both of these two approaches need elaborate calculations.

Chapter 3

Methods of finding ω_0

As explained in last section, the main task to solve (2.3) is to find the value of ω_0 for given parameters α, γ and p. After ω_0 being obtained, (2.3) then appears to be a normal initial value problem, therefore we turn our study on the solutions of equation (2.3) and pendulum equation (2.2) first to the study of the properties of ω_0. In this section we study mainly the methods how to get ω_0.

3.1   Solving algebraic equations(direct method)

First let us give a short discussion on the phase curves of (2.2). Rewriting the essential part of (2.2) in the following equivalent form:

$$\begin{aligned} \frac{d\Psi}{dt} &= \Phi, \\ \frac{d\Phi}{dt} &= -\sin\Psi. \end{aligned} \tag{3.1}$$

The singular points of (3.1) are $(\pm n\pi, 0), n = 0, 1, 2, \dots$. The coefficient matrixes of the linearized systems at the corresponding points are

$$\begin{bmatrix} 0 & 1 \\ -\cos(\pm n\pi) & 0 \end{bmatrix}, \quad n = 0, 1, 2, \dots.$$

The eigenvalues for $(\pm 2m\pi, 0)$ are $\pm i$, these singular points of nonlinear equation (3.1) could be either centers or focuses, but concerning the symmetry of the system, that is $F(\Psi, \Phi) := \begin{bmatrix} \Phi \\ -\sin\Psi \end{bmatrix}$ satisfies $F(-\Psi, -\Phi) = -F(\Psi, \Phi)$, $(\pm 2m\pi, 0)$ are centers [98]. While eigenvalues for $(\pm(2m+1)\pi, 0)$ are ± 1, so they are saddles of (3.1). The separatrixes

connecting these saddles form a boundary for the central zone, outside this boundary the phase curves of (3.1) are topologically straight lines.
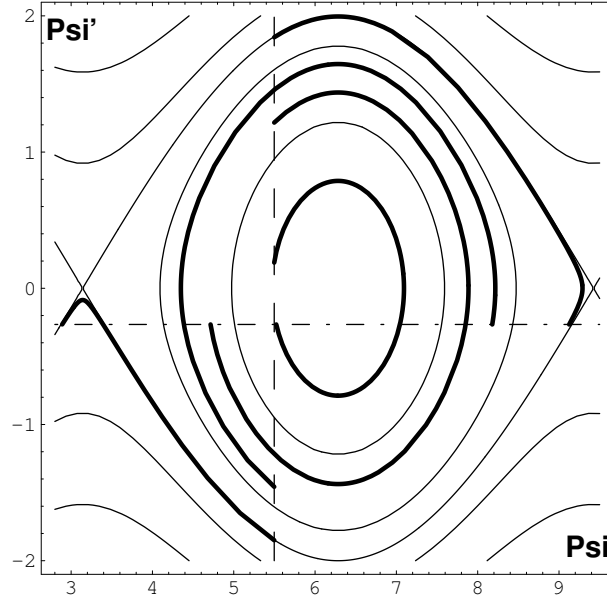

Figure 3.1: Possible phase curves of the BVP (2.2).

Integrating equation (2.2) in the usual way, we get

$$\frac{1}{2}\Psi'^2 = \cos\Psi + c.$$

Taking initial condition into consideration,

$$c = \frac{1}{2}\omega_0^2 + \cos(\gamma - \alpha).$$

Setting

$$k^2 := \frac{4}{2 + \omega_0^2 + 2\cos(\gamma - \alpha)},$$

we have

$$\Psi'^2 = \frac{4}{k^2}(1 - k^2 \sin^2\frac{\Psi}{2}), \quad t \geq 0.$$

This could be taken as the solution of the initial value problem:

$$\frac{d^2\Psi}{dt^2} = -\sin\Psi, \Psi(0) = \pi + \gamma - \alpha, \Psi'(0) = \omega_0.$$

If a solution of the initial value problem is also a solution of BVP (2.2), the boundary condition must be satisfied. It means that the phase curve related to the possible solution of (2.2) must end with $\Psi'(\sqrt{p}) = -\frac{2\gamma}{\sqrt{p}}$. This is shown in figure 3.1. Now we take the

boundary condition of (2.2) under consideration. When confining to orbits below the lower part of the separatrix, $\Psi' < 0$, thus

$$\Psi' = -\frac{2}{k}\sqrt{1 - k^2 \sin^2 \frac{\Psi}{2}}.$$

Let $u = \frac{\Psi}{2}$, then

$$u' = -\frac{1}{k}\sqrt{1 - k^2 \sin^2 u},$$

or

$$dt = -k\frac{du}{\sqrt{1 - k^2 \sin^2 u}},$$

integrating the last equation yields

$$t = -k\int_{\frac{1}{2}(\pi + \gamma - \alpha)}^{u} \frac{du}{\sqrt{1 - k^2 \sin^2 u}}.$$

The final values of $\sqrt{p}$ of the transit 'time' and $-\frac{2\gamma}{\sqrt{p}}$ of Ψ' then show up as

$$\sqrt{p} = k(F(\frac{1}{2}(\pi + \gamma + \alpha), k^2) - F(\frac{1}{2}\Psi_1, k^2)),$$

$$\frac{\gamma^2}{p} = \frac{1}{k^2} - \sin^2 \frac{\Psi_1}{2},$$

where $\Psi_1 = \Psi(\sqrt{p})$ and

$$F(v, k^2) = \int_0^v \frac{1}{\sqrt{1 - k^2 \sin^2 u}}du$$

is the elliptic integral of the first kind.

Now let

$$F_1(\omega_0, k, \Psi_1) := k^2 - \frac{4}{2 + \omega_0{}^2 + 2\cos(\gamma - \alpha)},$$

$$F_2(\omega_0, k, \Psi_1) := \sqrt{p} - k(F(\frac{1}{2}(\pi + \gamma - \alpha), k^2) + F(\frac{1}{2}\Psi_1, k^2)),$$

$$F_3(\omega_0, k, \Psi_1) := \frac{\gamma^2}{p} - \frac{1}{k^2} + \sin^2 \frac{\Psi_1}{2},$$

then a solution $(\bar{\omega}_0, \bar{k}, \bar{\Psi}_1)$ of the equations

$$\begin{cases} F_1(\omega_0, k, \Psi_1) = 0 \\ F_2(\omega_0, k, \Psi_1) = 0 \\ F_3(\omega_0, k, \Psi_1) = 0, \end{cases}$$

is the values needed to solve BVP (2.2) and then (2.3). Denoting the jacobian determinant of F_1, F_2, F_3 with respect to ω_0, k, Ψ_1 by $\frac{D(F_1, F_2, F_3)}{D(\omega_0, k, \Psi_1)}$, then $(\bar{\omega}_0, \bar{k}, \bar{\Psi}_1)$ is a simple point of system (2.2) if

$$\left.\frac{D(F_1, F_2, F_3)}{D(\omega_0, k, \Psi_1)}\right|_{(\bar{\omega}_0, \bar{k}, \bar{\Psi}_1)} \neq 0,$$

at each point of this kind holds the uniqueness of the solution. If

$$\left.\frac{D(F_1, F_2, F_3)}{D(\omega_0, k, \Psi_1)}\right|_{(\bar{\omega}_0, \bar{k}, \bar{\Psi}_1)} = 0$$

holds, then $(\bar{\omega}_0, \bar{k}, \bar{\Psi}_1)$ is a singular point of system (2.2), around which the uniqueness of solution will not be guaranteed.

From figure 3.1 we can see clearly that the possible orbits of (2.2) can also locate within the zone bounded by the two branches of the separatrix, for those orbits the expression of the transit 'time' is more involved since the entire orbits are possibly composed of several pieces, along which Ψ' may have different signs, so the above equations can not represent this case possibly. Theoretically we can solve the above three equations obtained from (2.2) to get the values of the three unknowns k, Ψ_1 and ω_0 for given p, α and γ, but owing to the nonlinearity of the equations and the fact that one set of (p, α, γ) there may correspond more than one value of k, Ψ_1 and ω_0, that is the multiplicity phenomenon would occur, it is difficult to find the three unknowns as explicit functions of p, α and γ exactly or numerically. This method was used in [77], [78] for discussion on the deformed elastic rings.

3.2   Method of extended system

By suitable transformation we can also put the bifurcation parameter p involved in the boundary value condition of (2.2) into principal equation and the equivalent equation of (2.2) is:

$$
\begin{aligned}
\Psi'' &= -\lambda \sin \Psi, \\
\Psi(0) &= \pi + \gamma - \alpha, \\
\Psi'(1) &= -2\gamma,
\end{aligned}
\tag{3.2}
$$

where $\lambda = p$. In [67] the author considered the general boundary value problem of differential equation:

$$\Psi' = F(\Psi, \lambda), B(\Psi(a), \Psi(b)) = 0, \tag{3.3}$$

where $\Psi = (\Psi_1, \Psi_2, ..., \Psi_n)^\top \in I\!\!R^n, F : I\!\!R^n \times I\!\!R^m \longrightarrow I\!\!R^n$ is a map differentiable to any order needed. $\lambda \in I\!\!R^m$ is considered as branching parameter, $B : I\!\!R^n \times I\!\!R^n \longrightarrow I\!\!R^n$ is a map

indicating boundary value condition. Normally λ is a constant vector in the discussions, that is $\lambda' = 0$. So we can write the BVP in a more general form:

$$\begin{bmatrix} \Psi \\ \lambda \end{bmatrix}' = \begin{bmatrix} F(\Psi, \lambda) \\ 0 \end{bmatrix}$$

with boundary condition

$$\begin{bmatrix} B(\Psi(a), \Psi(b)) \\ \Psi_k(a) - \eta \end{bmatrix} = \begin{bmatrix} 0 \\ 0 \end{bmatrix},$$

where $1 \le k \le n$ is an index and η is some constant (for example we can simply choose $\eta = 1$). By solving the above BVP we will get a value of λ which matches the given k and η. If $\Psi_l(a)$ is prescribed by $B(\Psi(a), \Psi(b)) = 0$, k must be different from l, otherwise a contradiction might be brought about [67],[68],[69].

When we discuss the branching problem of the BVP, we should take some more aspects into account. Suppose (Ψ_0, λ_0) is a branching point of (3.3), it means, there are more than one orbits passing through it, as discussed above, at this point the following conditions hold:

$$F(\Psi_0, \lambda_0) = 0, \quad \left[F'_\Psi(\Psi_0, \lambda_0)\right]^{-1} \text{dost} \quad \text{not} \quad \text{exist},$$

that is, equation $F'_\Psi(\Psi_0, \lambda_0)\psi = 0$ has non-trivial solution, so we consider also the following linear differential equation

$$\psi' = F'_\Psi(\Psi_0, \lambda_0)\psi$$

with boundary condition

$$J\psi(a) + K\psi(b) = 0,$$

where

$$J = \frac{\partial B(\Psi(a), \Psi(b))}{\partial \Psi(a)}, \quad K = \frac{\partial B(\Psi(a), \Psi(b))}{\partial \Psi(b)}$$

are $n \times n$ matrices obtained from boundary condition of (3.3). In emphasis of $\psi \ne 0$, we set some certain $\psi_k(a) = 1$. Put this BVP together with the original BVP (3.3) we get the extended BVP for branching point:

$$\begin{bmatrix} \Psi \\ \lambda \\ \psi \end{bmatrix}' = \begin{bmatrix} F(\Psi, \lambda) \\ 0 \\ F'_\Psi(\Psi, \lambda)\psi \end{bmatrix}, \quad \begin{bmatrix} B(\Psi(a), \Psi(b)) \\ \psi_k(a) - 1 \\ J\psi(a) + K\psi(b) \end{bmatrix} = 0. \tag{3.4}$$

All kinds of singular points of (3.3) are included in (3.4), in order to pick out the singular points with special characters, we need to add some more conditional equations to the above extended system (3.4), that is, it can be further extended. For instance, at bifurcation

points (we will give the exact definition and discussion on them in next chapter). at least two branching curves intersect with different tangents, the condition $\frac{\partial F(\Psi_0, \lambda_0)}{\partial \lambda} = 0$ holds for bifurcation point.

This method put every condition for branching point in an extended equation, but owing to the increase of the number of the extended equations, sometimes it could not reduce the difficulty for bifurcation calculation.

3.3   Using manifold in the phase plane of equation (2.2)

The character of (2.2) is: the equation is a nonlinear differential equation of order two defined on an interval $\left[0, \sqrt{p}\right]$, the right end of the interval is a parameter, the boundary conditions depend on p. First we discuss a general form of equation (2.2):

$$\Psi'' = F(\Psi, \Psi'), \Psi(a) = \Psi_a, \Psi'(b) = H(b), \tag{3.5}$$

where a and Ψ_a(independent of a) are some fixed constants, $b \in I\!R, b > a$ could be considered as the branching parameter, $F : I\!R \times I\!R \longrightarrow I\!R$ and $H : I\!R \longrightarrow I\!R$ are both smooth functions.

Actually we try to find the solution of the above BVP defined on the interval $[a, b]$. Instead of discussing the BVP, we consider the related initial value problem(IVP):

$$
\begin{aligned}
\Psi'' &= F(\Psi, \Psi'), \\
\Psi(a) &= \Psi_a, \\
\Psi'(a) &= \Psi'_a.
\end{aligned}
\tag{3.6}
$$

According to the wellknown existence and uniqueness theorem of the IVP for ordinary differential equations, for each given Ψ'_a, the above IVP has a unique solution, denoted by $\Psi(t, \Psi_a, \Psi'_a)$. Therefore if $\Psi(t, \Psi_a, \Psi'_a)$ is a solution of the above BVP (3.5), it must satisfy

$$\Psi'(b, \Psi_a, \Psi'_a) = H(b).$$

Now we consider the last situation in an another way. For each given fixed Ψ_a, the above discussion has a geometrical explanation as follows: on the $\Psi - \Psi'$ phase plane, $\Psi = \Psi_a$ represents a vertical straight line, at time moment a all orbits of (3.6) start from the points (Ψ_a, Ψ'_a) on this vertical straight line. This segment $\Psi = \Psi_a$ can be thought as the initial manifold M_a or starting manifold, at any time $t > a$, let ψ_t denote the flow [43] of (3.6) in

the $\Psi\Psi'$-phase plane and let $M_t = \{(\Psi(t, \Psi_a, \Psi_a'), \Psi'(t, \Psi_a, \Psi_a'))\}$, then $M_t = \psi_t(M_a)$. For fixed Ψ_a, M_t is a continuous curve parameterized by Ψ_a', we take it as the manifold at time t. Further we take the set $M_b = \{(\Psi(b, \Psi_a, \Psi_a'), \Psi'(b, \Psi_a, \Psi_a'))\}$ as the end manifold. For fixed Ψ_a and Ψ_a', M_t represents an orbit of (3.6) for $t \in [a, b]$. Summarizing the discussion we have the following result.

Theorem 3.1 *There is an one- to- one correspondence between the solutions of the BVP $\Psi'' = F(\Psi, \Psi'), \Psi(a) = \Psi_a, \Psi'(b) = H(b)$ and the roots of the equation $\Psi'(b, \Psi_a, \Psi_a') = H(b)$, or geometrically, there is an one- to- one correspondence between the orbits of the BVP $\Psi'' = F(\Psi, \Psi'), \Psi(a) = \Psi_a, \Psi'(b) = H(b)$ and the intersections of the end manifold with the horizontal straight line $\Psi' = H(b)$.*

If we denote $\Xi(b, \Psi_a, \Psi_a') := \Psi'(b, \Psi_a, \Psi_a') - H(b)$, then we should discuss the roots Ψ_a' of the equation $\Xi(b, \Psi_a, \Psi_a') = 0$ for given b and Ψ_a. According to the theory of implicit functions, we know if at some root, say $\bar{\Psi}_a'$, of the equation, there holds the condition $\Xi'_{\Psi_a'}(\bar{b}, \Psi_a, \bar{\Psi}_a') \neq 0$, then point $(\bar{b}, \bar{\Psi}_a')$ is called a regular point, geometrically, the end manifold intersects $\Psi' = H(b)$ transversally at this point, so this kind of point will still exist under small change of the parameters, or in analytical words: for this kind of point, there exists a $\epsilon > 0$, such that when $|b - \bar{b}| < \epsilon$, all corresponding BVP (3.5) has a solution with initial value (Ψ_a, Ψ_a') near $(\Psi_a, \bar{\Psi}_a')$. The singular point occurs only when $\Xi'_{\Psi_a'}(\bar{b}, \Psi_a, \bar{\Psi}_a') = 0$.

In some literature, for example in [8], the frequently referred BVP is of the following form:

$$\Psi'' = \lambda F(\Psi, \Psi'), \Psi(a) = \Psi_a, \Psi'(b) = \bar{\Psi}_b', \lambda \neq 0,$$

here F has the same property as given above, λ is a parameter, which is in the equation not in the boundary condition. After making a transformation $\sqrt{\lambda}t = \delta$ (provided $\lambda > 0$), then

$$\Psi_t' = \sqrt{\lambda}\frac{d\Psi}{d\delta}, \Psi_{tt}'' = \lambda\frac{d^2\Psi}{d^2\delta},$$

we get

$$\Psi_{\delta\delta}'' = F(\Psi, \Psi'), \Psi(\sqrt{\lambda}a) = \Psi_a, \Psi(\sqrt{\lambda}b) = \frac{1}{\sqrt{\lambda}}\bar{\Psi}_b',$$

the parameter λ is moved to the boundary condition and the equation is now of the form we discussed above. Therefore our discussion on (2.2) is also applicable to $\Psi'' = \lambda F(\Psi, \Psi')$.

Applying the above discussion to our pendulum equation, in the (Ψ, Ψ')-phase plane of system (2.2), for each given γ, we can define a manifold $M(\alpha, p)$ in the following way: for
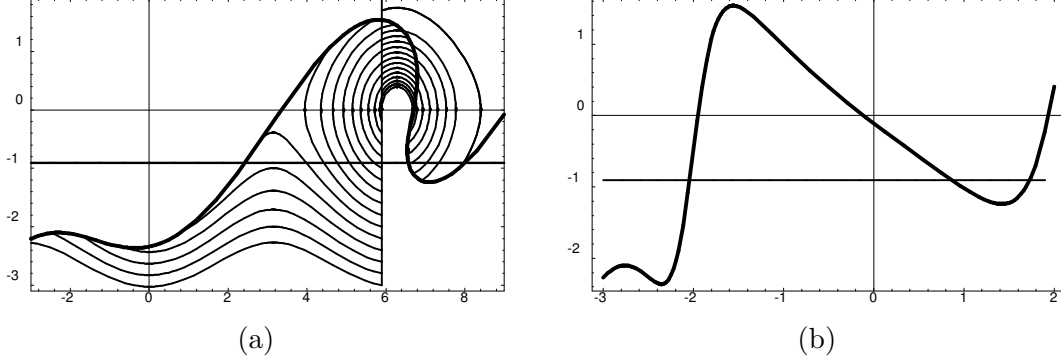
(a)   (b)

Figure 3.2: (a): Manifold $M(-\frac{3\pi}{8}, 12)$ for $\gamma = \frac{\pi}{2}$. (b): Ψ'_1 vs. ω_0 with $\gamma = \frac{\pi}{2}, \alpha = -\frac{3\pi}{8}, p = 12$.

fixed α, the initial manifold M_α is the vertical straight line $\{(\pi + \gamma - \alpha, \omega_0)|\omega_0 \in \mathbb{R}\}$. Let Ψ_t be the flow of the pendulum equation (2.2), consider M_α under that flow and let $M(\alpha, p) := \Psi_{\sqrt{p}}(M_\alpha)$, then M is composed of points $(\Psi(\sqrt{p}), \Psi'(\sqrt{p}))$(note: we denote them as (Ψ_1, Ψ'_1)), it is a plane smooth curve parameterized by ω_0 for given γ, α and p(see figure 3.2(a)). Each intersection of $M(\alpha, p)$ with the horizontal straight line $\Psi' = -\frac{2\gamma}{\sqrt{p}}$ is an end point of the possible phase curve, the coordinate $\bar{\omega}_0$ of the start point of which is the value we intend to find. That means, from this value of ω_0 we can get an orbit of (2.2) which starts at $(\pi + \gamma - \alpha, \bar{\omega}_0)$, ends at a point on $\Psi' = -\frac{2\gamma}{\sqrt{p}}$ and the transit 'time' along it is $\sqrt{p}$. Since the final value of Ψ' along each possible orbit of (2.2) is to be negative and owing to the fact that the phase curve of (2.2) can not meet the separatrix (except separatrix itself), we need not take points of M_α above the upper part of the separatrix into consideration, *i.e.*, $\omega_0 < 2$. In our following discussion we suppose M_α is a half straight line. Figure 3.2(a) shows the manifold defined by (2.2) for $\gamma = \frac{\pi}{2}, \alpha = \frac{-3\pi}{8}$. In figure 3.2(a) the thin curves are the phase curve (2.2), the thick solid curve represents part of the end manifold $M(-\frac{3}{8}\pi, 12)$ for $\gamma = \frac{\pi}{2}$ (the corresponding undeformed elastic rod is a half ring), in this case there are three mentioned intersections, which correspond to three values of ω_0. It indicates that, for $\gamma = \frac{\pi}{2}, \alpha = -\frac{3}{8}\pi, p = 12$, system (2.2) has three orbits, each takes the above ω_0 as initial velocity, and further (2.3) has three solutions.

With the same consideration , for fixed γ, α and p we can consider Ψ'_1 as a function of ω_0, namely $\Psi'_1 = \Psi'_1(\omega_0)$, it defines a continuous curve in $\omega_0\Psi'_1$- plane, the ω_0-coordinates of the intersections of this curve with the horizontal straight line $\Psi' = -\frac{2\gamma}{\sqrt{p}}$ are the values of ω_0 we wanted. Figure 3.2(b) shows a sample curve of this kind, which corresponds to the situation shown in figure 3.2(a). Comparing figure 3.2(a) and 3.2(b), it is obvious that 3.2(b) can be

obtained from 3.2(a), but 3.2(b) shows the relation between the intersection and ω_0 more clearly than 3.2(a).

The obvious advantages of this method (we call it manifold method) are:

a) With this method we can relatively more easily investigate the behavior of the possible phase curves (or solutions) of system (2.2);

b) We can find the number of $\omega_0's$ and give estimations to ω_0 more easily compared with the frequently used numerical methods, these estimations are extremely important for almost all numerical treatments;

c) We can get a prediction to the change tendency of ω_0 visually;

d) With this method we can discuss the phase curves and possible orbits both outside and inside of the zone bounded by the separatrix at the same time, without giving special attention to their location;

e) With this method, for given γ and α we need not deal with the *three* nonlinear equations about k, Ψ_{re} and ω_0 in **3.1**, but only function $\Psi'(\omega_0)$, determined by end manifold.

For determination of the relation between ω_0 and the parameters γ, α and p, we could use other methods mentioned above, for instance, recalling the extended system (3.4), taking

$$F(\Psi_1, \Psi_2) = \begin{bmatrix} \Psi_2 \\ -\sin \Psi_1 \end{bmatrix}, \quad \lambda = \Psi_3,$$

$$B(\Psi(a), \Psi(b)) = \begin{bmatrix} \Psi_1(0) - \pi - \gamma + \alpha \\ \Psi_2(1) + 2\gamma \end{bmatrix} = 0,$$

thus

$$F'_\Psi = \begin{bmatrix} 0 & 1 \\ -\Psi_3 \cos \Psi_1 & 0 \end{bmatrix},$$

$$J = \begin{bmatrix} 1 & 0 \\ 0 & 0 \end{bmatrix}, \quad K = \begin{bmatrix} 0 & 0 \\ 0 & 1 \end{bmatrix},$$

further let $\psi = (\Psi_4, \Psi_5)^\top, \Psi_5(0) = 1$, at last we get the following equations:

$$\begin{bmatrix} \Psi_1 \\ \Psi_2 \\ \Psi_3 \\ \Psi_4 \\ \Psi_5 \end{bmatrix}' = \begin{bmatrix} \Psi_2 \\ -\Psi_3 \sin \Psi_1 \\ 0 \\ \Psi_5 \\ -\Psi_3 \Psi_4 \cos \Psi_1 \end{bmatrix}, \quad \begin{bmatrix} \Psi_1(0) \\ \Psi_2(1) \\ \Psi_5(0) \\ \Psi_4(0) \\ \Psi_5(1) \end{bmatrix} = \begin{bmatrix} \pi + \gamma - \alpha \\ -2\gamma \\ 1 \\ 0 \\ 0 \end{bmatrix}$$

Solving above equations gives the relation between $\Psi_2(0)$ and $\Psi_3(0)$, which correspond to ω_0 and p respectively.

To solve the above mentioned equations numerically, we could use some numerical methods suitable for differential equations, such as shooting, Runge-Kutta, continuation, imbedding, finite difference and so on [21], [47], or we may call for some existing mathematical softwares, for instance *Mathematica, Maple* or *Matlab, etc*. In this work we used *Mathematica* to deal with the numeric calculation. With the help of this software, we can get satisfactory results with not too complex program. Taking main part of the procedure for finding the value of ω_0 for example, we use the following short *Mathematica* program:

$$End[\omega_{0-}, \gamma_-, \alpha_-, p_-] := \text{Module}[\{\Psi, \Phi\}, \text{Evaluate}[\{\Psi[\sqrt{p}], \Phi[\sqrt{p}]\}]/.$$
$$\text{NDSolve}[\{\Psi'[t] == \Phi[t], \Phi'[t] == -\sin\Psi[t], \Psi[0] == \pi + \gamma - \alpha, \Phi[0] == \omega_0\},$$
$$\{\Psi, \Phi\}, \{t, 0, \sqrt{p}\}]];$$
$$\omega_0[\gamma_-, \alpha_-, p_-] := \text{FindRoot}[End[\omega_0, \gamma, \alpha, p][[1, 2]] == -\frac{2\gamma}{\sqrt{p}}, \{\omega_0, \omega_{01}, \omega_{02}\}],$$

where ω_{01}, ω_{02}, which are needed in the *Mathematica* command 'FindRoot' and can be found by considering the end manifold, are two approximate values of ω_0, with $\omega_{01} \leq \omega_{02}$. In this program, $End(\omega_0, \gamma, \alpha, p)$ determines the end manifold, while $\omega_0(\gamma, \alpha, p)$ is the ω_0 coordinate of intersection produced by end manifold and the horizontal line $\Psi' = \frac{-2\gamma}{\sqrt{p}}$. We can also increase the precision of the calculation for ω_0 by means of reducing the difference of $\omega_{02} - \omega_{01}$ and choosing some extra options in 'FindRoot' with no big problem. With this method we need not to know where the orbit lies, inside or outside the zone bounded by the separatrix, and the nonlinearity plays a little role.

After ω_0 being obtained with the above methods, for fixed p, α and γ, we can calculate k easily with $k^2 = \frac{4}{\omega_0^2 + 2 + 2\cos(\gamma - \alpha)}$ and for orbits below the separatrix, we have

$$\Psi' = -\frac{2}{|k|}\sqrt{1 - k^2 \sin^2 \frac{\Psi}{2}}$$

or

$$\frac{d\Phi}{\sqrt{1 - k^2 \sin^2 \Phi}} = -\frac{1}{|k|}dt.$$

Thus

$$t = -|k|\int_{\frac{\pi+\gamma-\alpha}{2}}^{\frac{\Psi(t)}{2}} \frac{d\Phi}{\sqrt{1 - k^2 \sin^2 \Phi}}$$
$$= |k|(F(\frac{\pi+\gamma-\alpha}{2}, k^2) - F(\frac{\Psi(t)}{2}, k^2)), 0 \leq t \leq \sqrt{p}.$$

The above equation determines an implicit function

$$\Psi = \Psi(t, \alpha, \gamma), 0 \leq t \leq \sqrt{p}.$$

Substituting this expression in system (2.3), we obtain the solution of it

$$
\begin{aligned}
x(\sigma) &= \int_0^\sigma \cos(\Psi(\xi\sqrt{p}, \alpha, \gamma) + \alpha - \pi)d\xi, \\
y(\sigma) &= \int_0^\sigma \sin(\Psi(\xi\sqrt{p}, \alpha, \gamma) + \alpha - \pi)d\xi, 0 \le \sigma \le 1,
\end{aligned}
$$

and further

$$
\theta(\sigma) = \omega_0\sqrt{p}\sigma + \gamma + p\int_0^\sigma (y(\xi)\cos\alpha - x(\xi)\sin\alpha)d\xi, 0 \le \sigma \le 1,
$$

where p, α and γ are parameters.

For orbits inside of the zone bounded by the separatrix, Ψ' changes its sign when the orbits meet the Ψ-axis, at these points we have

$$
\Psi'^2 = \frac{4}{k^2}(1 - k^2\sin^2\frac{\Psi}{2}) = 0.
$$

Let $\bar\Psi$ be a solution of the last equation, the corresponding 'time' is

$$
\bar t = |k|\int_{\frac{\pi+\gamma-\alpha}{2}}^{\frac{\bar\Psi}{2}} \frac{d\Phi}{\sqrt{1 - k^2\sin^2\Phi}}.
$$

Therefore if an orbit meets the Ψ-axis only once, then the corresponding implicit solution of (2.2) is

$$
\begin{aligned}
t &= \begin{cases}
|k|\int_{\frac{\pi+\gamma-\alpha}{2}}^{\frac{\Phi(t)}{2}} \frac{d\Phi}{\sqrt{1-k^2\sin^2\Phi}} & 0 \le t \le \bar t \\[2mm]
|k|\int_{\frac{\pi+\gamma-\alpha}{2}}^{\frac{\bar\Psi}{2}} \frac{d\Phi}{\sqrt{1-k^2\sin^2\Phi}} - |k|\int_{\frac{\bar\Psi}{2}}^{\frac{\Psi(t)}{2}} \frac{d\Phi}{\sqrt{1-k^2\sin^2\Phi}} & \bar t < t \le \sqrt{p},
\end{cases} \\[3mm]
&= \begin{cases}
|k|(F(\frac{\Psi(t)}{2}, k^2) - F(\frac{\pi+\gamma-\alpha}{2}, k^2)) & 0 \le t \le \bar t \\[1mm]
|k|(2F(\frac{\bar\Psi}{2}, k^2) - F(\frac{\Psi(t)}{2}, k^2) - F(\frac{\pi+\gamma-\alpha}{2}, k^2)) & \bar t < t \le \sqrt{p}.
\end{cases}
\end{aligned}
$$

Similarly we can get the solution of (2.3) in this case. It may be possible that an orbit of (2.2) meets the Ψ axis more than once, the corresponding expression of the solution of (2.3) should be more complex. For very special system, sometimes we can handle the system directly.

For example, let $\gamma = 0, \alpha = \pi$ (Euler's rod) and assume that the deformation of the originally straight rac under the action of p is sufficiently small. The pendulum equation now is of the following form:

$$
\frac{d^2\Psi}{dt^2} = -\sin\Psi, \Psi(0) = 0, \Psi'(\sqrt{p}) = 0. \tag{3.7}
$$

With our direct method, if we take the initial value of the derivative ω_0 at left end of the rod as the unknown parameter, then we have the following equations:

$$\sqrt{p} = \frac{2}{\omega_0} \int_{\Phi_1}^0 \frac{d\Phi}{\sqrt{1 - \frac{4}{\omega_0^2} \sin^2 \Phi}} \tag{3.8}$$

where $\Phi_1 = -\arccos\left(1 - \frac{1}{2}\omega_0^2\right)$ representing the value of Ψ at the free end of the rod.

If we take Ψ_1 as the unknown parameter, then we handle the equation as following. Integrating the pendulum equation one time gives the result: $\frac{1}{2}\Psi'^2 = \cos\Psi + c$, concerning the boundary value condition $\Psi'(\sqrt{p}) = 0$, we have $c = -\cos\Psi(\sqrt{p}) := -\cos\beta$. Thus

$$\frac{d\Psi}{dt} = \pm\sqrt{2(\cos\Psi - \cos\beta)},$$

if we take the case $d\Psi > 0$ into account, then we have

$$\sqrt{p} = \frac{1}{\sqrt{2}} \int_0^\beta \frac{d\Psi}{\sqrt{\cos\Psi - \cos\beta}} = \frac{1}{2} \int_0^\beta \frac{d\Psi}{\sqrt{\sin^2\frac{\beta}{2} - \sin^2\frac{\Psi}{2}}}. \tag{3.9}$$

Let

$$\lambda = \sin\frac{\beta}{2}, \sin\frac{\Psi}{2} = \lambda\sin\psi = \sin\frac{\beta}{2}\sin\psi,$$

then

$$\sqrt{\sin^2\frac{\beta}{2} - \sin^2\frac{\Psi}{2}} = \lambda\cos\psi.$$

Finally we get the result

$$\sqrt{p} = \int_0^{\frac{\pi}{2}} \frac{d\psi}{\sqrt{1 - \lambda^2\sin^2\psi}} = K(\lambda^2).$$

If only small deformation of the rod is concerned, then β and λ can be considered to be very small, by neglecting the term $\lambda^2\sin^2\psi$, then we have the approximate value for critical force:

$$\sqrt{p} = \frac{\pi}{2},$$

or

$$\frac{L\sqrt{P}}{\sqrt{EI}} = \frac{\pi}{2},$$

that is

$$P = \frac{\pi^2 EI}{4L^2}.$$

This value of P is the smallest critical load (Euler's 1_{st} critical load obtained via linearization) which corresponds the first singular point for pendulum equation with $\gamma = 0, \alpha = \pi$.

For this arc, getting the displacement of its free end from its original position is not difficult.
From equation

$$\frac{dy}{d\sigma} = \sin\theta(\sigma),$$

we have

$$\frac{dy}{dt} = \sin\theta(\sigma)\frac{1}{\sqrt{p}} = \frac{\sin\theta d\theta}{\sqrt{2p}dt\sqrt{\cos\theta - \cos\beta}}.$$

Using the transformation

$$\sin\frac{\theta}{2} = \lambda\sin\psi,$$

we have

$$\frac{1}{2}\cos\frac{\theta}{2}d\theta = \lambda\cos\psi d\psi,$$

$$\cos\frac{\theta}{2} = \sqrt{1 - \lambda^2\sin^2\psi},$$

$$\sin\theta = 2\lambda\sin\psi\sqrt{1 - \lambda^2\sin^2\psi},$$

thus

$$y(\sqrt{p}) = \frac{1}{2\sqrt{p}}\int_0^\beta \frac{\sin\theta d\theta}{\sqrt{\sin^2\frac{\beta}{2} - \sin^2\frac{\theta}{2}}} = \frac{2\lambda}{\sqrt{p}}\int_0^{\frac{\pi}{2}}\sin\psi d\psi = \frac{2\lambda}{\sqrt{p}}. \qquad (3.10)$$

Similarly, from

$$dx = \frac{\cos\theta d\theta}{\sqrt{2p}\sqrt{\cos\theta - \cos\beta}}$$

and the transformation used for y-coordinate, we obtain

$$x(\sqrt{p}) = \frac{2}{\sqrt{p}}\int_0^{\frac{\pi}{2}}\sqrt{1 - \lambda^2\sin^2\psi}d\psi - \frac{1}{\sqrt{p}}\int_0^{\frac{\pi}{2}}\frac{d\Psi}{\sqrt{1 - \lambda^2\sin^2\Psi}}$$

$$= \frac{2}{\sqrt{p}}E(\lambda^2) - \frac{1}{\sqrt{p}}K(\lambda^2),$$

in the result $E(\lambda^2)$ is elliptic integral of the second kind.

Therefore if we need to get the displacement of the right end of the deformed arc for a
certain small p, we can get the value of λ from $\sqrt{p} = K(\lambda^2)$ first, then using the expression
above to get $x(\sqrt{p})$ and $y(\sqrt{p})$.

After ω_0 obtained, we can use the following *Mathematica* program to draw the phase
curves of (2.2):

$$\gamma = \gamma_0; \alpha = \alpha_0; p = p_0; \omega_0 = \bar\omega_0;$$

$$\text{Phase}[t_-, \gamma_-, \alpha_-, p_-, \omega_{0-}] := \text{NDSolve}[\{\Psi'(t) == \Phi(t), \Phi'(t) == -\sin\Psi(t),$$

$$\Psi(0) == \pi + \gamma - \alpha, \Phi(0) == \omega_0\}, \{\Psi(t), \Phi(t)\}, \{t, 0, \sqrt{p}\}];$$

$$\Psi[t\_, \gamma\_, \alpha\_, p\_, \omega_0\_] := \text{Phase}[t, \gamma, \alpha, p, \omega_0][[1,1]];$$

$$\Phi[t\_, \gamma\_, \alpha\_, p\_, \omega_0\_] := \text{Phase}[t, \gamma, \alpha, p, \omega_0][[1,2]];$$

$$\text{ParametricPlot}[\{\Psi[t, \gamma, \alpha, p, \omega_0], \Phi[t, \gamma, \alpha, p, \omega_0]\}, \{t, 0, \sqrt{p}\}].$$

The solution of (2.3) can be obtained with the following program:

$$\gamma = \gamma_0; \alpha = \alpha_0; p = p_0; \omega_0 = \bar{\omega}_0;$$

$$\text{Conf}[\sigma\_, \gamma\_, \alpha\_, p\_, \omega_0\_] := \text{NDSolve}[\{x'(\sigma) == \cos\theta(\sigma), y'(\sigma) == \sin\theta(\sigma),$$

$$\theta'(\sigma) == p[y(\sigma)\cos\alpha - x(\sigma)\sin(\alpha)] + \omega_0\sqrt{p},$$

$$x(0) == 0, y(0) == 0, \theta(0) == \gamma\}, \{x(\sigma), y(\sigma), \theta(\sigma)\}, \{\sigma, 0, 1\}];$$

$$x[\sigma\_, \gamma\_, \alpha\_, p\_, \omega_0\_] := \text{Conf}[\sigma, \gamma, \alpha, p, \omega_0][[1,1]];$$

$$y[\sigma\_, \gamma\_, \alpha\_, p\_, \omega_0\_] := \text{Conf}[\sigma, \gamma, \alpha, p, \omega_0][[1,2]];$$

$$\theta[\sigma\_, \gamma\_, \alpha\_, p\_, \omega_0\_] := \text{Conf}[\sigma, \gamma, \alpha, p, \omega_0][[1,3]];$$

We can use the *Mathematica* command 'ParametricPlot' to draw the configuration of (2.3), which we will show in next section:

$$\text{ParametricPlot}[\{x[\sigma, \gamma, \alpha, p, \omega_0], y[\sigma, \gamma, \alpha, p, \omega_0]\}, \{\sigma, 0, 1\}].$$

Chapter 4

Study on multiplicity and bifurcation

As discussed above, the study of the deformation of the elastic arcs (or solution of (2.3)) is reduced to the study of the BVP of the related pendulum equation (2.2), and this is then turned to the study on ω_0. Normally, of the three parameters in (2), we take the normalized acting force p as bifurcation parameter. When the parameters are given, the number of the possible solutions of the pendulum equation will be the same as the number of $\omega_0's$, because there is clearly an one -to-one correspondence between these two numbers. So from now on we will put ω_0 at the same place as the solution of (2.2) and (2.3) to be found. In the following we will concentrate our discussion on the relation between ω_0 and the three parameters γ, α and p.

First we introduce some concepts for general situations. Generally the BVP of the autonomous differential equation can be written in the following form:

$$\Psi' = F(\Psi, \lambda, \beta), B(\Psi(a), \Psi(b)) = 0, \tag{4.1}$$

where $\Psi \in I\!\!R^n, \lambda \in I\!\!R, \beta \in I\!\!R^l, F \in C^1 : I\!\!R^n \times I\!\!R \times I\!\!R^l \longrightarrow I\!\!R^n$ and $B \in C^1 : I\!\!R^{n_1} \times I\!\!R^{n_2} \longrightarrow I\!\!R^n$ with $n_1 + n_2 = n$.

In the following discussion we need a definition related to bifurcation,

Definition 4.1 *The set $D(F) = \{(\lambda, \Psi)|F(\Psi, \lambda, \beta) = 0\}$ is called the bifurcation diagram of F for fixed β. The set $B(F) = \{\beta|F(\Psi, \lambda, \beta) = 0, rank(DF) < n\}$, here DF denotes the differential of F with respect to Ψ and λ but not β, is called branching diagram of F.*

To give a geometrical explanation to this definition, we consider a very simple example:

$$F(\Psi, \lambda, \beta) = \Psi^3 - \lambda\Psi + \beta = 0,$$

taking λ as bifurcation parameter and β as branching parameter, the relation $\Psi\, vs.\, \lambda$ for fixed β is ahown in figure 4.1, in this figure the vertical coordinate is Ψ.

From the above definitions and example we know the bifurcation parameter and other parameters play an important role in the study of multiplicity and bifurcation. As the explicit expressions of the solutions of the bifurcation problems and the differential equations are difficult to find, the numerical handling is necessary. About numerical treatment of bifurcation problem a plenty of work can be found [4], [16], [35], [34], [61], [63], [75], [84]. In our work we will study bifurcation diagram with manifold method and get the result with the help of some available mathematical softwares. We try to give a through survey to the influence of all parameters on the system.

4.1 The relation between ω_0 and α, γ as well as p

As described above, the most important work for solving system (2.3) is to find ω_0. In this section we will especially concentrate our attention to ω_0 and its character, such as its existence, multiplicity, change tendency, numerical value and the relations between ω_0 and phase curves of (2.2) and configurations of (2.3) as well. As shown in figure 3.2, ω_0 changes with the parameters γ, α and p or we can say ω_0 is a function of the parameters: $\omega_0 = \omega_0(\gamma, \alpha, p)$. It is obvious that one set of (γ, α, p) may correspond with more than one value of ω_0, therefore $\omega_0(\gamma, \alpha, p)$ represents a complex hypersurface in $I\!\!R^4$ geometrically, which is composed of several branches of simple surface. For simplicity and clearness and making it more visual, we will discuss the projection of it on different planes, or we will discuss the intersection of this surface with planes which are parallel to the coordinate planes of the parameter coordinate system (γ, α, p), that is, in our following discussion we
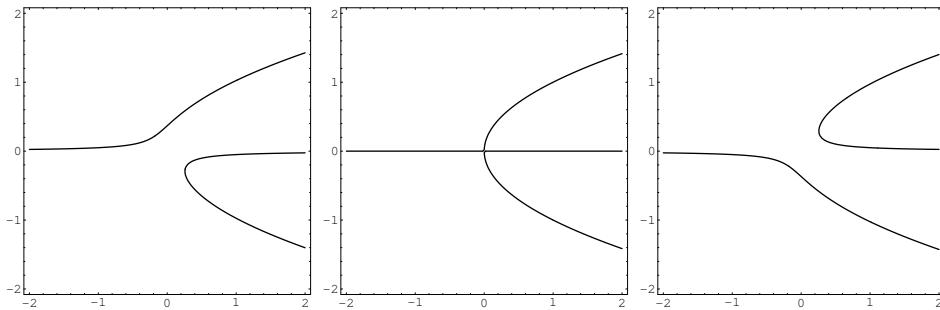

Figure 4.1: The bifurcation diagram of $F(\Psi, \lambda, \beta) = \Psi^3 - \lambda\Psi + \beta = 0$ for $\beta < 0$ (left), $\beta = 0$ (middle) and $\beta > 0$ (right).
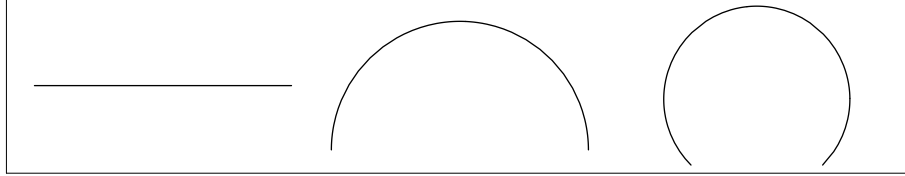
Figure 4.2: The undeforemed arcs for $\gamma = 0$ (left), 0.5π (middle) and 0.75π (right).

will set some parameters fixed. Because it is almost not possible to get the exact analytical expressions of the solutions of the corresponding problem in large scale, the results will be shown by bifurcation diagrams.

4.1.1 The relation between ω_0 and p for fixed γ(alsoα)

In this section we intend to make clear the relation between ω_0 and p. First we choose some typical values of $\gamma, (0(\frac{\pi}{4})\pi)$, then for each fixed γ, choose some different values of α. In this section we give the bifurcation diagram for $\gamma = 0, \gamma = 0.5\pi$ and $\gamma = 0.75\pi$ in figure 4.3, 4.4, 4.5 separately, the corresponding undeformed arcs are shown in figure 4.2. Other bifurcation diagrams are given in appendix 3 together. These figures show clearly: for fixed γ and α, when p is relatively small, to one p there corresponds only one ω_0, the points (p, ω_0) compose a curve in each diagram in $p\omega_0$- plane, the configurations of (2.3) corresponding to these values of ω_0 are said to be 'normal', because they are of practical significance, according to the engineers.

This states the fact that small acting force does not bring extra configurations to system (2.2). When p grows further the number of the ω_0 has a 'jump', for relatively large p, the correspondence between p and ω_0 is no more one-to-one, it is represented by several pieces of curves on the $p - \omega_0$ plane. When γ is fixed, these curves move with α, observing the following rules: considering the two curves located above the normal one, 1.) if one is above the other when $\alpha = -0.5\pi$, then the upper one moves rightwards, while the other one moves leftwards as α increases, and they meet together for some definite α to form a singular point, then they split again to form two new curves with one is located at the right of the other, and then these two new curves move rightwards. 2.) If the two curves have a left-right position when $\alpha = -0.5\pi$, then they move rightwards with α. For the curves below the normal one, they move rightwards with α. It is possible, one of them
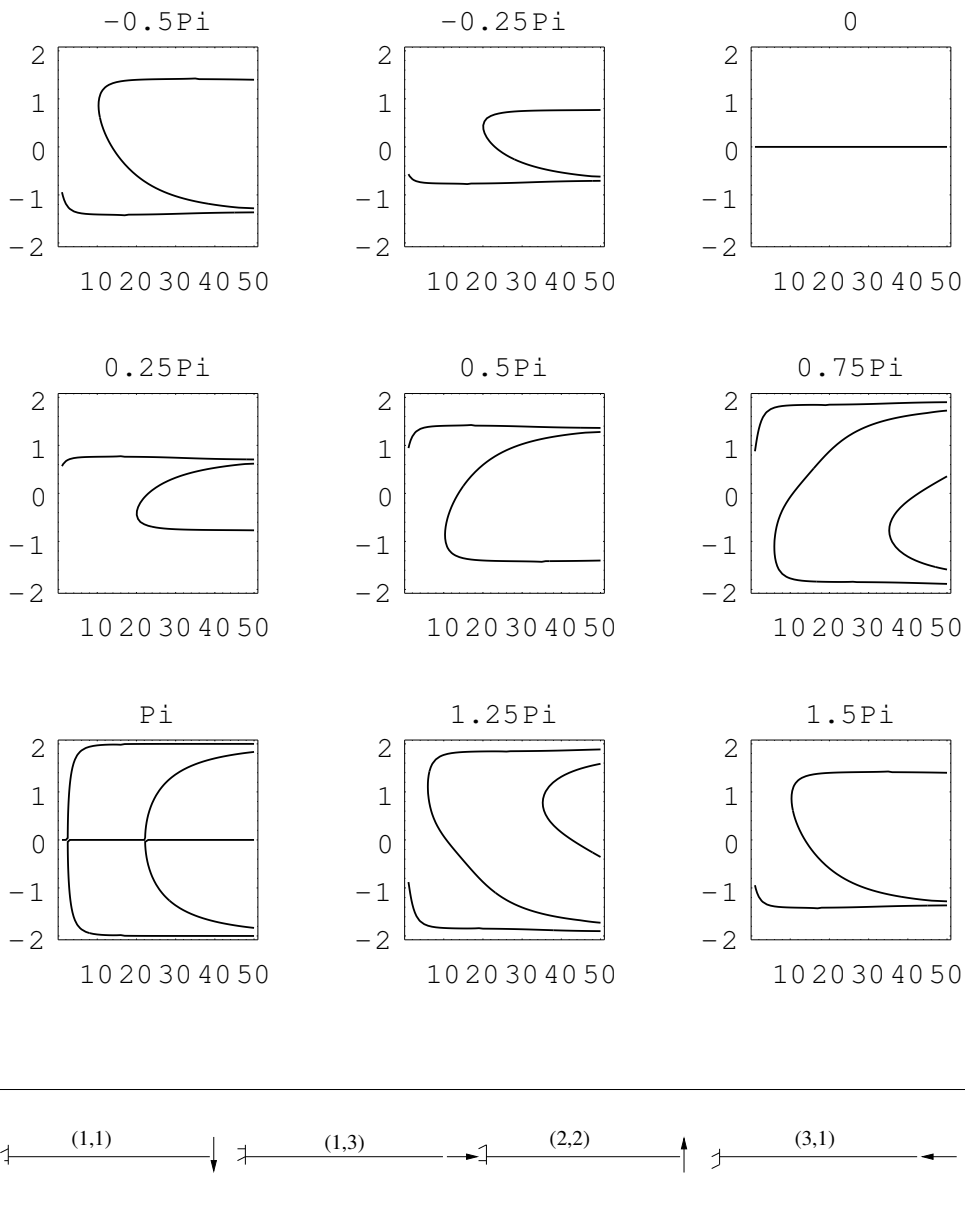
Figure 4.3: Bifurcation diagram $\{(p, \alpha, \omega_0) | \alpha \text{ fixed}, p \in [0, 50]\}$ for $\gamma = 0$, (α values above diagrams)(upper) and some typical cases of acting forces(lower).
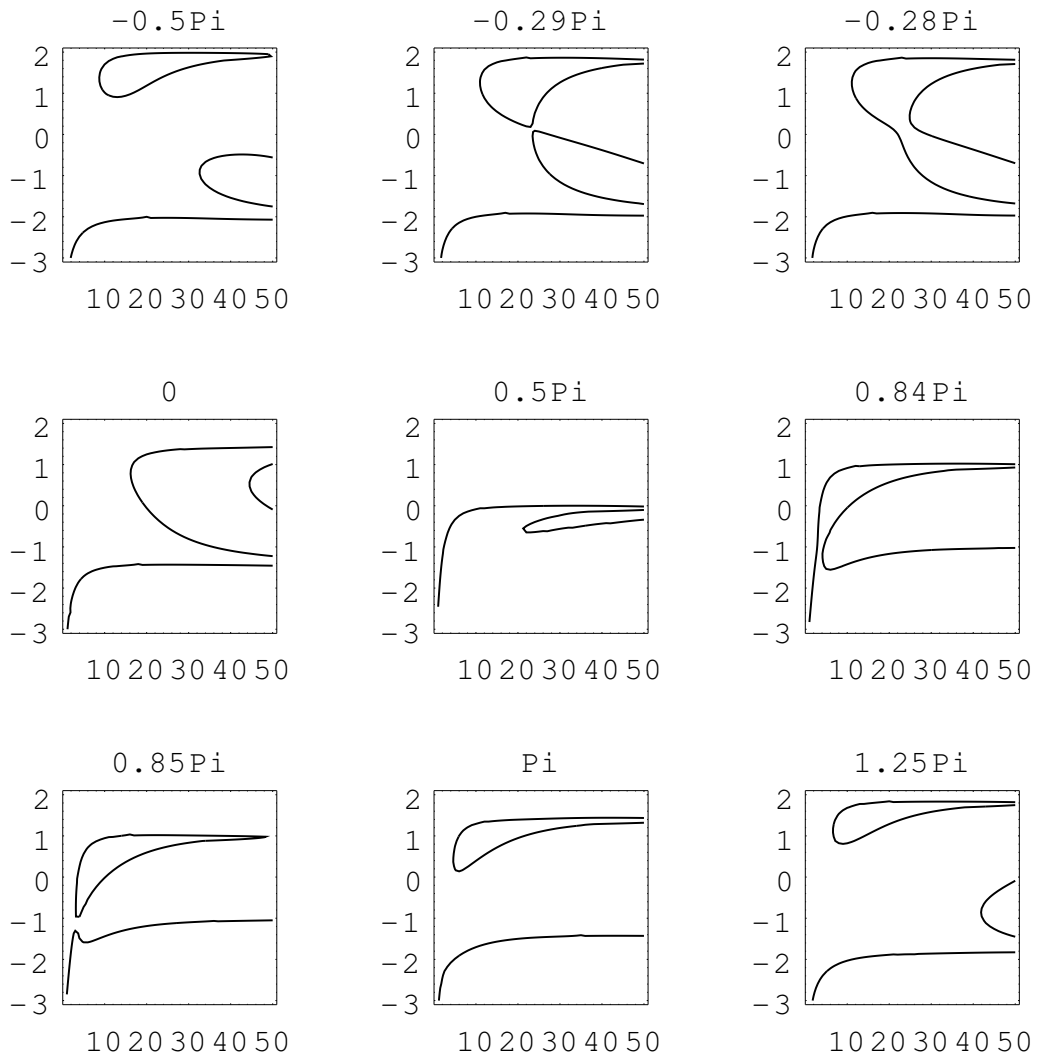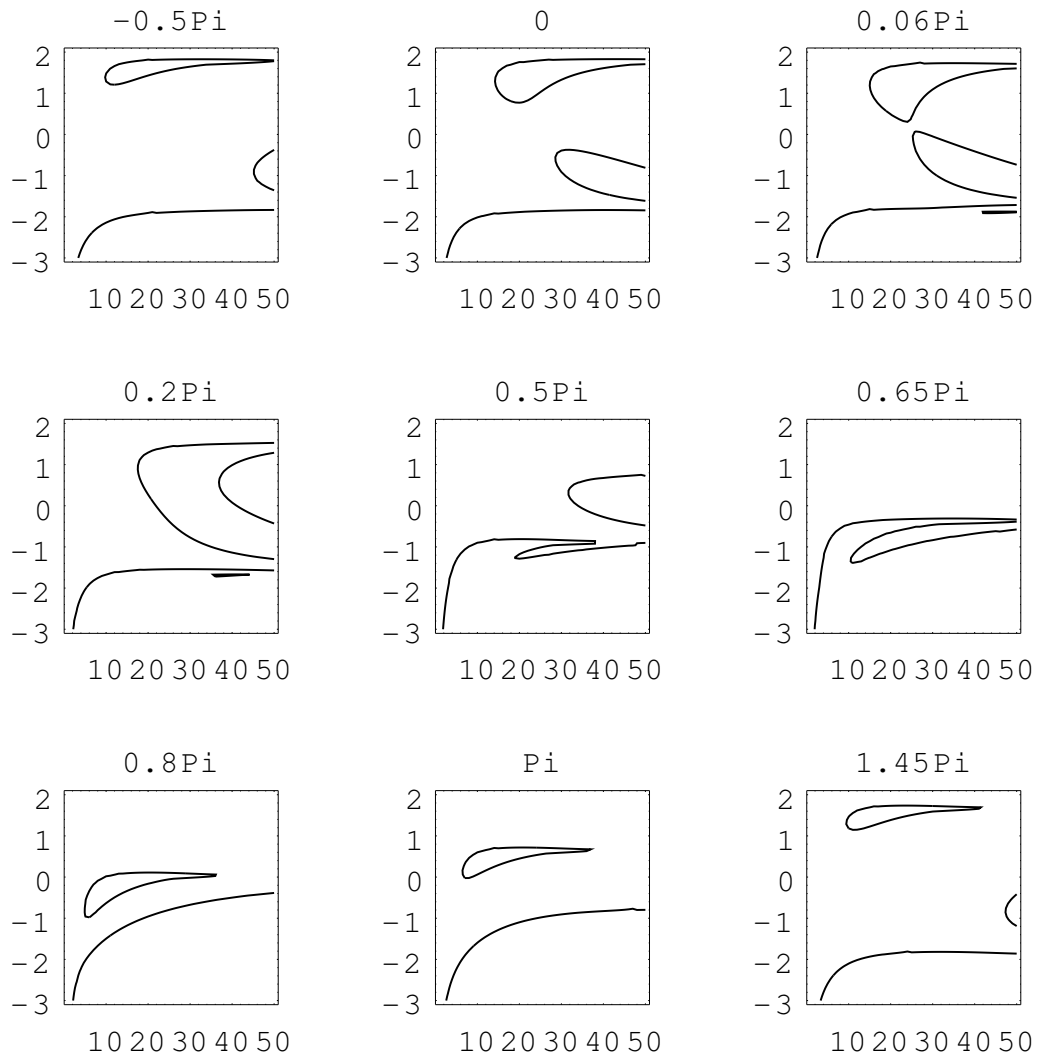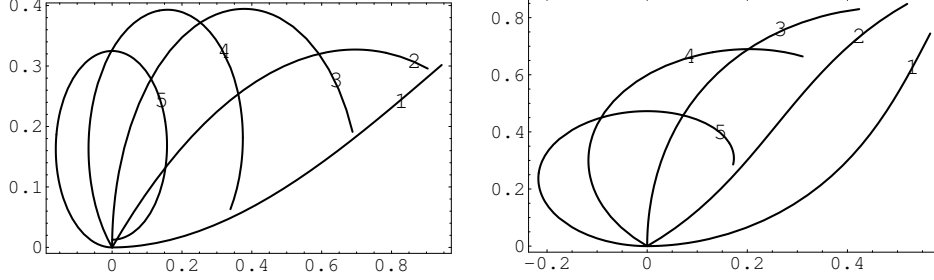
Figure 4.4: Bifurcation diagram $\{(p, \alpha, \omega_0) | \alpha$ fixed, $p \in [0, 50]\}$ for $\gamma = 0.5\pi$, (α values above diagrams).

Figure 4.5: Bifurcation diagram $\{(p, \alpha, \omega_0) | \alpha \text{ fixed}, p \in [0, 50]\}$ for $\gamma = 0.75\pi$, (α values above diagrams).

Figure 4.6: The normal configurations for $\alpha = 0.5\pi$ and $\gamma = 0, \gamma = 0.25\pi, \gamma = 0.5\pi, \gamma = 0.75\pi$ and $\gamma = \pi$ (distinguished by 1, 2, 3, 4 and 5 separately) with $p = 1$ (left) and $p = 6$ (right).

will meet the normal one for some certain α to form a singular point, and then it changes position with the normal one to become the curve above and moves obeying the rule for curves above the normal one. This phenomenon can be explained by recalling the phase curve of (2.2). The value $\pi + \gamma - \alpha = \pi$ or $\gamma = \alpha$ is a special value, for given γ if α makes the value $|\alpha - \gamma|$ bigger, the vertical line $\Psi = \pi + \gamma - \alpha$ is much apart from the vertical line $\Psi = \pi$, so there are more possibilities for orbit starting from a point on $\Psi = \pi + \gamma - \alpha$ to reach $\Psi' = \frac{-2\gamma}{\sqrt{p}}$, that means (2.2) could have multiple solutions for relatively smaller p. In course of this procedure, the normal curve moves with α too, but upwards or downwards. Specifically, when $0 \leq \gamma \leq \frac{3\pi}{4}$, it moves upwards first, meets the curve below it to form a singular point, then moves downwards to reach a lowest position, after that it moves upwards again. But for $\gamma = \pi$, it moves in the opposite direction.

These figures show also the developing tendency of ω_0. For each fixed γ and α (beside $\alpha = \gamma$, in this case $\Psi(0) = \pi$ and because $(\pi, 0)$ is the saddle point of pendulum equation (2.2), so ω_0 must be always negative), when p tends to infinity. ω_0 has two limit values, which corresponds to the upper and lower branches of the separatrix of (2.2) respectively, that means, when p increases infinitely, the corresponding phase curves of (2.2) will approach to the two branches of separatrix and the endpoints of the phase curves will tend to the saddle points. The separatrix then acts as the limit curve of the phase curves and the saddle points are limit points of the endpoints of the phase curves of (2.2) with boundary conditions.

We now give a theoretical description to this limit phenomenon with the following theorem.

Theorem 4.1 *The function $\omega_0 = \omega_0(p)$ determined by*

$$End(\alpha, \gamma, \omega_0, p) + \frac{2\gamma}{\sqrt{p}} = 0,$$

for every fixed γ and α, is single-valued for small p and multiple-valued for sufficiently large p (except $\gamma = \alpha = 0$), geometrically it has different branches. For $\alpha \neq \gamma$, it has two limit values as $p \to \infty$, which correspond to the vertical coordinates of the two intersections of vertical line $\Psi = \pi + \gamma - \alpha$ with the separatrix.

Before the proof of this theorem, we state that, for any fixed α and γ (except $\gamma = \alpha = 0$), there is a p_c (dependent on α and γ), when $p < p_c$, $\omega_0(p)$ *vs* p is one-to-one. But for big p, $\omega_0(p)$ could have as many as branches provided that p is big enough.

Proof: From the pendulum equation $\Psi'' = -\sin\Psi$ we have $\frac{1}{2}\Psi'^2 = \cos\Psi + c$. Without loss of generality, we confine $-\pi \leq \Psi \leq \pi$. Along each possible orbit the arc from a start point on vertical line $\Psi = \gamma + \alpha - \pi$ to a point on Ψ-axis in the first quadrant of $\Psi - \Psi'$ coordinate system, the transit 'time' is

$$t = k \int_{\frac{\pi+\gamma-\alpha}{2}}^{\Phi_1} \frac{d\Phi}{\sqrt{1 - k^2 \sin^2\Phi}},$$

where $\Phi_1 = \frac{\bar{\Psi}}{2}$ corresponding to the intersection between the mentioned arc with the Ψ-axis. The arc along the separatrix from a point on Ψ'-axis to a point on Ψ-axis in the first quadrant corresponds $c = 1$ and $k = 1$ and $\Phi_1 \to \frac{\pi}{2}$, but

$$\lim_{k \to 1} \int_0^{\frac{\pi}{2}} \frac{d\Phi}{\sqrt{1 - k^2 \sin^2\Phi}} = \infty.$$

So in the procedure of $p's$ approaching to ∞, the horizontal line $\Psi' = \frac{-2\gamma}{\sqrt{p}}$ approaches to Ψ-axis, the above mentioned arc on an orbit of the pendulum equation approaches to the arc segment on separatrix from the intersection made by the vertical line and the separatrix to the saddle point, Φ approaches to $\frac{\pi}{2}$, or in other words, the related ω_0 approaches to the vertical coordinate of the intersection, meanwhile the transit 'time' approaches to ∞.□

At the same time the configurations of (2.3) change also with p, for instance in the case of $\gamma = 0, \alpha = \pi$, when p is very big, the free ends of two of the configurations will tend to the negative x-axis, while in the case of $\gamma = 0.5\pi, \alpha = 0.5\pi$, one of the configuration will tend to the positive y-axis (see 4.8 and 4.9).

Note: When $\gamma = \alpha$, the vertical line is $\Psi = \pi$, the possible ω_0 has only one limit value 0 as $p \to \infty$.

From the proof of this theorem we can also get a conclusion about the change of the number of ω_0:

1. let γ and p be fixed, the curves in bifurcation diagram change with α, as $\pi + \gamma - \alpha$ is near 0, the p needed for the existence of multiple solutions is relatively small, and when $\pi + \gamma - \alpha$ closes to $\pm\pi$, the p needed is relatively big.

2. let γ and α be fixed, we see the bigger the p is, the more ω_0's there will be, that is because, when p grows, the horizontal line $\Psi' = -\frac{2\gamma}{\sqrt{p}}$ goes to Ψ-axis, more phase curves could arrive this line.

3. when α, p are fixed, the situation is more complex, because both $\Psi = \pi + \gamma - \alpha$ and $\Psi' = -\frac{2\gamma}{\sqrt{p}}$ move with γ, the number of ω_0 does not change monotonously with γ.

Here we give some sample phase curves (2.2) and corresponding configurations of (2.3) to match the above given discussions on bifurcation diagrams in figure 4.7 -4.10:
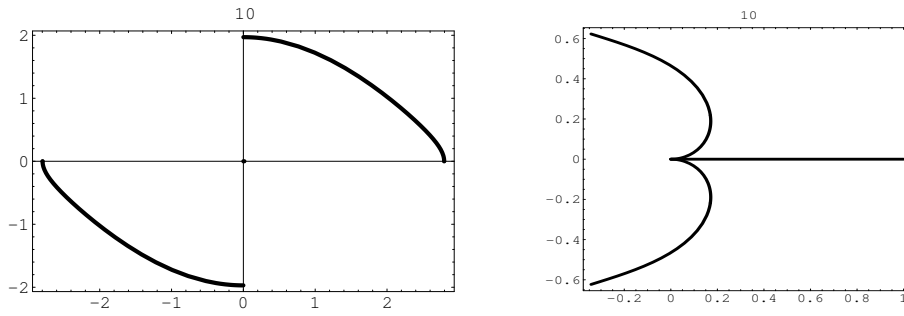
Figure 4.7: The phase curves of (2.2) (left) and configurations of (2.3)(right) for $\gamma = 0, \alpha = \pi$ and $p = 10$.

In order to get more information about the character of ω_0, we take also some fixed values of $\alpha, (-0.5\pi(0.25\pi)1.25\pi)$. For each chosen α, we choose some values of $\gamma, (0(0.25\pi)\pi)$ to discuss the relation between ω_0 and p. The results are geometrically shown in figures 8.3-8.10 in appendix 3.

These figures show, for each fixed α and $0 \leq \gamma \leq \pi$, there is at most only one singular point. It is formed in the following way: the two $p - \omega_0$ curves above the normal one, having the left-right position, move leftwards first when γ increases from 0 to π, they meet together for some definite γ to form a singular point, then they split again to become two new curves having upper-lower position and then move rightwards. While the two $p - \omega_0$ curves below the normal one move leftwards for $\alpha \leq 0$ (when exist) and move rightwards for $\alpha > 0$ (when exist) first, either to reach an extra right position and then move leftwards,
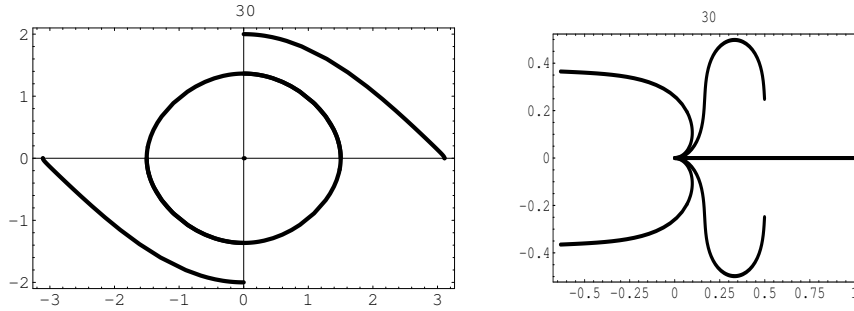
Figure 4.8: The phase curves of (2.2) (left) and configurations of (2.3) (right) for $\gamma = 0, \alpha = \pi$ and $p = 30$.

or to meet the normal one to form a singular point and then become the curves above the normal one. In this procedure, the normal $p - \omega_0$ curve moves upwards or downwards. For each fixed γ and $-\pi/2 \leq \alpha \leq 3\pi/2$, when $p \leq 50$, there are two singular points. When $p \geq 50$, there should be more bifurcation points other than these two. In fact, simply for $\gamma = 0, \alpha = \pi$, the system (2.2) could have as many as singular points provided p is sufficiently big.

4.1.2 The relation between ω_0 and α for fixed γ(also p)

With the same method as used in 4.1.1, in this section we choose some typical values of γ first, then for each fixed γ we select some values of p to discuss how ω_0 changes with α. That is, in this section we intend to discuss the influence of the acting direction of p on the deformation of the elastic arcs. The results are shown in figure 8.11- 8.15. For each fixed p (γ is fixed), the diagram shows the projection of $\omega_0(\gamma, \alpha, p)$ on a cylinder of radius p in a planar manner, so the vertical edges of each diagram are to be identified. For smaller p, the relation between α and ω_0 is one-to-one and the curve is wavelike, the wave peak turns clockwise as p increases, meanwhile the number of ω_0 increases. And these figures show also for smaller p, the bigger the value of γ is, the flatter are the $\alpha - \omega_0$ curves and the lower is the position of them. This can be explained by the location of the horizontal line $\Psi' = \frac{-2\pi}{\sqrt{p}}$ and the fact that the endpoints of the possible orbits lie on this line. For relatively big p, the bigger the value of γ is, the narrower is the peak of the $\alpha - \omega_0$ curve. For each fixed γ, we can see clearly from these figures that, only the curves below the normal one may intersect with the vertical straight line $\alpha = \gamma$, this agrees with the
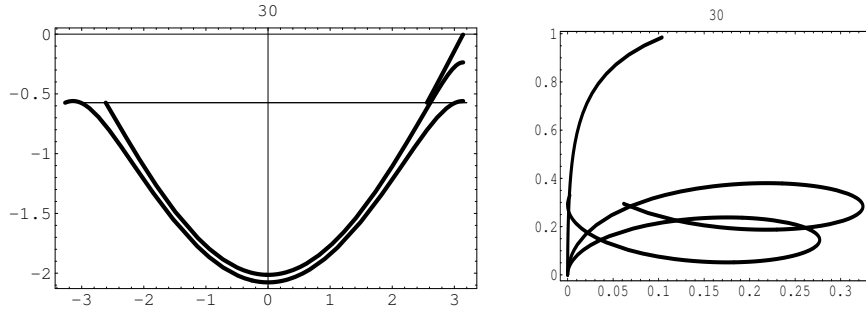
Figure 4.9: The phase curves of (2.2) (left) and configurations of (2.3)(right) for $\gamma = 0.5\pi, \alpha = 0.5\pi$ and $p = 30$.

discussion before.

When we take some fixed values of $\alpha, (-0.5\pi(0.25\pi)1.5\pi)$ and for each fixed α choose some values of p to discuss the relation between ω_0 and γ, we can see also clearly some characters of the normal $\gamma - \omega_0$ curve and some other interesting phenomena. For instance, for very small p(say $p = 1$), the normal curve becomes steeper when α changes from -0.5π to 0.5π, then becomes less steeper. For fixed α, it becomes flatter as p increases. These characters can be explained by phase portrait of (2.2), for fixed $\gamma \neq 0$, the bigger the value of p is, the closer the horizontal line $\Psi' = \frac{-2\gamma}{\sqrt{p}}$ goes to the Ψ-axis, and the bigger the curvature of phase curve becomes, so the value of ω_0 changes more quickly. In this group of bifurcation diagrams, some branches of the $\gamma - \omega_0$ curves are closed (see $\alpha = -0.5\pi, p = 10$, etc) and some two branches may meet together to form a singular point(see $\alpha = 0.5\pi, p \in (20, 25)$, etc).

As a conclusion of the discussion on bifurcation diagram, we give a partition on the $p\alpha$-parameter plane as shown in figure 4.11- 4.15 according to the number of solutions of the equations 2.2 and (2.3). In these figures we use roman numbers $I, II, etc.$ to represent the zone in which the number of the solution is equal to this roman number. The curves in these figures correspond to the turning points and the arabic number on these curves represents the number of solutions. The pinpoints in each diagram correspond to a singular point of the bifurcation diagram. The intersection of two curves corresponds to a situation in which two turning points of the bifurcation diagram exist at the same time.
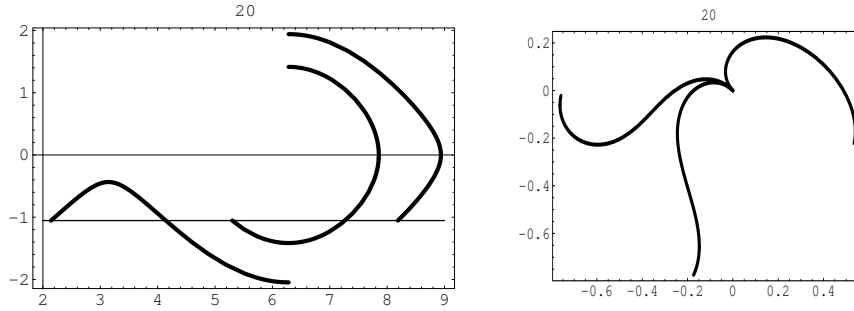
Figure 4.10: The phase curves of (2.2) (left) and configurations of (2.3) (right) for $\gamma = 0.75\pi, \alpha = -0.25\pi$ and $p = 20$.
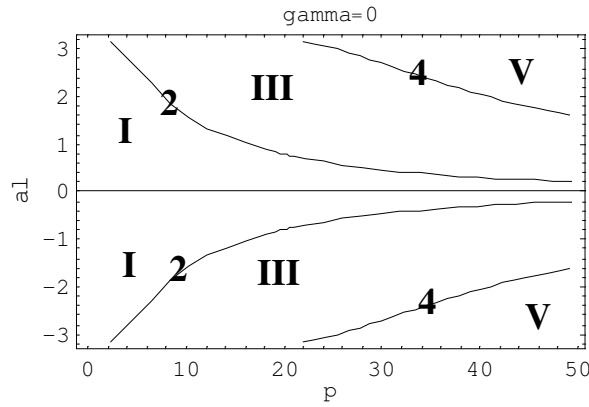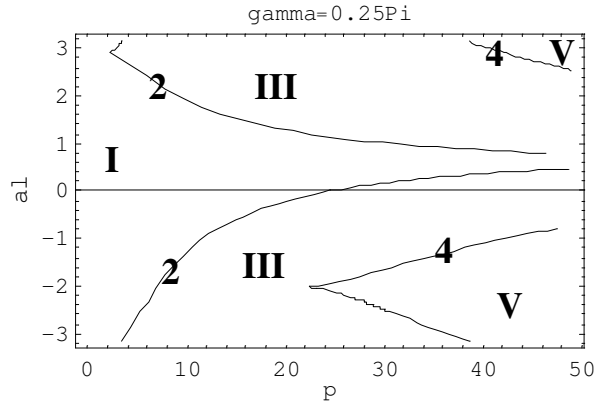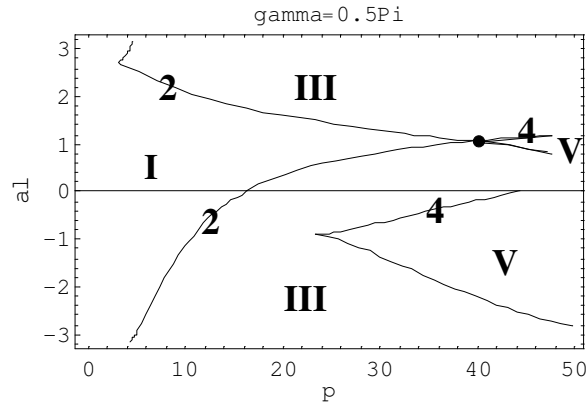

Figure 4.11: Partition of $p - \alpha$ plane for $\gamma = 0$.

4.2 Investigation of bifurcation

According to the discussion results in 4.1, we can divide the points on the curves in bifurcation diagrams geometrically into four kinds:

1. Regular point, the corresponding p has a neighborhood, in which the number of ω_0 keeps not changed.

2.) Turning point, the corresponding point $(\bar{p}, \bar{\omega}_0)$ has a neighborhood U, denoting the number of ω_0 for $p < \bar{p}\,(p > \bar{p})$ with $n_l(n_r)$ in U respectively, then $|n_r - n_l| = 2$.

3. Bifurcation point, at which two different curves meet together with different tangents.

4. Hysteresis point, at which the branching curve has a vertical tangent and the number of ω_0 keeps the same in a small neighborhood of it.
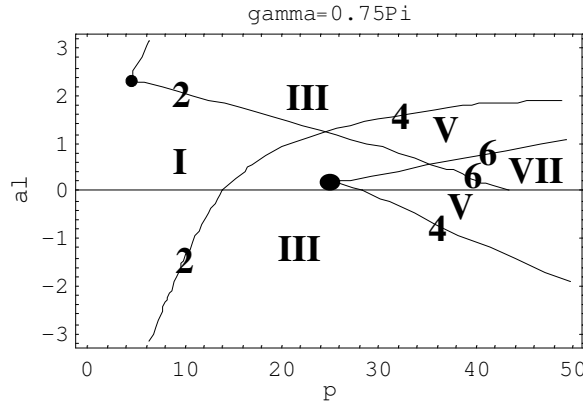
Figure 4.12: Partition of $p - \alpha$ plane for $\gamma = 0.25\pi$.

Figure 4.13: Partition of $p - \alpha$ plane for $\gamma = 0.5\pi$.

There are different analytic definitions about the above classification. We use the following definition (see for example [32]).

Definition 4.2 *A point* (Ψ_0, λ_0) *is a simple stationary bifurcation point of the equation*

$$F(\Psi, \lambda) = 0,$$

where $\Psi \in I\!R^n, \lambda \in I\!R, F : I\!R^n \times I\!R \longrightarrow I\!R^n$ *is sufficiently smooth, if the following conditions hold:*

(1). $F(\Psi_0, \lambda_0) = 0,$

(2). $rank F'_\Psi(\Psi_0, \lambda_0) = n - 1,$

(3). $F'_\lambda(\Psi_0, \lambda_0) \in Range F'_\Psi(\Psi_0, \lambda_0),$

(4). exact two branches of stationary solutions intersect at point (x_0, λ_0) *with two different tangents.*

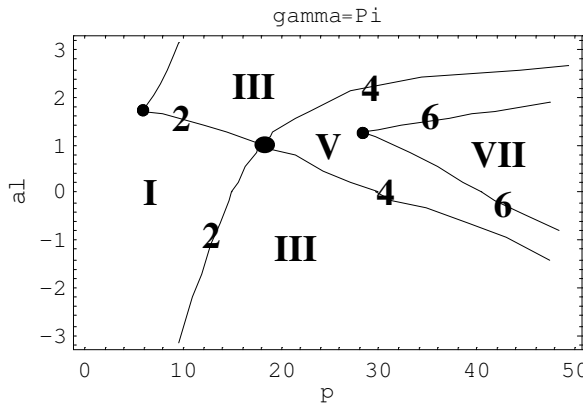Figure 4.14: Partition of $p - \alpha$ plane for $\gamma = 0.75\pi$.

Figure 4.15: Partition of $p - \alpha$ plane for $\gamma = \pi$.

Definition 4.3 *A point of* (Ψ_0, λ_0) *is a turning point of stationary solution of the equation* $F(\Psi, \lambda) = 0$, *where F is the same as in last definition, if the following conditions hold:*
(1).,(2). are the same as in last definition,

(3). $F'_\lambda(\Psi_0, \lambda_0) \notin RangeF'_\Psi(\Psi_0, \lambda_0)$, *or* $rank(F'_\Psi(\Psi_0, \lambda_0)|F'_\lambda(\Psi_0, \lambda_0))$
   $= n$,

(4). *there is a parameterization* $\Psi(\sigma), \lambda(\sigma)$ *with* $\Psi(\sigma_0) = \Psi_0, \lambda(\sigma_0) = \lambda_0$
   and $\frac{d^2\lambda(\sigma_0)}{d\sigma^2} \neq 0$.

For understanding of definition 4.2 we can simply consider $F(\Psi, \lambda) = \Psi^3 - \lambda\Psi$ as an example, here $F : \mathbb{R} \times \mathbb{R} \longrightarrow \mathbb{R}$. $(\Psi_0, \lambda_0) = (0,0)$ satisfies (1), $F'_\Psi(0,0) = 0$, that is $rankF'_\Psi(0,0) = 1 - 1 = 0$. $F'_\lambda(0,0) = 0 \in RangeF'_\Psi(0,0)$, so condition (2) and (3) are satisfied, from the following figure we see (4) is also satisfied. That is a pitchfork bifurcation point is a simple stationary bifurcation point.

For definition 4.3 we consider $F(\Psi, \lambda) = \Psi^2 - \lambda$, conditions (1),(2) are true at $(\Psi_0, \lambda_0) =$

$(0, 0)$. Now $F'_\lambda(0, 0) = -1 \notin RangeF'_\Psi(0, 0) = \{0\}$. If we let $\delta = \Psi, \lambda = \delta^2$, then $\delta = 0$ corresponds to $(0, 0)$, $\frac{d^2\lambda(0)}{d\delta^2} = 2$, so (3), (4) are true, $(0, 0)$ is a turning point for $F(\Psi, \lambda) = \Psi^2 - \lambda$.

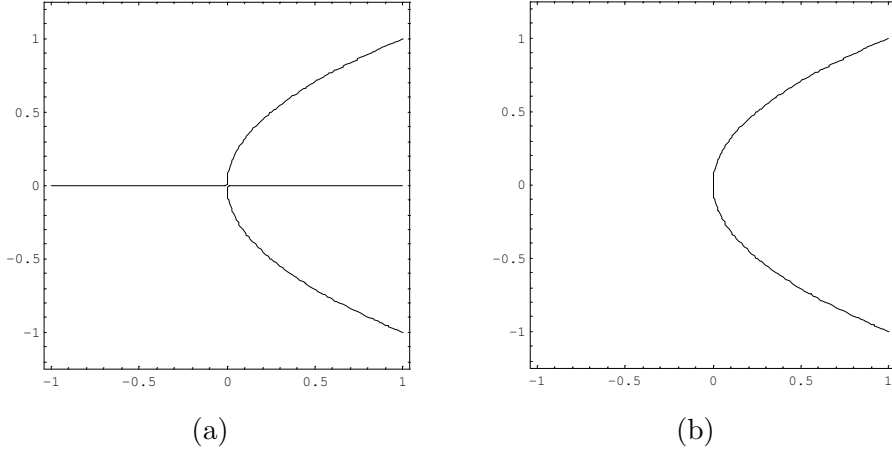We give an explanation to the conditions in these two definitions: For branching point

(a)   (b)

Figure 4.16: The bifurcation diagrams of $\Psi^3 - \lambda\Psi = 0$ (a) and $\Psi^2 - \lambda$ (b).

the preliminaries of (1). and (2). in both definitions are obvious, because at these points the uniqueness of Ψ to λ is invalid. Without loss of generality, let λ be $(n+1)_{st}$ component of Ψ, say $\Psi_{n+1} = \lambda$. Now $F(\Psi, \lambda) =: F(\hat{\Psi}) = 0$ includes n equations with $n+1$ unknowns, $F_i(\Psi_1, \Psi_2, ...\Psi_n, \Psi_{n+1}) = 0, (i = 1, 2, ..., n)$, and

$$\left[\frac{\partial F}{\partial \Psi}, \frac{\partial F}{\partial \lambda}\right] = \left[\frac{\partial F}{\partial \Psi_1}, \frac{\partial F}{\partial \Psi_2}, ..., \frac{\partial F}{\partial \Psi_n}, \frac{\partial F}{\partial \Psi_{n+1}}\right].$$

Now we take one of the $n + 1$ components as a parameter, say $\Psi_k = \varsigma$. Then the rest variables $\Psi_1, \Psi_2, ..., \Psi_{k-1}, \Psi_{k+1}, ..., \Psi_n, \Psi_{n+1}$ depend on ς with a jacobian matrix by moving the k_{th} column from $\left[\frac{\partial F}{\partial \Psi}, \frac{\partial F}{\partial \lambda}\right]$. As long as

$$rank\left[\frac{\partial F}{\partial \Psi}, \frac{\partial F}{\partial \lambda}\right] = n,$$

the existence of such k is guaranteed. Removing the k_{th} column a nonsingular square matrix gives

$$\left[\frac{\partial F}{\partial \check{\Psi}}\right] := \left[\frac{\partial(F_1, F_2, ..., F_n)}{\partial(\Psi_1, ..., \Psi_{k-1}, \Psi_{k+1}, ..., \Psi_{n+1})}\right],$$

where $\check{\Psi} = (\Psi_1, ..., \Psi_{k-1}, \Psi_{k+1}, ..., \Psi_{n+1})^\top$. That means if we take Ψ_k as bifurcation parameter, the branching (turning) point is removed, as the implicit function theorem works

again to $\check{\Psi}$. The geometrical interpretation is: the bifurcation diagram $\Psi\ vs\ \varsigma$ is obtained by rotating the bifurcation diagram $\Psi\ vs\ \lambda$ to 90^0, then the turning point disappears. This situation is reflected in conditions (3). and (4). of definition 4.3. For bifurcation point, we are not able to remove it by rotating the bifurcation diagram to 90^0, or in other words, we could not get a nonsingular matrix by moving a single column from $\left[\frac{\partial F}{\partial\Psi},\frac{\partial F}{\partial\lambda}\right]$. It means there are c_i such that

$$F_\lambda' = \frac{\partial F}{\partial\Psi^{n+1}} = \sum_{i=1}^n c_i\frac{\partial F}{\partial\Psi_i},$$

it means $\frac{\partial F}{\partial\lambda}\in RangeF_\Psi'$. This is the third condition in definition 4.2, the condition (4) is simply from the geometrical consideration. From the explanation of the conditions in the two definitions one can easily see the geometrical difference between turning point and bifurcation point.

Among these four kinds of points, turning point and bifurcation point, especially bifurcation point is frequently given a special consideration, because the character of phase curve of (2.2) and configuration of (2.3) will change qualitatively at these points.

From figure 4.17, we see the end manifold turns as p increases, in this procedure more intersections are born. So in our study on bifurcation, we must take the dependence of the end manifolds on p into account. We first discuss some special cases. As shown in bifurcation diagrams obtained in last section, the situation for $\gamma = 0$ is very special. As the system is symmetric, the bifurcation diagrams for $\alpha = \pi+\triangle\alpha$ and $\alpha = \pi-\triangle\alpha, \triangle\alpha > 0$ are also symmetric. So $\alpha = 0$ and $\alpha = \pi$ are two limit cases.

For $\gamma = 0, \alpha = 0$, the initial manifold is the vertical line $\Psi = \pi$, the target manifold is the Ψ-axis, it is fixed for any $p > 0$. From the phase portrait we know there are two possibilities for orbits of (2.2) to start from $(\pi, 0)$ to reach the target manifold, namely saddle point $(\pi, 0)$ and the lower separatrix from $(\pi, 0)$ to $(-\pi, 0)$. But the transit 'time' along the separatrix is infinity, so for any finite $p > 0$ it is not the phase curve of (2.2). The unique solution is therefore the p-independent saddle point, which corresponds to $\omega_0 = 0$. In bifurcation diagram it is represented by the p-axis (or $\omega_0 = 0$).

For $\gamma = 0, \alpha \neq 0$, the possible phase curves of (2.2) are p-dependent, because the transit time is $\sqrt{p}$, different p will correspond to different phase curves. Or in other words, different p correspond to different ω_0. From the bifurcation diagrams we know $\gamma = 0, \alpha = 0$ is the only case exhibiting one $p-$independent equilibrium.

Now we discuss the case of $\gamma = 0, \alpha = \pi$, the initial manifold and target manifold are Ψ'- and Ψ- axis respectively. Obviously $(0, 0)$ is a solution of (2.2) for any $p > 0$. The end manifold is symmetric to $(0, 0)$, and it intersects with Ψ- axis transversally from the third
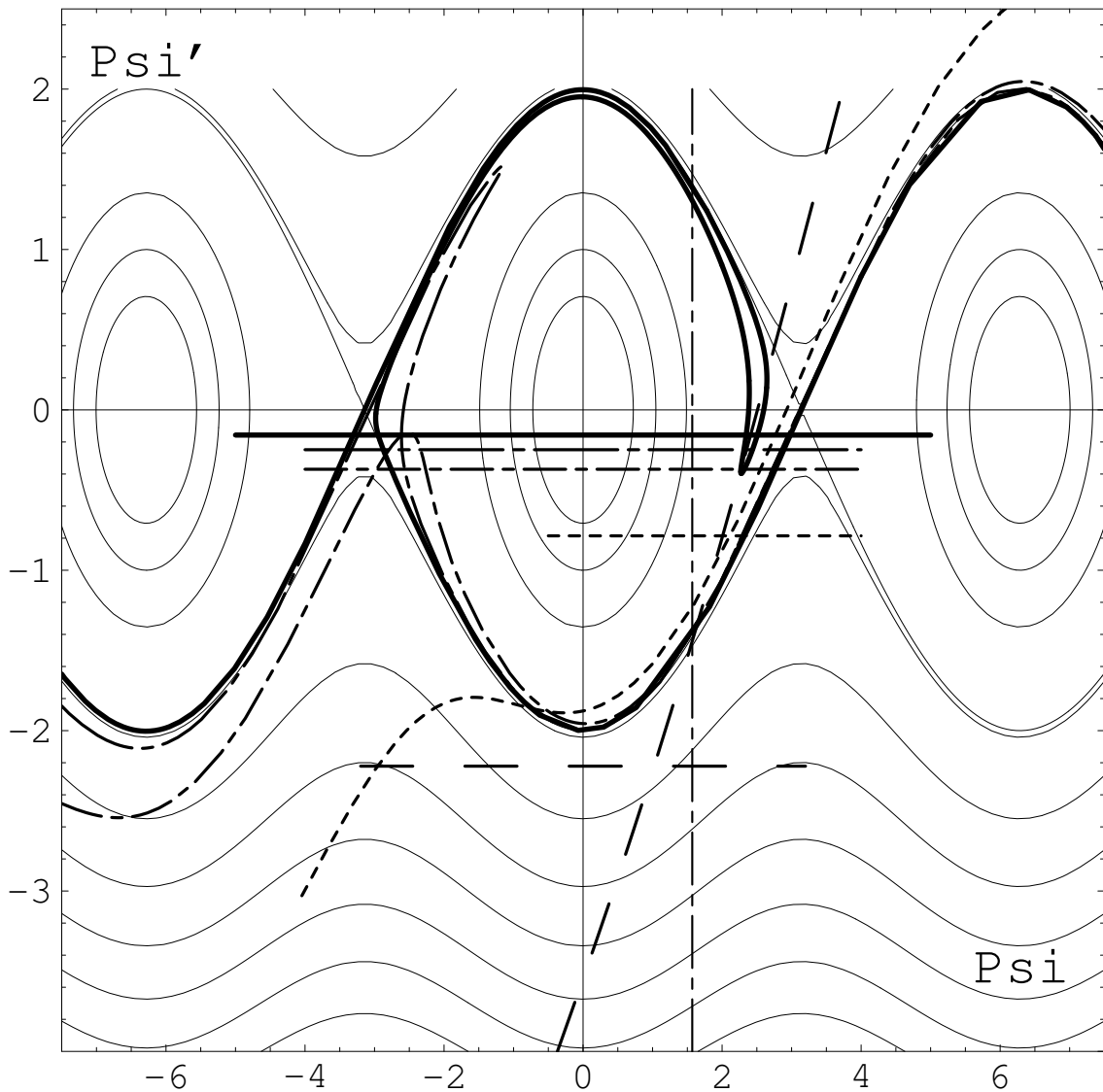
Figure 4.17: A sample phase portrait of (2.2) with the initial manifold (vertical dash-dotted line), five different end manifolds (thick curves) corresponding to $p = 0.5, p = 4, p = 18, p = 40, p = 100$ respectively, the end manifolds listed upwards for increasing p are drawn in the same sort of lines as the target manifolds.

quadrant to the first quadrant if p is small. If for big p (2.2) has solutions other than $(0,0)$, then the corresponding ω_0 must be born in pairs, one is positive and another is negative, they have the same absolute value. The new ω_0 are born in the following manner: for small p the end manifold intersects with the Ψ-axis transversally from the third quadrant to the first quadrant, as p increases, the end manifold approaches a situation that the manifold intersects with the Ψ- axis at $(0,0)$ with its tangent parallel to the Ψ-axis. As p increase further, the end manifold intersects the Ψ-axis transversally again, but from the second quadrant to the fourth quadrant, as other parts of the end manifold are still in the third and the first quadrant, then two more intersections are produced form $(0,0)$. So for this case we have the conclusion: when $\gamma = 0, \alpha = \pi$, (2.2) has an odd number of solutions, the singular points of its bifurcation diagrams are all pitchforks. All new curves in bifurcation diagram are first bifurcated from pitchfork, so these pitchforks together with the curves passing them form a cluster of curves opening to the right and no secondary bifurcation. Now we try to explain that it is the only case for $\alpha = \pi$ that the bifurcation diagram has only pitchforks as its singular points when $\gamma = 0$ is fixed. When $\alpha \neq \pi$, the initial manifold is $\pi - \alpha$ and the target manifold is still the Ψ-axis, without loss of generality, we take $0 < \alpha < \pi$. All possible phase curves of (2.2) lie in the zone bounded by the separatrix. For small p, the end manifold intersects with the Ψ-axis once transversally, the intersection point corresponds to a positive ω_0. This kind of intersection will exist for any $p > 0$, as at this kind of point the end manifold intersects the Ψ-axis transversally, there will be no new intersections born from these points. In bifurcation diagram the corresponding $\omega_0's$ lie on a curve. When p increases further, new intersections may be produced, but they could only be produced in the following way: As p increases, the end manifold approaches to a situation gradually for $p = p_1$, in which the end manifold meets the $\Psi-$ axis from below with its 'nose', one new phase curve is produced, now there are two intersections altogether. When $p > p_1$, this new intersection splits into two, now there are three intersections, so p_1 corresponds to a turning point in the bifurcation diagram. If p increases further, the new intersection will be produced in the same way as discussed above. We show this procedure by figure 4.18. Therefore the bifurcation diagrams for $\gamma = 0$ and different α have only turning points as their singular points.

As $\gamma = 0, \alpha = \pi$ is a special case and has the above character. We intend to discuss the bifurcation diagrams for $(\gamma, \alpha) \neq (0, \pi)$, but (γ, α) is near to $(0, \pi)$. As the case $\gamma = 0, \alpha \neq \pi$ is already discussed above, we now discuss the case $\gamma \neq 0, \alpha = \pi$. The initial manifold is now $\Psi = \gamma$, the target manifold is $\Phi = -\frac{2\gamma}{\sqrt{p}}$. When p is very small, the target manifold lies below the lower part of the separatrix, the end manifold will intersect the target manifold
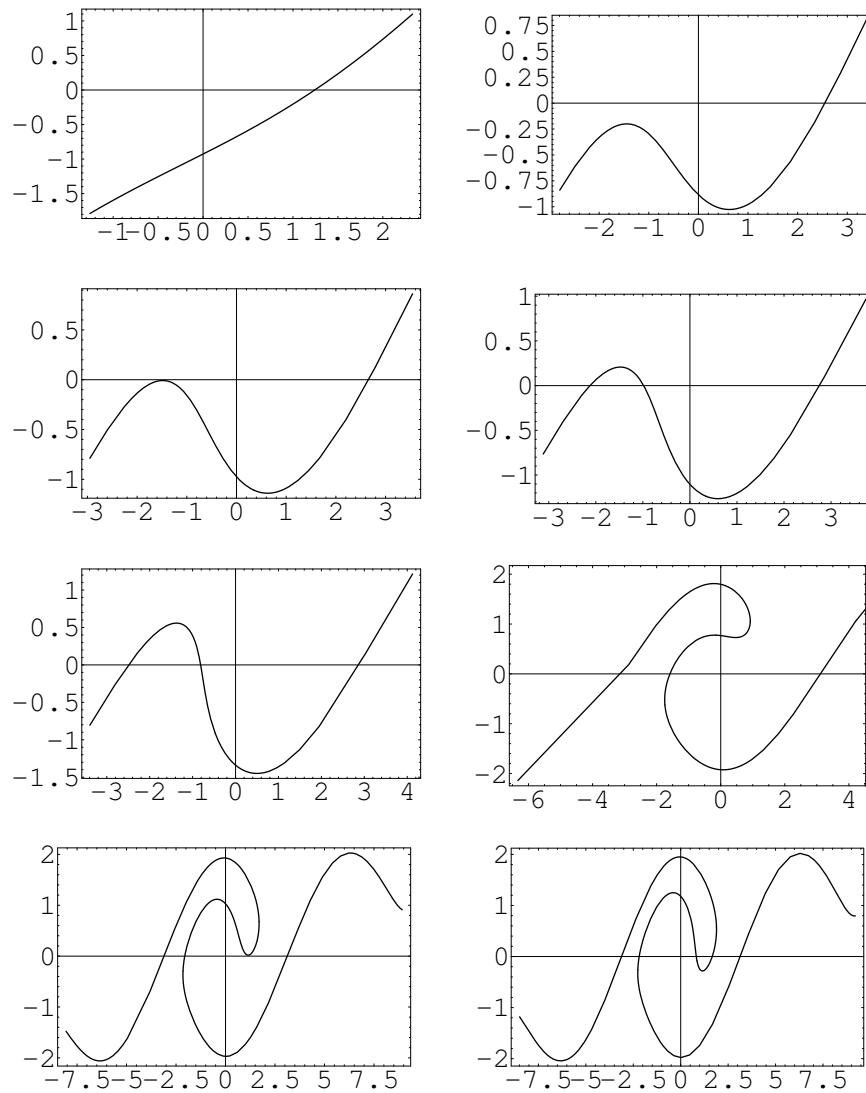
Figure 4.18: The end manifolds for $\gamma = 0, \alpha \neq \pi$ with increasing p along (1,1)-(1,2)-(2,1)-(2,2)-(3,1)-(3,2)-(4,1)-(4,2).
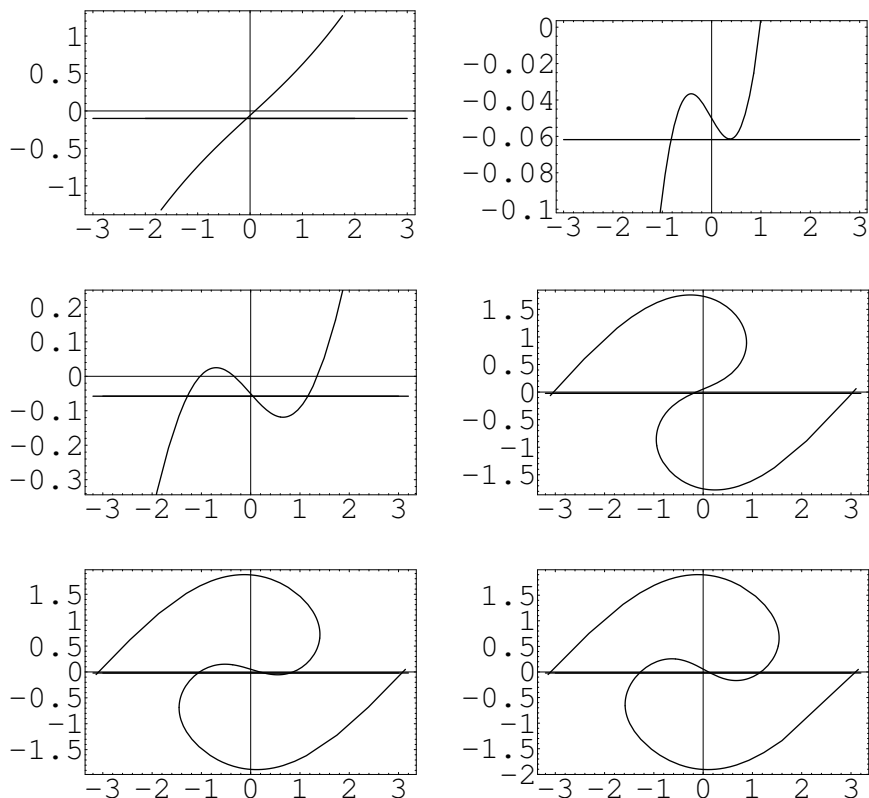
Figure 4.19: The end manifolds for very small γ and $\alpha = \pi$ with increasing p along (1,1)-(1,2)-(2,1)-(2,2)-(3,1)-(3,2).

transversally, and the corresponding $\omega_0 < 0$. This kind of intersection will always exist for $p > 0$, the corresponding $\omega_0' s$ lie on a curve below the p-axis in $p\omega_0$-plan. When p grows, the target manifold moves upwards. After $p = \frac{\gamma^2}{\cos^2(\gamma/2)}$, part of the target manifold lies above the lower part of the separatrix and it is possible for an orbit to start from a point on part of the initial manifold lying in the zone bounded by the separatrix to reach the target manifold and to produce new intersection. But as the discussion given before, a new intersection is born first at the moment when the end manifold meets the target manifold and is parallel to it, then this new intersection splits into two, that is, the corresponding new $\omega_0' s$ can be produced only from turning points.(see figure 4.19). The bifurcation diagram has therefore only turning points as its singular points.

With the detailed discussion on the end manifold, we can distinguish the difference be-

tween the bifurcation diagrams for $\gamma = 0, \alpha$ is close to π and for $\alpha = \pi, \gamma$ is close to 0. The turning points for $\gamma = 0, \alpha \neq 0$ and the curves passing these points form a cluster with the character that the curve passing the turning point corresponding to bigger p lies in the area bounded by the curve passing the turning points corresponding to smaller p. While for $\alpha = \pi$, γ near zero the turning points and the curves passing these them are divided into two groups, one group consists of the first turning point and the curve passing it. The others form a cluster like the one in the last case. We demonstrate this result by the following two examples.

Example 1: $\gamma = 0, \alpha = 0.9\pi$.

In this case, if p is small, the end manifold has one intersection with Ψ- axis (see figure 4.20), the only ω_0 is denoted by ω_0^1.
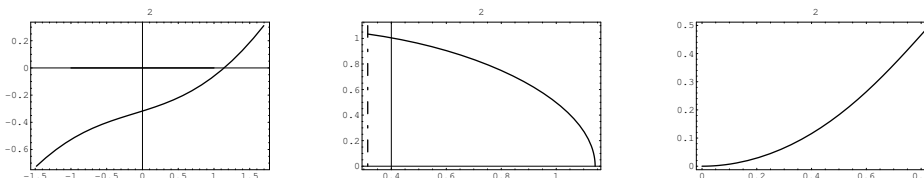
Figure 4.20: The end manifold (left), phase curves (middle) of equation(2.2) and configurations of (2.3) for $\gamma = 0, \alpha = 0.9\pi$ and $p = 2$.

As p increases, 'noses' are formed to the left of the first intersection below the Ψ-axis, they turn clockwise when p increases, at a certain value p_2 of p, one of them meets the Ψ-axis from below (see figure 4.21) with $\omega_0 = \omega_0^2$, then it splits into two, so ω_0^2 corresponds to a turning point.
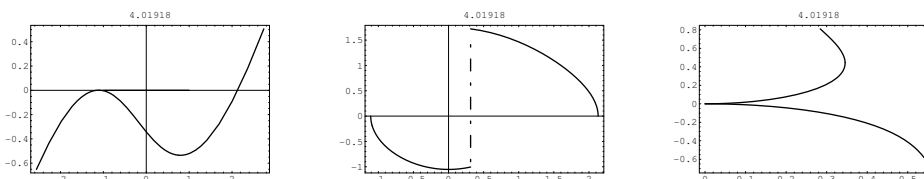

Figure 4.21: The end manifold (left), phase curves (middle) of equation(2.2) and configurations of (2.3) for $\gamma = 0, \alpha = 0.9\pi$ and $p = 4.01918$.

The two new values of ω_0, denoted by $\omega_0^{2,1} < \omega_0^{2,2}$, are both less than ω_0^1. As p increases from p_2, the 'nose' turns further (see figure 4.22) and then meets the Ψ-axis again from above for some $p = p_3$ (see figure 4.23), the corresponding ω_0^3 lies between $\omega_0^{2,1}$ and $\omega_0^{2,2}$.

As p increases from $p = p_3$, the intersection corresponding to p_3 splits into two, which correspond to two values $\omega_0^{3,1} < \omega_0^{3,2}$, so ω_0^3 corresponds also to a turning point, which locates in the area bounded by the bifurcation curve passing the first turning point.
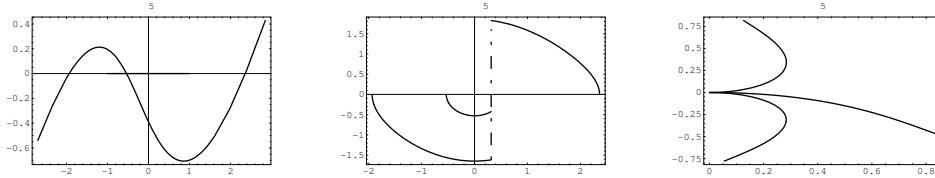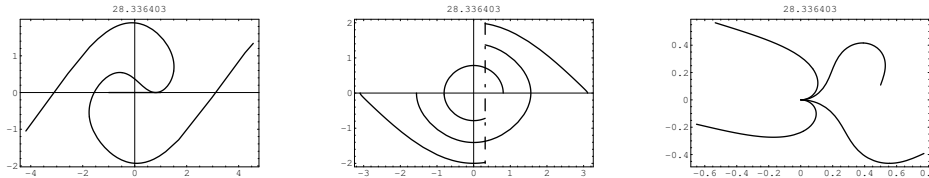

Figure 4.22: The end manifold (left), phase curves (middle) of equation(2.2) and configurations of (2.3) for $\gamma = 0, \alpha = 0.9\pi$ and $p = 5$.

Figure 4.23: The end manifold (left), phase curves (middle) of equation(2.2) and configurations of (2.3) for $\gamma = 0, \alpha = 0.9\pi$ and $p = 28.336403$.
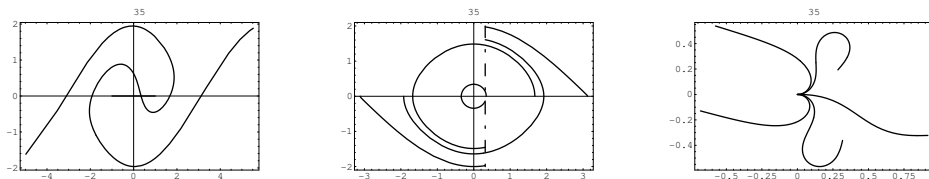

Figure 4.24: The end manifold (left), phase curves (middle) of equation(2.2) and configurations of (2.3) for $\gamma = 0, \alpha = 0.9\pi$ and $p = 35$.

Following this procedure we get the conclusion: equation (2.2) for $\gamma = 0, \alpha = 0.9\pi$ can have any number of tuning points with $p \in [0, p_e]$, provided p_e is sufficiently large. The curves passing these turning points do not meet and their positions follow the following role: the bifurcation curve passing the turning point corresponding to p_i lies in the area bounded by the bifurcation curve passing turning point corresponding to $p_{i-1}, (p_i > p_{i-1})$.
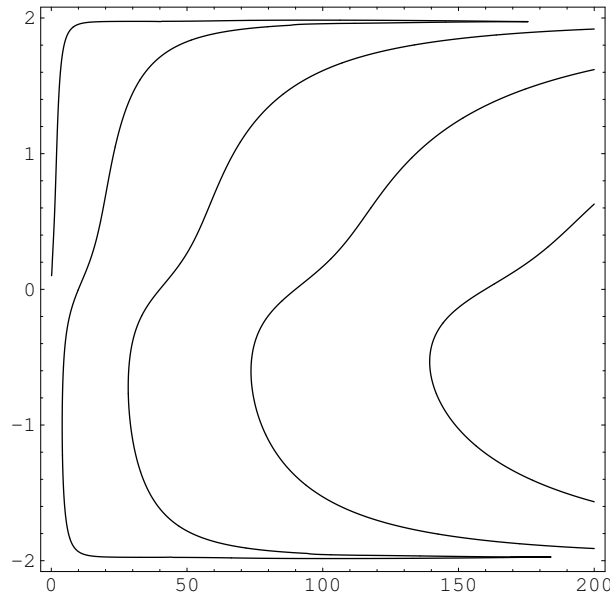
Figure 4.25: Bifurcation diagram of (2.2) for $\gamma = 0, \alpha = 0.9\pi$.

So the bifurcation diagram for $\gamma = 0, \alpha = 0.9\pi$ has the form as shown in figure 4.25.

Example 2: $\gamma = 0.1, \alpha = \pi$. In this case, for small p, the end manifold intersects with the horizontal line $\Psi' = -\frac{2\gamma}{\sqrt{p}}$ only once (see figure 4.26), the corresponding values of p and ω_0 are denoted by p_1 and ω_0^1. As p increases, 'noses' are formed above the horizontal
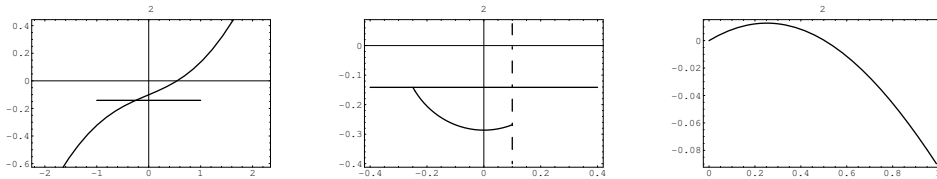

Figure 4.26: The end manifold (left), phase curve (middle) of equation(2.2) and configuration of (2.3) for $\gamma = 0.1, \alpha = \pi$ and $p = 2$.

line right to the first intersection and they turn clockwise as p increases and one of them meets the horizontal line to the right of the first intersection from above for some certain p_2 (see figure 4.27), the corresponding value of ω_0 is denoted by ω_0^2. As p increases from p_2, the 'nose' turns and the intersection splits into two, the corresponding values of ω_0 are denoted by $\omega_0^{2,1} < \omega_0^{2,2}$, they are both greater than ω_0^1, then ω_0^2 corresponds to a turning point (see figure 4.28).
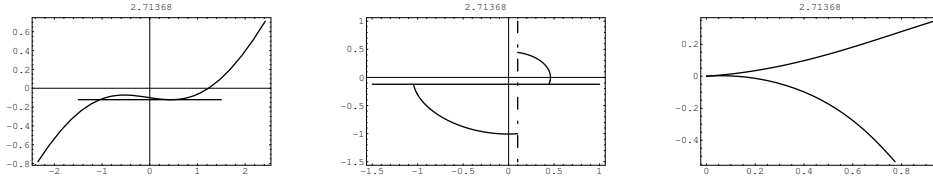
Figure 4.27: The end manifold (left), phase curves (middle) of equation(2.2) and configurations of (2.3) for $\gamma = 0.1, \alpha = \pi$ and $p = 2.71368$.
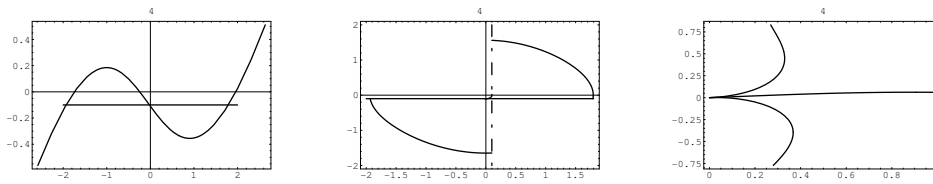

Figure 4.28: The end manifold (left), phase curves (middle) of equation(2.2) and configurations of (2.3) for $\gamma = 0.1, \alpha = \pi$ and $p = 4$.

As p increases further, another 'nose' meets the horizontal line from above for some p_3, the corresponding ω_0^3 satisfies $\omega_0^1 < \omega_0^3 < \omega_0^{2,1}$ (see figure 4.29). When $p > p_3$, the intersection
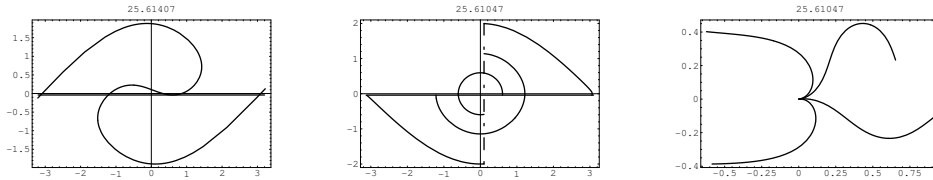

Figure 4.29: The end manifold (left), phase curves (middle) of equation(2.2) and configurations of (2.3) for $\gamma = 0.1, \alpha = \pi$ and $p = 25.61047$.

splits into two, the corresponding $\omega_0^{3,1}, \omega_0^{3,2}$ satisfy

$$\omega_0^1 < \omega_0^{3,1} < \omega_0^{3,2} < \omega_0^{2,1},$$

so ω_0^3 corresponds to a turning point, but this turning point lies outside of the area bounded by the bifurcation curve passing the first turning point. When p continues to increase, the end manifold meets the horizontal line for the fourth time for some $p = p_4$. Denoting the corresponding value of ω_0 with ω_0^4, then we have:

$$\omega_0^1 < \omega_0^{3,1} < \omega_0^4 < \omega_0^{3,2} < \omega_0^{2,1},$$
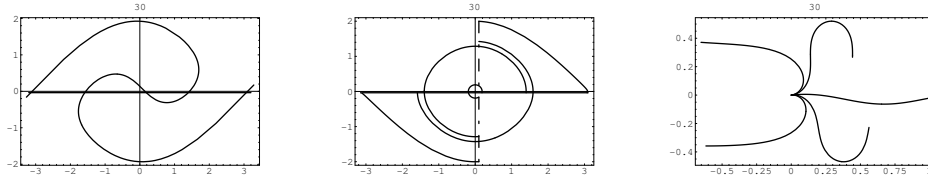
Figure 4.30: The end manifold (left), phase curves (middle) of equation(2.2) and configurations of (2.3) for $\gamma = 0.1, \alpha = \pi$ and $p = 30$.
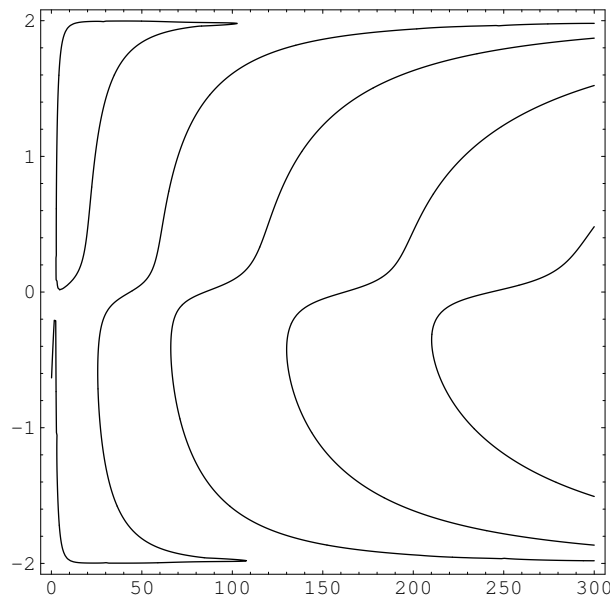

Figure 4.31: Bifurcation diagram of (2.2) for $\gamma = 0.1, \alpha = \pi$.

when $p > p_4$, the intersection splits into two, so ω_0^4 corresponds to a turning point. Denoting the corresponding values of ω_0 by $\omega_0^{4,1}, \omega_0^{4,2}$, then we have

$$\omega_0^1 < \omega_0^{3,1} < \omega_0^{4,1} < \omega_0^{4,2} < \omega_0^{3,2} < \omega_0^{2,1},$$

that means the turning point corresponding to ω_0^4 is located in the area bounded by the bifurcation curve passing the second turning point. After the second turning point, the turning point for p_i is located in the area bounded by the bifurcation curve passing the turning point for p_{i-1} ($i = 4, 5, 6...$). So the bifurcation diagram for $\gamma = 0.1, \alpha = \pi$ is as shown in figure 4.31. From the discussion of the two cases, we see, if γ, α is slightly different from $0, \pi$, the corresponding singular points of the bifurcation diagrams are only turning points. In detail, the curves passing these turning points of (2.2) for $\gamma = 0, \alpha = \pi - \triangle\alpha(\triangle\alpha$ is very small) are in one group, opening to the right, the bifurcation curve which crosses
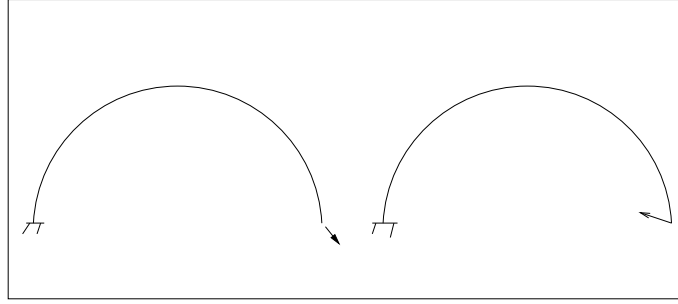
Figure 4.32: The undeformed arcs with $\gamma = 0.5\pi, \alpha = -0.289521\pi$ (left) and 0.84978675π (right).

the turning point corresponding to larger p is located in the area bounded by the curves which cross the turning points corresponding to smaller p. While the curves passing the turning points for $\gamma = \triangle\gamma(\triangle\gamma > 0$ is very small) and $\alpha = \pi$ consists of two groups, one group consists only one curve passing a turning point, the another group consists of the all other curves passing the other turning points and it has the same character as the group for $\gamma = 0, \alpha = \pi - \triangle\alpha$.

For the discussion of bifurcation points which belong to the system for γ, α are far from $0, \pi$, we take $\gamma = \frac{\pi}{2}$ for example. The bifurcation diagrams show obviously there are two bifurcation points, their numerical coordinates (α, p) are $(-0.289521\pi,$
23.394$) := (\alpha_{b1}, p_{b1})$ and $(0.84978675\pi, 3.335735) := (\alpha_{b2}, p_{b2})$ respectively. The undeformed arcs for these two values of α are sketched in 4.32. The manifolds, phase curves and configurations for values of α and p lie near (α_{b1}, p_{b1}) are illustrated in figure 4.33 $(\alpha = \alpha_{b1})$.

When the values of α and p lie near (α_{b2}, p_{b2}), the corresponding diagrams are shown in figure 4.34 $(\alpha = \alpha_{b2})$.

In figure 4.33 we can see that, if $|p - p_{b1}|$ is very small and $p \leq p_{b1}$, the corresponding system (2) has three phase curves, when $|p - p_{b1}|$ is very small and $p > p_{b1}$, system (2) has 5 phase curves, that is, when p passes through p_{b1} two extra phase curves (also configurations) appear near the one which corresponds to the bifurcation point. Bifurcation point (α_{b1}, p_{b1}) is of pitchfork type (see [91]). With the same discussion for (α_{b2}, p_{b2}) and referring to figure 4.34, we see that, when p is near and less than p_{b2}, system (2) has three phase curves, the two lower ones become closer and closer to each other in the course of p approaching to p_{b2} and coincide into one when $p = p_{b2}$, which splits into two again when p increases further. It means that when p passes through p_{b2} one phase curve (also configuration) disappears. Point (α_{b2}, p_{b2}) is of x-type. This is the qualitative difference
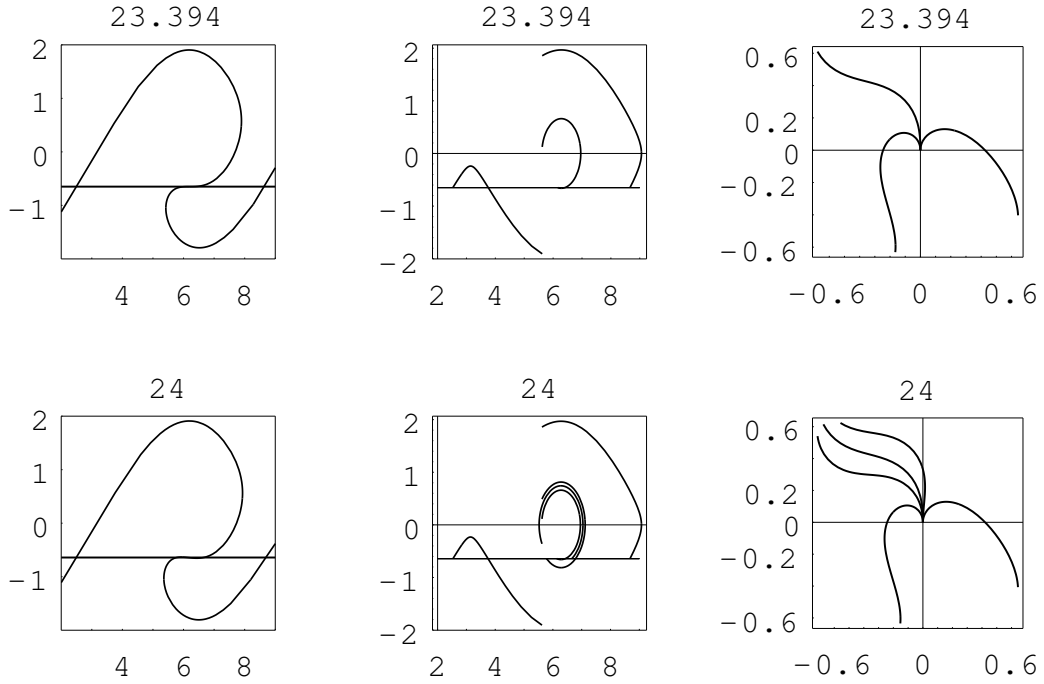
Figure 4.33: Final manifolds, phase curves and configurations for $\gamma = 0.5\pi, \alpha = -0.289521\pi, p$ takes two different values standing above the diagrams.

of the two bifurcation points.

From the bifurcation diagrams we see: for each fixed $\gamma > 0$ and $\alpha \in [-0.5\pi, 1.5\pi), p \in [0, 50]$, there are two bifurcation points, one is of pitch-fork form and the other of X form. $\gamma = 0$ is a special case, the two bifurcation points are both of pitch-fork form and we take $\gamma = 0$ as a reference, because the $p-\omega_0$ relation diagrams are symmetrical about $\alpha = \pi$ and the two bifurcations correspond to same value of α. The bifurcation points change with γ and α as follows: The left bifurcation point for $\gamma = 0, \alpha = \pi$ becomes X-form for $\gamma > 0$ and the corresponding α decreases from π when γ changes from 0 to π. While the right bifurcation for $\gamma = 0, \alpha = \pi$ keeps pitch-fork type for $\gamma > 0$ and the corresponding α varies from π through 1.5π(the corresponding system (2.2) is identical to that for $\alpha = -0.5\pi$), 0 to 0.5π.
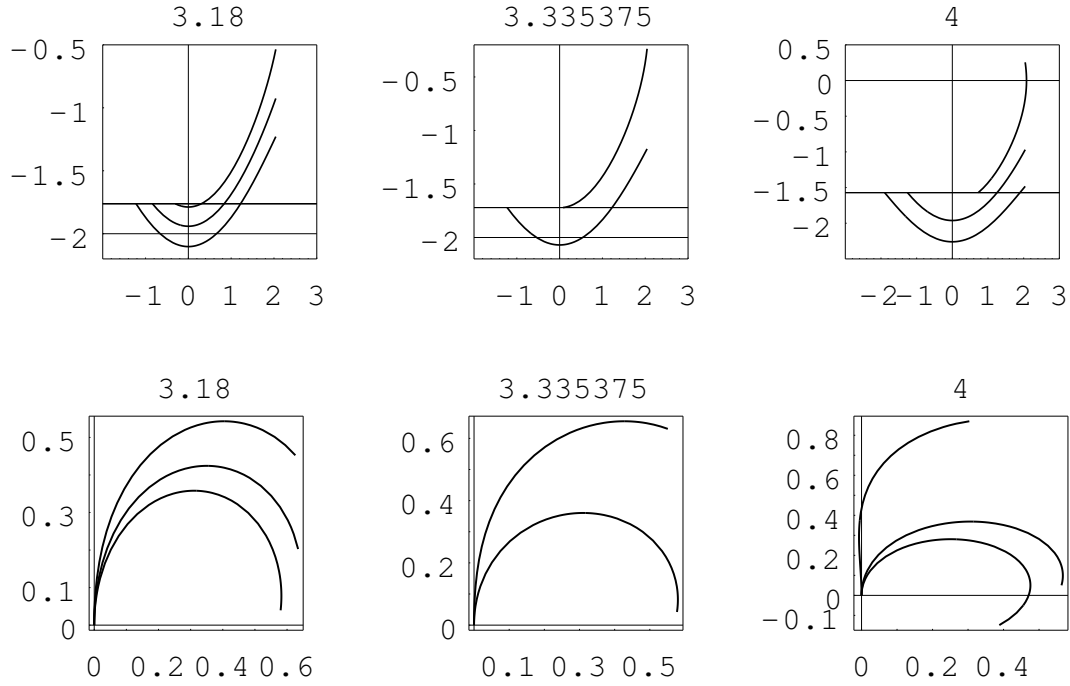
Figure 4.34: Phase curves and configurations for $\gamma = 0.5\pi, \alpha = 0.84978675\pi, p$ takes three different values standing above the diagrams.

4.3 Theoretical study of system 2.2 for $\gamma = \frac{\pi}{2}$ and $\alpha = \pm\frac{\pi}{2}$

In order to give a theoretical description to the method used in investigation of bifurcation diagram of system (2.2) and compare the result obtained, we take $\gamma = \frac{\pi}{2}$, $\alpha = \pm\frac{\pi}{2}$ for example, which correspond to the deformation of the half ring under the force acting vertically at its free end.

4.3.1 Phase curve discussion of (2.2) for $\alpha = \frac{\pi}{2}$

From system (2.2), when $\gamma = \alpha = \frac{\pi}{2}$, the corresponding system (2.2) is :

$$\Psi'' = -\sin\Psi, \Psi(0) = \pi, \Psi'(\sqrt{p}) = -\frac{\pi}{\sqrt{p}}.$$

and the energy integral is now
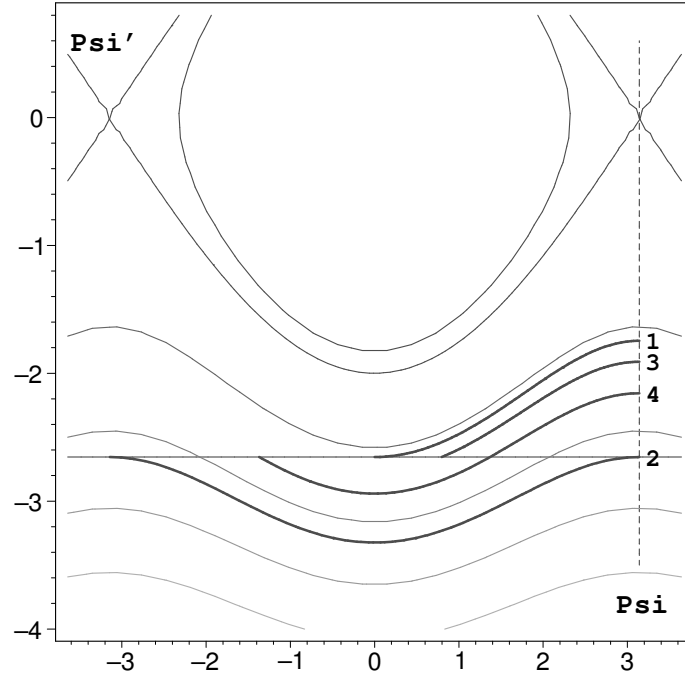
$$\Psi'^2 = \omega_0^2 - 4\cos^2\frac{\Psi}{2}.$$

Figure 4.35: Possible phase curves of (2.2) for $\gamma = \frac{\pi}{2}$, $\alpha = \frac{\pi}{2}$.

As the phase curve (or trajectory) starting at (π, ω_0) could not meet the separatrix (except the separatrix itself), all possible phase curves lie below the separatrix, that is, all possible $\omega_0's$ are negative. We show the case in figure 4.35, in this figure the phase curves numbered with 1, 2, 3, 4 are chosen in the following way: phase curve 1 starts from a point above the horizontal line $\Psi' = -\frac{\pi}{\sqrt{p}}$, it is parallel to the horizontal line at its end point, that means it is not possible for the phase curves above it to meet the horizontal line. The phase curve 2 is parallel to the horizontal line at both its start and end points, so the phase curves below it have no chance to meet the horizontal line. Therefore beside phase curves 1, 2, the other possible phase curves must lie between these two phase curves, or the start points of other possible phase curves must be located between the start points of 1 and 2 on the vertical line $\Psi = \pi$. Phase curves 3, 4 in figure 4.35 are representatives of the possible phase curves with 3 meets the horizontal line once and 4 meets it twice.
Let
$$\Psi'(\sqrt{p}) = -\frac{\pi}{\sqrt{p}} = \omega_1,$$
the possible ω_0 satisfies
$$\omega_1 \leq \omega_0 \leq \bar{\omega}_0,$$

here $(\pi, \bar{\omega}_0)$ is the start point of the phase curve which ends at $(0, \omega_1)$. So

$$\omega_1^2 = \bar{\omega_0}^2 + 4$$

and therefore

$$-\frac{\pi}{\sqrt{p}} \leq \omega_0 \leq -\sqrt{\frac{\pi^2}{p} - 4}.$$

For trajectory 1 in figure 4.35, let

$$k = \frac{2}{\sqrt{\omega_0^2 + 4}}, u = \frac{\Psi}{2},$$

then

$$u' = -\frac{1}{k}\sqrt{1 - k^2 \sin^2 u}, u(0) = \frac{\pi}{2}, u'(\sqrt{p}) = -\frac{\pi}{2\sqrt{p}}$$

and

$$t = -k \int_{\frac{\pi}{2}}^{u(t)} \frac{du}{\sqrt{1 - k^2 \sin^2 u}}.$$

The transit 'time' along trajectory 1 $T_1 = \sqrt{p}$ is equivalent to

$$\sqrt{p} = k \int_0^{\frac{\pi}{2}} \frac{du}{\sqrt{1 - k^2 \sin^2 u}} = kK(k^2).$$

$\bar{\omega}_0 = \sqrt{\frac{\pi^2}{p} - 4}$ gives $k = \frac{2\sqrt{p}}{\pi}$, thus

$$K(k^2)) = \frac{\pi}{2}.$$

But

$$K(k^2) = \int_0^{\frac{\pi}{2}} \frac{du}{\sqrt{1 - k^2 \sin^2 u}} > \int_0^{\frac{\pi}{2}} du = \frac{\pi}{2}.$$

This means trajectory 1 does not exit.

Along trajectory 2,

$$\omega_0 = \omega_1 = -\frac{\pi}{\sqrt{p}}, u(0) = \frac{\pi}{2}, u(\sqrt{p}) = -\frac{\pi}{2},$$

so the implicit expression of the trajectory is

$$t = -k \int_{\frac{\pi}{2}}^{u(t)} \frac{du}{\sqrt{1 - k^2 \sin^2 u}}.$$

The transit 'time' along it $T_2 = \sqrt{p}$ is equivalent to

$$2kK(k^2) = \sqrt{p},$$

where

$$k = \frac{2}{\sqrt{\omega_0^2 + 4}} = \frac{2}{\sqrt{\omega_1^2 + 4}} = \frac{2\sqrt{p}}{\sqrt{4p + \pi^2}}.$$

The above equation can be satisfied for relatively large p, it implies that trajectory 2 exists for some p.

Along trajectory 3 we have

$$-k \int_{\frac{\pi}{2}}^{u_3} \frac{du}{\sqrt{1 - k^2 \sin^2 u}} = \sqrt{p} = k(K(k^2) - F(u_3, k^2)).$$

and

$$\frac{\pi^2}{4p} = \frac{1}{k^2}(1 - k^2 \sin^2 u_3).$$

From the above two equations we get

$$K(k^2) - F(u_3, k^2) = \frac{\pi}{2\sqrt{1 - k^2 \sin^2 u_3}},$$

or

$$\int_{u_3}^{\frac{\pi}{2}} \frac{\sqrt{1 - k^2 \sin^2 u_3}}{\sqrt{1 - k^2 \sin^2 u}} du = \frac{\pi}{2},$$

the equality is true for some $0 < u_3 < \frac{\pi}{2}$. So trajectory 3 always exists.

With the same consideration, for trajectory 4 we have

$$\sqrt{1 - k^2 \sin^2 u_4} K(k^2) + \int_0^{u_4} \frac{\sqrt{1 - k^2 \sin^2 u_4}}{\sqrt{1 - k^2 \sin^2 u}} du = \frac{\pi}{2}.$$

Because the left side of the above expression is greater than $\frac{\pi}{2}$ when $u_4 = 0$, and when $u_4 = \frac{\pi}{2}$, it is equal to

$$2\sqrt{1 - k^2} K(k^2) = \frac{2|\omega_0|}{\sqrt{\omega_0^2 + 4}} K(k^2),$$

while ω_0 can be very small when p is sufficiently big, so the left side of the discussed expression may be smaller than $\frac{\pi}{2}$, that means, the discussed equation can be satisfied for some relative big p or in other words, trajectory 4 can exist. Following the discussion for trajectory (4), we can imagine that for even bigger p, there could be more solutions other than these three.

The discussion result on the phase curves of (2.2) and further configurations of (2.3) for $\gamma = \alpha = 0.5\pi, p = 25.2691$ are shown in figure 4.36.

Recalling the bifurcation diagram for $\gamma = \alpha = \frac{\pi}{2}$ in last section, we see, the theoretical and numerical results are exactly identical.
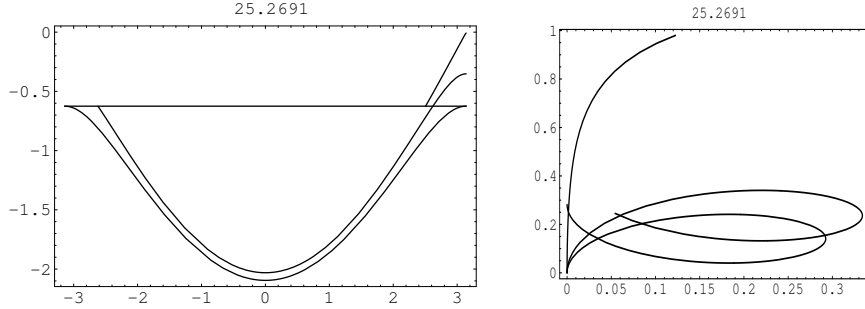
Figure 4.36: The phase curves of (2.2) (left) and configurations of (2.3) for $\gamma = \alpha = 0.5\pi$ and $p = 25.2691$. The aspect ratio of this figure is not 1.

4.3.2   Phase curve discussion of (2.2) for $\alpha = -\frac{\pi}{2}$

When $\alpha = -\frac{\pi}{2}$, the energy integral in section 3 is now the following expression with the corresponding boundary conditions:

$$\Psi'^2 = \omega_0^2 + 2(\cos\Psi - 1) = \omega_0^2 - 4\sin^2\frac{\Psi}{2},$$
$$\Psi(0) = 2\pi, \Psi'(\sqrt{p}) = -\frac{\pi}{\sqrt{p}} := \omega_1. \tag{4.2}$$

As the separatrix corresponds to $\omega_0 = \pm 2$, and $\omega_1 = -2$ implies $p = \frac{\pi^2}{4}$, we discuss the phase curves of system (4.2) in three cases.

Case I. $p < \frac{\pi^2}{4}$. We have $\omega_1 < -2$. In this case, the principal phase curves are shown in figure 4.37, in this figure the phase curves are so chosen as for $\alpha = \frac{\pi}{2}$.
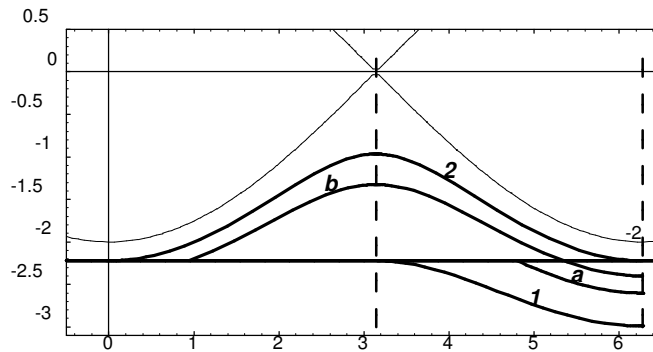

Figure 4.37: Possible phase curves of (2) for $\gamma = \frac{\pi}{2}$, $\alpha = -\frac{\pi}{2}$ and $p < \frac{\pi^2}{4}$.

From this figure, we see several possibilities for the phase curves starting at $(2\pi, \omega_0)$ on the

vertical line $\Psi = 2\pi$, the end points of which lie on the horizontal straight line $\Psi' = -\frac{\pi}{\sqrt{p}}$. Our aim is to determine which possibility can come true. It is necessary that the possible ω_0 satisfy the inequality:

$$\underline{\omega_0} \leq \omega_0 \leq \omega_1$$

where $\underline{\omega_0}$ corresponds to the final point (π, ω_1): $\omega_1^2 = \underline{\omega_0}^2 - 4$. Therefore

$$-2\sqrt{1 + \frac{\pi^2}{4p}} \leq \omega_0 \leq -\frac{\pi}{\sqrt{p}}.$$

Below the separatrix

$$\omega_0^2 > 4, k = \frac{2}{|\omega_0|},$$

let $u := \frac{\Psi}{2}$, then system (4.2) is now

$$u' = -\frac{1}{k}\sqrt{1 - k^2 \sin^2 u}, \quad u(0) = \pi, \quad u'(\sqrt{p}) = -\frac{\pi}{2\sqrt{p}}. \qquad (4.3)$$

Along trajectory 1, $\omega_0 = \underline{\omega_0}$, the transit 'time' is

$$
\begin{aligned}
T_1 \quad &= \quad -k(p) \int_\pi^{\frac{\pi}{2}} \frac{1}{\sqrt{1 - k^2 \sin^2 u}} du \\
&\overset{u := \pi - v}{=} \quad k(p) \int_0^{\frac{\pi}{2}} \frac{1}{\sqrt{1 - k^2 \sin^2 v}} dv \\
&= \quad k(p) K(k^2(p)),
\end{aligned}
$$

where

$$K(k^2) := \int_0^{\frac{\pi}{2}} \frac{1}{\sqrt{1 - k^2 \sin^2 u}} du$$

and

$$k(p) = \frac{1}{\sqrt{1 + \pi^2/4p}}$$

or

$$p = \frac{\pi^2 k^2}{4(1 - k^2)}.$$

If trajectory 1 exist, then

$$T_1(p) = \sqrt{p}$$

or

$$\sqrt{1 - k^2} K(k^2) = \frac{\pi}{2}. \qquad (4.4)$$

Since

$$\frac{\pi}{2} < K(k^2) < \frac{\pi}{2} \frac{1}{\sqrt{1 - k^2}}, (k \neq 0)$$

(4.4) can not be true, *i.e.*, trajectory 1 does not exist.

Along trajectory 2, with

$$k = \frac{2}{|\omega_1|}, \omega_0 = \omega_1,$$

$$T_2(p) = -k \int_\pi^0 \frac{1}{\sqrt{1 - k^2 \sin^2 u}} du = 2kK(k^2) = \sqrt{p}$$

is equivalent to

$$K(k^2) = \frac{\pi}{4},$$

which is not true owing to $K(k^2) > \frac{\pi}{2}$. So trajectory 2 does not exist either. Thus, all possible phase curves lie between trajectories 1 and 2, or the corresponding possible ω_0 satisfy

$$\underline{\omega_0} < \omega_0 < \omega_1.$$

For trajectory a in figure 4.37,

$$T_a = -k \int_\pi^{u_1} \frac{1}{\sqrt{1 - k^2 \sin^2 u}} du$$

with

$$\frac{\pi^2}{4p} = \frac{1}{k^2}(1 - k^2 \sin^2 u_1).$$

For trajectory b

$$\begin{aligned}
T_b &= -k \int_\pi^{u_2} \frac{1}{\sqrt{1 - k^2 \sin^2 u}} du \\
&= k \int_0^\pi \frac{1}{\sqrt{1 - k^2 \sin^2 u}} du - T_a \\
&= 2kK(k^2) - T_a.
\end{aligned}$$

From figure 4.37 we know,

$$T_a = k \int_0^{u_2} \frac{1}{\sqrt{1 - k^2 \sin^2 u}} du = kF(u_2, k^2).$$

$T_a = \sqrt{p}$ means

$$F(u_2, k^2) = \frac{\pi}{2} \frac{1}{\sqrt{1 - k^2 \sin^2 u_2}}$$

or

$$\int_0^{u_2} \frac{\sqrt{1 - k^2 \sin^2 u_2}}{\sqrt{1 - k^2 \sin^2 u}} du = \frac{\pi}{2}.$$

Since

$$0 \le u \le u_2 < \frac{\pi}{2} \Rightarrow \frac{\sqrt{1 - k^2 \sin^2 u_2}}{\sqrt{1 - k^2 \sin^2 u}} < 1,$$

it follows

$$\frac{\pi}{2} = \int_0^{u_2} \frac{\sqrt{1 - k^2 \sin^2 u_2}}{\sqrt{1 - k^2 \sin^2 u}} du < u_2 < \frac{\pi}{2}.$$

So trajectory a can not exist.

In order to discuss the existence of trajectory b, we define the following function

$$g(u_2) = 2K(k^2) - F(u_2, k^2) - \frac{\pi}{2} \frac{1}{\sqrt{1 - k^2 \sin^2 u_2}},$$

with

$$\frac{\pi^2}{4p} = \frac{1}{k^2}(1 - k^2 \sin^2 u_2).$$

Then

$$
\begin{aligned}
g(0) &= 2K(k^2) - \frac{\pi}{2} = \int_0^{\frac{\pi}{2}} \left(\frac{2}{\sqrt{1 - k^2 \sin^2 u}} - 1 \right) du > 0, \\
g\left(\frac{\pi}{2}\right) &= 2K(k^2) - K(k^2) - \frac{\pi}{2} \frac{1}{\sqrt{1 - k^2}} \\
&= \int_0^{\frac{\pi}{2}} \left(\frac{1}{\sqrt{1 - k^2 \sin^2 u}} - \frac{1}{\sqrt{1 - k^2}} \right) du < 0.
\end{aligned}
$$

Thus, $\exists$ some $\overline{u_2}$, with $0 < \overline{u_2} < \frac{\pi}{2}$, such that $g(\overline{u_2}) = 0$. For this $\overline{u_2}$, $T_b = \sqrt{p}$. Furthermore, as $u_2 = 0$ means $\frac{\pi}{4p} = \frac{1}{k^2}$, we have

$$-k \int_\pi^0 \frac{1}{\sqrt{1 - k^2 \sin^2 u}}\, du = 2kK(k^2) \geq k\pi > \sqrt{p}.$$

From the above discussion, we know that this kind of u_2 corresponds to the trajectory b in figure 4.37.

Case II. $p = \frac{\pi^2}{4}$. The discussion is the same as that for $p < \frac{\pi^2}{4}$.

Case III. $p > \frac{\pi^2}{4}$, we have $\omega_1 > -2$. There are several possibilities for both $\omega_0 > 0$ and $\omega_0 < 0$ (see figure 4.38).

First we investigate the existence of trajectories 3 and 4 in figure 4.38. Trajectory 3 lies on the separatrix, so

$$\omega_0 = -2, \omega_1 = -\frac{\pi}{\sqrt{p}}.$$

From equation (4.3) we have

$$\omega_1^2 = \frac{\pi^2}{p} = \omega_0^2 + 2(\cos \Psi_1 - 1) = 4\cos^2 \frac{\Psi_1}{2},$$

or,

$$
\begin{aligned}
\cos^2 u_3 &= \frac{\pi^2}{4p}, \qquad u_3 \in \left(\frac{\pi}{2}, \pi\right) \\
\cos u_3 &= -\frac{\pi}{2\sqrt{p}} \\
u_3(p) &= \arccos\left(-\frac{\pi}{2\sqrt{p}}\right) = \pi - \arccos\left(\frac{\pi}{2\sqrt{p}}\right).
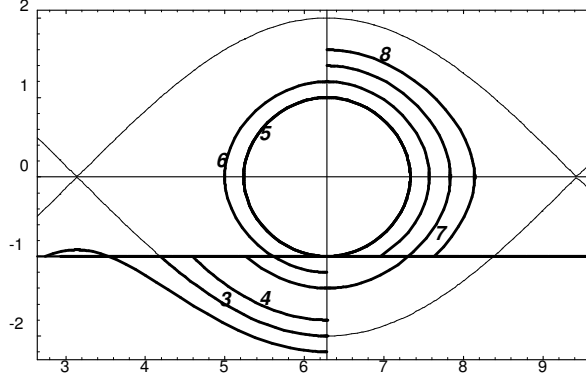\end{aligned}
$$

Figure 4.38: Possible phase curves of (2.2) for $\gamma = \frac{\pi}{2}, \alpha = -\frac{\pi}{2}$ and $p > \frac{\pi^2}{4}$.

Along trajectory 3, $u' = \cos u$,

$$T_3(p) = \int_{\pi}^{u_3} \frac{1}{\cos u} du = \log\left(\frac{2}{\pi}\sqrt{p}\left(1 + \sqrt{1 - \frac{\pi^2}{4p}}\right)\right).$$

So

$$\log\left(\frac{2}{\pi}\sqrt{p}\right) < T_3(p) < \log\left(\frac{4}{\pi}\sqrt{p}\right).$$

If $T_3(p) = \sqrt{p}$, then

$$\log\left(\frac{2}{\pi}\sqrt{p}\right) < \sqrt{p} = \frac{\pi}{2}\frac{2}{\pi}\sqrt{p} < \log\left(2 \cdot \frac{2}{\pi}\sqrt{p}\right).$$

Because $\frac{2}{\pi}\sqrt{p} > 1$, the above inequality is not true. Thus trajectory 3 does not exist. Inside the separatrix

$$\Psi'^2 = 2(\cos\Psi - \cos\hat{\Psi})$$

with $\cos\hat{\Psi} = 1 - \frac{1}{2}\omega_0^2$. Let

$$k^2 := \sin^2\frac{\hat{\Psi}}{2}, \quad \sin\frac{\Psi}{2} =: \sin\frac{\hat{\Psi}}{2}\sin u.$$

Then we have

$$u'^2 = 1 - k^2\sin^2 u.$$

Along trajectory 4 the transit 'time' is

$$T_4 = \int_{u_4}^{\pi} \frac{1}{\sqrt{1 - k^2\sin^2 u}} du$$

with

$$\frac{\pi^2}{4p} = k^2\cos^2 u_4, \quad \frac{\pi}{2} < u_4 \le \pi.$$

$T_4 = \sqrt{p}$ is equivalent to

$$\frac{\pi}{2k|\cos u_4|} = \int_{u_4}^{\pi} \frac{1}{\sqrt{1 - k^2 \sin^2 u}}\, du.$$

But

$$
\begin{aligned}
\int_{u_4}^{\pi} \frac{k|\cos u_4|}{\sqrt{1 - k^2 \sin^2 u}}\, du \quad &< \quad -\int_{u_4}^{\pi} \frac{k \cos u}{\sqrt{1 - k^2 \sin^2 u}}\, du \\
&= \quad \int_0^{\pi - u_4} \frac{k \cos v}{\sqrt{1 - k^2 \sin^2 v}}\, dv \\
&= \quad \arcsin\left(k \sin\left(\pi - u_4\right)\right) = \arcsin\left(\sin\left(\pi - \frac{\Psi_1}{2}\right)\right) \\
&= \quad \pi - \frac{\Psi_1}{2} < \frac{\pi}{2}.
\end{aligned}
$$
(4.5)

Thus $T_4 = \sqrt{p}$ can not be satisfied or trajectory 4 does not exist.

For trajectory 5,

$$\omega_0 = \omega_1 = -\frac{\pi}{\sqrt{p}},$$

$$\cos\hat{\Psi} = 1 - \frac{1}{2}\omega_0^2 = 1 - \frac{\pi^2}{2p}.$$

$$k^2 = \sin^2\frac{\hat{\Psi}}{2} = \frac{\pi^2}{4p}, \quad \sin\frac{\Psi}{2} = \sin\frac{\hat{\Psi}}{2}\sin u,$$

then we get (period for one cycle)

$$T_5 = 4\int_0^{\frac{\pi}{2}} \frac{1}{\sqrt{1 - k^2 \sin^2 u}}\, du = 4K(k^2).$$

While $T_5 = \sqrt{p}$ is equivalent to

$$4K(k^2) = 4K\left(\frac{\pi^2}{4p}\right) = \sqrt{p},$$

the numerical solution of this equation is $p = 40.7266$. With the same discussion, we know that trajectories 6, 7, 8 can also exist for some greater p. We illustrate part of the discussion in this section with figure 4.39, in which the final manifold, phase curves and configurations for $p = 40.7266$ are drawn.

From the above discussion, it is obvious that, the theoretical investigation supports the results obtained from manifold method.
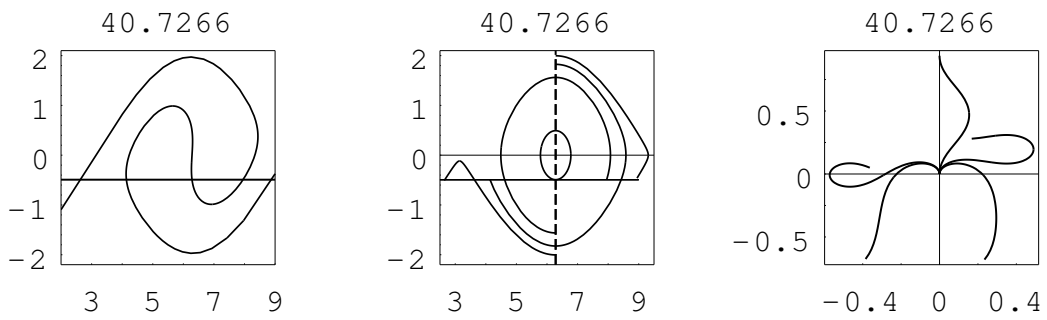
Figure 4.39: Final manifold, phase curves and configurations for $\gamma = 0.5\pi, \alpha = -0.5\pi, p = 40.7266$.

Chapter 5

Study of stability

5.1 General related concepts

Stability and loss of stability exist in nature and in almost every area of science and technology. The stability study of the solutions of differential equations was greatly developed by Liapunov, the stability theory and method have been modified, extended and complemented by a great number of mathematicians and other scientists, the research areas have been greatly widened after Liapunov. The infiltration of stability study into non-mathematical areas makes it develop rapidly. In our study of deformation of circular elastic arcs, we also noticed the problem of stability. Here we intend to mention some related definitions and methods which have something to do with our theme. In the above sections, our study based on the discussion of the pendulum equation. In our stability study we also take the pendulum equation under consideration. As already mentioned, in the study of stability, parameters p and γ will be given more emphasis. We introduce some definitions for the general differential equation

$$\frac{d\Psi}{dt} = F(\Psi, t) \tag{5.1}$$

where $\Psi \in I\!\!R^n, t \in (-\infty, \infty), F : I\!\!R^n \times I\!\!R \longrightarrow I\!\!R^n$ is sufficiently smooth. Let $\Psi(t, t_0, \Psi_0)$ be solution of the equation satisfying $\Psi(t_0) = \Psi_0$.

Definition 5.1 *(Liapunov stability) A solution $\bar{\Psi}(t)$ of equation (5.1) is said to be stable if it holds the following condition: for each t_0 and $\epsilon > 0$, there exists a $\delta(\epsilon, t_0) > 0$ such that $\|\Psi_0 - \bar{\Psi}(t_0)\| \leq \delta \Longrightarrow \|\Psi(t, t_0, \Psi_0) - \bar{\Psi}(t)\| \leq \epsilon$ for $t > t_0$.*

This definition is frequently used in the study of dynamical system and the most popular method suitable for this definition is Liapunov direct method or Liapunov function method

(note: in some references it is known as Liapunov second method) [46],
[51], [58]. This kind of stability concerns mainly the behavior of the solution when t
keeps extremely large and the influence of the initial value on the solutions. In the course
of the study the system (or the parameters in the system) keeps generally not changed.
The stability study of this kind is often accompanied by the discussion of the orbits and is
carried out in the phase plane. This definition is belonged to Liapunov. It is a fundamental
definition of the stability of motion, work on this kind of stability is a very important
component of stability study, another part of stability is structural stability, which based
on the concepts of equivalence (see appendix 2 and [33], [34]).

Definition 5.2 *Two differential equations $\Psi' = F(\Psi)$ and $\Psi' = G(\Psi)$ are said to be
topologically equivalent if there is a homeomorphism h such that h takes the orbits of one
differential equation to the orbits of the other and preserves the sense of directions in time.*

In much literature if there is an above mentioned homeomorphism [23], [55] between two
differential systems then these two systems are said to have the same structure. The
following two definitions can be found in books on differential equations and bifurcations,
for instance [2] and [34].

Definition 5.3 *Let $\Psi' = F(\Psi, \lambda)$ be a differential system with $\lambda \in I\!\!R^m, m \geq 1$. For fixed
value of $\lambda = \lambda_0$, system $\Psi' = F(\Psi, \lambda_0)$ is said to be structurally stable if there is an $\delta \geq 0$
such that $\Psi' = F(\Psi, \lambda)$ has the same structure as $\Psi' = F(\Psi, \lambda_0)$ for all $||\lambda - \lambda_0|| \leq \delta$.*

Definition 5.4 *A solution $(\Psi_0, \lambda_0, \beta_0)$ of equation $F(\Psi, \lambda, \beta) = 0$ is said to be structurally
stable if for any smooth G, for any neighborhood U of $(\Psi_0, \lambda_0, \beta_0)$ and for any ϵ ($|\epsilon|$ suf-
ficiently small), the small perturbed problem $\hat{F}_\epsilon(\Psi, \lambda, \beta) = F(\Psi, \lambda, \beta) + \epsilon G(\Psi, \lambda, \beta)$ has a
singularity of the same type at a point in U.*

Note: According to this definition, we know the simple node, saddle and focus of differen-
tial equations are structurally stable, but center is not structural stable, this can be easily
explained by consideration of eigenvalues of the corresponding singularities.
The differential equations originated from practical problems contain normally several coef-
ficients, namely branching (or bifurcation) parameter and other parameters, which describe
the mechanical characters or properties of materials. One task of the stability study of the
differential equations is to determine the effect of these parameters on the system, in other
words we intend to make clear how a given solution and qualitative structure of entire
system change with these parameters.
The stability definition of Timoschenko [82], [9], which is more related to our mathematical
model, is stated with words as follows:

Definition 5.5 *The straight form of elastic equilibrium is stable under an acting force which means that if a lateral force is applied and a small deflection produced, the deflection disappears when the lateral force is removed and bar returns to its straight form. If the acting force is gradually increased, a condition is reached in which a small lateral force will produce a deflection which does not disappear when the lateral force is removed, then the straight form of equilibrium becomes unstable.*

We illustrate this definition via a deformed elastic arc in figure 5.1. The straight form of the arc in (a) is stable, but it is unstable in (b), (c) and (d).
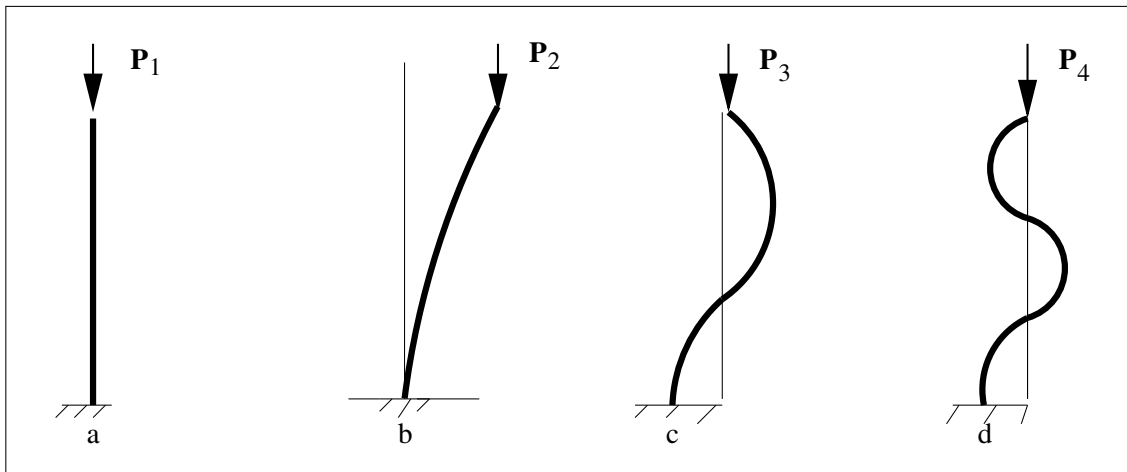

Figure 5.1: Deformation of an elastic straight bar under acting force p.

This definition is specially used in the study of the elastic straight bars under some external acting forces. Related to this definition, we can find some other definitions and methods quoted in [6]. Energy method is an often used method and it is connected with the following definition.

Definition 5.6 *An equilibrium configuration of an elastic rod under conservative loads is stable if and only if the potential energy assumes a weak proper minimum value at the equilibrium configuration in the class of finite virtual displacement satisfying the kinetic constraints (see figure 5.2).*

The above definitions are somewhat not exact, but easy to be understood. From these definitions we know the stability of an equilibrium and structure stability of a system strongly depend on the values of parameters in a system. A same equilibrium may be stable for some value of parameters and unstable for some other value of same parameters. It is an usual case that a very small change of parameters would bring a great perturbation to an
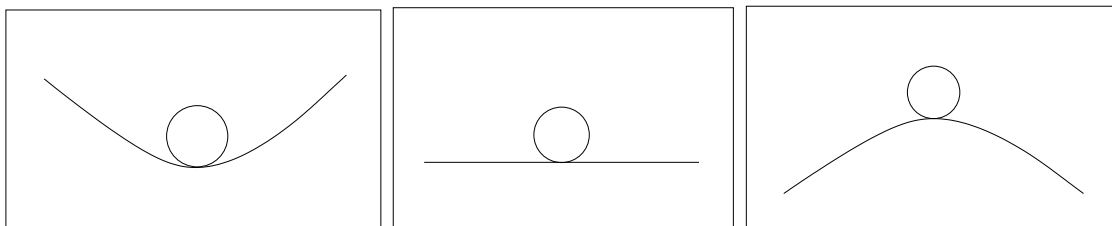
Figure 5.2: Stability behavior of a heavy ball moving along a parabola.

equilibrium or a system, this phenomenon of losing stability is encountered in many areas of applied science and technology, an overview about this situation was given by [86]. Here we intend to give some more explanation about structure stability and other definitions of stability:

1. Liapunov's stability(or stability of motion) concerns mainly the influence of a small perturbation to the initial value on a specially indicated equilibrium or a motion. If the displacement of the motion from a special motion remains small after a small perturbation to the initial value, then the motion is stable, otherwise unstable, or geometrically speaking, when all other motions starting from a small neighborhood of the special motion remain always in a small neighborhood of the special motion. But structural stability concerns chiefly whether the system studied keeps the same topological characters as the unperturbed system after a small perturbation on the parameters included in the system, while changes introduced to initial value play no role. In this point of view the researching object of structure stability is entire system, but stability of motion deals with a specially indicated motion.

2. In stability study on a special equilibrium or a motion and structural stability on a system, the critical values of parameters, for which a system or an indicated motion loses or gains (structural) stability, play a very important role. Generally speaking the conditions of structural instability contain the critical value for stability of motion.

3. Concerning the research methods used in both stability, they have also many connections.

5.2 Structural stability

According to the definitions given before and the results on bifurcation diagram, we discuss the structural stability of (2.2) in this section. In this part we take p as bifurcation

parameter.

For structural stability of the originally straight line we have the following result

Theorem 5.1 *For pendulum equation (2.2) with $\alpha = \pi, \gamma = 0$ (Euler's rod), there exist infinite many critical values of p, the system is structurally stable with respect to the small perturbation of p for p is different from the critical values (for $p \leq 50$, there exist two critical values of $p, p_c < p_d$).*

Note: When $\gamma = 0, \alpha = \pi$, our model is specially Euler's rod. According to the bifurcation diagram we know the two critical values $p_c \approx 2.47, p_d \approx 22.2$, they agree with the Euler's classical result on critical values $p_c = \frac{\pi^2}{4}, p_d = \frac{9\pi^2}{4}$ obtained by linearization.

The description for this result can be easily got from the bifurcation diagram 4.3, concerning also the symmetry, the system for different p has same number of solutions and the solutions have same characteristics, provided that the perturbation on p is small and $p \neq p_c, p \neq p_d$. From this result we know the critical values for structural stability include values which correspond to bifurcation points. Recalling the bifurcation diagrams for α, γ other than π, 0, we know we must take the values which correspond to turning points into consideration, because the number of the solutions changes at these points . About structural stability we have the following result:

(1). In pendulum equation (2.2) let γ and α be fixed, the equation is an one-parameter system. Let S_p be the set of all p which correspond to turning points or bifurcation points in bifurcation diagram, then the system is structurally stable for $p \notin S_p$.

(2). In (2.2) let γ and p be fixed, the qualitative structure is determined by the value of α. In the bifurcation diagram no bifurcation appears, but we meet two kinds of critical points: 1. turning points, let the corresponding value of $\alpha = \alpha_0$, the number of solutions at this point is n_0, the number of solution for $\alpha < \alpha_0 (\alpha > \alpha_0)$ is $n_l(n_r)$, then $n_0 = n_l - 1 = n_r + 1$, provided that $|\alpha - \alpha_0|$ sufficiently small (see bifurcation diagrams figure 8.11- 8.2 for relatively bigger p). $F(\Psi, \lambda) = \Psi^2 + \lambda = 0$ has an equilibrium of this kind at $(0, 0)$. 2. hysteresis point, at this kind of point, the branching curve in bifurcation diagram has a vertical tangent. $F(\Psi, \lambda, \beta) = \Psi^3 - \lambda + \beta\Psi = 0$ has an equilibrium of this kind at $\beta = 0$ (see figure 5.3). As shown in the figure the number of ω_0 keeps the same in a small neighborhood of α_0. Let S_α be the set of all α which correspond the above mentioned turning points, then the system is structurally stable when $\alpha \notin S_\alpha$.
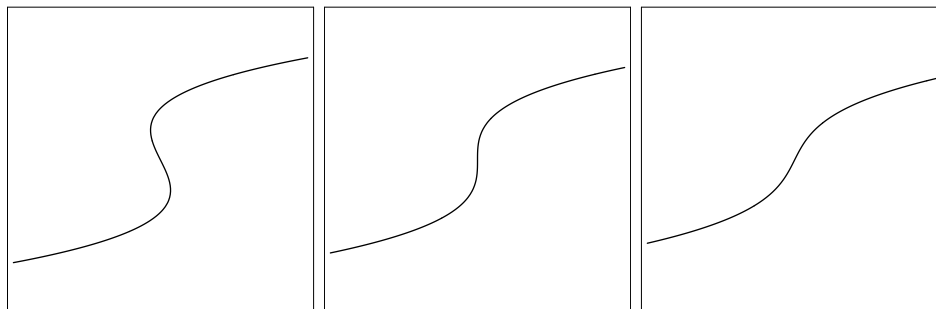
Figure 5.3: The formation procedure of a hysteresis (in the middle) defined by $\Psi^3 - \lambda + \beta\Psi = 0$ for $\beta < 0$ (left), $\beta = 0$ (middle) and $\beta > 0$ (right).

(3). Let α and p be fixed, there is no bifurcation point of pitchfork type, but turning point (both types) and bifurcation point of X-type. Let S_γ denote the set of all γ which correspond to turning points and bifurcation points, then the system is structurally stable if $\gamma \notin S_\gamma$.

This conclusion indicates that bifurcation points, turning points are critical points of structural stability, the corresponding parameters consist of the boundary of structural stability of (2.2) on the parameter plane, so the parameter partition diagram figures 4.11- 4.15 are also diagrams for structural stability. For fixed γ, when parameter pair (p, α) is located on the curves, then the corresponding system (2.2) is not structurally stable.

Note: Here we should claim that the study about structural stability of (2.2) was based on only mathematical consideration, we did not take the practical background of the model into account anymore. Sometimes there are some differences between mathematical stability and practical stability, a solution exists following mathematical consideration and calculation, but it may not appear in practical observation or a simulation experiment.

5.3 Stability of equilibrium of (2.2)

On stability of equilibrium of differential systems, the most frequently used method is Liapunov direct method and many delicate modifications, but it is not always an easy work to build a suitable Liapunov function for a given system, which can be used to determine the stability of an equilibrium. On stability study of equilibrium of elastic system we intend to mention the three frequently used methods [6]: 1. adjacent method of Euler, it is based on the fact that a stable equilibrium should exist and keep its qualitative and motion distinction under a small perturbation, that is it will not split into more than one equilibrium or join with other equilibrium, so the key point of the method is to find the

boundary of stability- or critical value of bifurcation parameter. 2. energy method, this method is based on the fact that in a dynamic system, the potential energy of a system takes a minimum value at a stable equilibrium, this is geometrically shown by a heavy ball moving along a parabola(see figure 5.2), visually it is clear that a small perturbation can make a small displacement from the lowest position, but the ball will turn back to the lowest point at end. The key point of this method is therefore to construct an energy functional and to find its minimum value from all possible equilibriums. 3. dynamic method, this method was based on Liapunov direct method, the key point of this method is to construct a Liapunov function which is positive (or negative) definite and its derivative along the orbit is negative (positive) definite in a sufficiently small neighborhood of an equilibrium. These three methods are proved to be especially useful for the stability study of constant solutions. In rod theory they are used in the investigation of the stability of trivial equilibrium which corresponds to originally straight rod. Except these methods we mention some other work: Drawshi and Betten [22] discussed the stability of equilibrium with deformation maps geometrically, Suire and Cederbaum [79] gave explanation to stability by means of a numerical calculation. Afagh and Lee [1] represented their work on stability with eigenvalue and Galerkin method. Wu's [95] work on stability study based on dynamic method and eigenvalue of linearization part at equilibrium. Bhallacharyya [10] used numerical method in stability study related to a Mathieu-Hill equation:

$$\frac{d^2y}{d\psi^2} + F(\psi)y = 0,$$

where $F(\psi) = R(\psi) - P^2(\psi) - \frac{dP(\psi)}{d\psi}$ is a even, π-periodic function of ψ.

In our study on large deformations of elastic circular arcs, γ can take any value in $[0, \pi]$. If $\gamma \neq 0$, there is no more trivial equilibrium for (2.2), the above mentioned methods might not be used directly in the stability study in our model.

In this section we will introduce a method to stability study of an equilibrium of a general differential system. The idea comes from the work on the stability of steady-state solution (or stationary solution) of partial differential equations, see for example [80].

In the stability study of the solution of given autonomous ordinary differential equation of first order:

$$\frac{d\Psi}{dt} = F(\Psi, \lambda),$$

we obtain the singular point of the equation by solving equation $F(\Psi, \lambda) = 0$, the stability of the singular points can be determined by several known methods, the most frequently used way should be Liapunov method and linearization. For instance, let (Ψ_0, λ_0) be a singular point of the equation, that is $F(\Psi_0, \lambda_0) = 0$. After making a transformation

$\hat{\Psi} = \Psi - \Psi_0$, we get $\frac{d\hat{\Psi}}{dt} = DF(\Psi_0, \lambda_0)\hat{\Psi} + O(\hat{\Psi}^2)$, here $DF(\Psi_0, \lambda_0)$ is Jacobian matrix of F at point (Ψ_0, λ_0). If all eigenvalues of $DF(\Psi_0, \lambda_0)$ have negative real parts, then (Ψ_0, λ_0) is stable. If at least one of the eigenvalues has positive real part, then (Ψ_0, λ_0) is unstable. If no eigenvalue has positive part, but some eigenvalue has zero real part, in this case the nonlinear term $O(\hat{\Psi})$ should be considered.

If we deal with an equilibrium problem $G(\Psi, \lambda) = 0$, we could think of $G(\Psi, \lambda)$ as a controller of a motion described by the following equation:

$$\frac{d\Psi}{dt} = G(\Psi, \lambda),$$

then we can define and discuss the stability of an equilibrium of $G(\Psi, \lambda)$ similarly as in the stability study for a singular point of the equation $\frac{d\Psi}{dt} = G(\Psi, \lambda)$, that is, if (λ_0, Ψ_0) is stable (unstable) as a singular point of a differential equation, we say it is stable (unstable) as an equilibrium of $G(\Psi, \lambda)$. In this consideration, an equilibrium of $G(\Psi, \lambda)$ and the singular point of the corresponding differential equation can be thought to be identical.

With the similar consideration as on the ordinary differential equation of first order, we could carry out our study on differential equation of order 2.

Let the boundary value problem of differential equations of order two be of the following form:

$$\psi'' + F(\psi, \psi', \lambda) = 0 \tag{5.2}$$

here F is a smooth function of state variable ψ and its derivative ψ' as well as parameter λ, $''$ is the 2-order derivative with respect to $s \in [a, b]$. The boundary condition is:

$$B(\psi(a), \psi(b), \psi'(a), \psi'(b)) = 0.$$

When $F : \mathbb{R}^n \times \mathbb{R}^n \times \mathbb{R} \longrightarrow \mathbb{R}^n$, then normally $B \in \mathbb{R}^{2n}$. For solutions of (5.2), we take them as the stationary solutions of the partial differential equation of parabolic type:

$$\frac{\partial \psi}{\partial t} - \frac{\partial^2 \psi}{\partial s^2} = F(\psi, \psi', \lambda)$$
$$B(\psi(t, a), \psi(t, b), \psi'(t, a), \psi'(t, b)) = 0. \tag{5.3}$$

It is obvious that solutions of (5.2) satisfying the boundary condition are independent of t, they are also solutions of (5.3). The systematic theory and methods about partial differential equations can be found in many books [24], [26], [92]. Now let $\psi_0(s)$ be a solution of (5.2), whose stability is to be studied. We construct a partial differential equation of parabolic type:

$$\frac{\partial \psi}{\partial t} - \frac{\partial^2 \psi}{\partial s^2} = F(\psi, \psi', \lambda), \quad s \in [a, b], t > 0$$
$$B(\psi(a, t), \psi(b, t), \psi'(a, t), \psi'(b, t)) = 0, \quad t > 0, \tag{5.4}$$
$$\psi(0, s) = \psi_0(s) + \tilde{\psi}(s).$$

Let $\psi = \psi(t,s)$ be a solution of (5.4), then $\psi_0(s)$ is called nunstable (not unstable) stationary state (note: it is also regarded as steady state) of (5.3), if $\psi(t,s)$ lies always in any given neighborhood of $\psi_0(s)$ for all $t > 0$ provided that $\psi(0,s)$ is sufficiently close to $\psi_0(s)$. Or in other words (see for example reference [73]): a stationary solution $\psi_0(s)$ is a nunstable solution of (5.3), if for every $\epsilon > 0$, there is a $\delta > 0$ such that if $||\tilde{\psi}(s)|| < \delta$, then $||\psi(s,t) - \psi_0(s)|| < \epsilon$ for all $t > 0$. If $\psi_0(s)$ is nunstable and there holds also the following condition

$$\lim_{t \to \infty} \psi(t,s) = \psi_0(s),$$

then $\psi_0(s)$ is said to be stable (asymptotically stable) solution of (5.4). $\psi_0(s)$ is unstable, if we can find solutions starting arbitrarily close to $\psi_0(s)$ which leave some given small neighborhood of $\psi_0(s)$ as $t \to \infty$. Now we say $\psi_0(s)$ is a P-nunstable, P-stable or P-unstable solution of (5.2) with boundary condition. Here we use P-stability to distinguish it from other definition of stability, "P" is especially used to emphasize that this stability is defined with the help of the Liapunov stability of a stationary solution of a corresponding parabolic partial differential equation.

With this method the stability study of solutions of equation (5.2) is turned to the stability study of the stationary solution of (5.3).

For study of partial differential equation (5.3) or (5.4) there are some methods available and many publications to find. Nishinra and Fujii [53] discussed the system of reaction-diffusion equation of the form:

$$\begin{cases} \frac{\partial u}{\partial t} = \epsilon^2 \frac{\partial^2 u}{\partial s^2} + f(u,v), \\ \frac{\partial v}{\partial t} = D \frac{\partial^2 v}{\partial s^2} + g(u,v), & (t,s) \in (0,\infty) \times [0,1], \\ u'_s = 0 = v'_s, & (t,s) \in (0,\infty)I, \partial I = \{0,1\}, \end{cases}$$

where $\epsilon > 0$ is a small parameter and $D > 0$. Using spectral analysis shows there exists a unique real critical eigenvalue $\lambda(\epsilon) \approx \tau\epsilon$ as $\tau \to 0$, other non-critical eigenvalues have negative real parts independent of ϵ, therefore if $\tau < 0$, the system is stable. Gardmer and Jones [31] discussed the stability of steady state solution of the partial differential equation of the form

$$\begin{cases} \frac{\partial u}{\partial t} = D \frac{\partial^2 u}{\partial s^2} + f(s,u,u'_s), & s \in (0,1) \\ u(s,0) = u_0(s), \\ B_0 u = 0, B_1 u = 0. \end{cases}$$

where $u \in \mathbb{R}^n, f : \mathbb{R}^{2n+1} \to \mathbb{R}^n$ is C^2, D is a positive diagonal matrix, by introduction of a stability index $\epsilon(K)$, which counts the number of eigenvalues inside a simple closed

curve K not intersecting the spectrum itself, they declared that, if K is chosen, so that it includes the origin and a suitably large portion of the unstable half plane, then K contains all potentially unstable eigenvalues, if this index is zero for such a curve K, the underlying solution is stable. Cónsul and Solá -Morales [18] studied the system

$$\begin{cases} \frac{\partial u}{\partial t} = \Delta u, & \text{in} \quad D, \\ u_0 = kf(u), & \text{on} \quad \partial D, \end{cases}$$

here D is a non-convex domain, $\triangle$ is Laplace operator. Under some assumption, they got the criterion for the existence of at least one stable nonconstant equilibrium solution. Heinemann and Poore [36], [39] studied the stability of a class of partial differential systems originated from tubular reactors in chemical engineering.

For numerical treatment, apart from the classical methods [29], Finite Element Method is a powerful method. Theoretically we could investigate the stability of any solution of (5.2) with this concept of P-stability, and with the help of the existing mathematical softwares, such as $Maple, Matlab, Scilab$ and so on, one can be able to deal with the partial differential equations numerically more easily than using the classical method directly. This method is obviously developed to turn the stability study of solutions of (2.2) to the stability study of the stationary solutions of (5.4), but inversely it gives a hint that we can also investigate (5.3) by means of an ordinary differential system, this idea was used in [27], [28] in the study of evolution equation of the type:

$$\frac{\partial u}{\partial t} - \lambda \frac{\partial^2 u}{\partial s^2} + \frac{\partial u}{\partial s} - u = 0$$

with boundary condition

$$u(0, t) = u(\pi, t) = 0.$$

Now we give a discussion to partial differential equation (5.4). Obviously each λ corresponds to a new system. Now let λ be fixed. The state at t is $\psi(s, t)$, which is a function of s, with notation of [19], considering $\psi : t \longrightarrow \psi(., t)$ with $\psi(., t) : s \longrightarrow \psi(s, t)$. Writing $\psi(t)$ instead of $\psi(s, t)$, then $\psi(t)$ is a function for fixed t and it has the character of $\psi(t)(s) = \psi(s, t)$. Then we define $G(\lambda, .)$ by

$$G(\lambda, \psi) = \frac{d^2 \psi}{ds^2} + F(\psi, \psi', \lambda),$$

and domain of G is defined as

$$D(G) = \{\psi | \psi \in C^2[a, b], B(\psi(a), \psi'(a), \psi(b), \psi'(b)) = 0\}.$$

As $\psi(s,t)$ is replaced by $\psi(t)$, we write $\frac{\partial \psi}{\partial t}$ as $\frac{d\psi}{dt}$, thus (5.4) can be written as

$$\frac{d\psi}{dt} = G(\lambda, \psi), \psi(0) = \psi_0. \tag{5.5}$$

For each known solution of $G(\lambda, \psi) = 0$, say $\psi = \psi_0(\lambda)$, let $u + \psi_0 = \psi$, then $\frac{du}{dt} = G(\lambda, u + \psi_0) := \bar{G}(\lambda, u)$. The stability of ψ_0 or $u = 0$ can be stated as: 0 is P-nunstable provided that solutions of last equation are close to 0 for all $t > 0$ and 0 is P-stable if it is P-stable and $u(t) \longrightarrow 0$ as $t \longrightarrow \infty$ by choosing $\psi(0)$ sufficiently small. This consideration gives a hint that a partial differential equation could be possibly studied as an ordinary differential equation. One of the most common methods used in stability study for ordinary equation is linearization.

Let $\psi_0(s)$ be a solution of (5.2) whose stability is to be studied, $\psi(t,s)$ be an any solution of (5.4) which starts from a sufficiently small neighborhood of $\psi_0(s)$. Let

$$\bar{\psi}(s,t) = \psi(s,t) - \psi_0(s)$$

be difference of these two solutions. Substituting it into (5.3), we have

$$\frac{\partial \bar{\psi}}{\partial t} = \frac{\partial \psi}{\partial t} = F(\psi_0(s) + \bar{\psi}, \psi_0'(s) + \bar{\psi}') + \frac{\partial^2 \psi_0}{\partial s^2} + \frac{\partial^2 \bar{\psi}}{\partial s^2},$$

The linearization of the above equation is

$$\begin{aligned}
\frac{\partial \bar{\psi}}{\partial t} &= \psi_0'' + \bar{\psi}'' + F(\psi_0, \psi_0') + F_\psi'(\psi_0, \psi_0')\bar{\psi} + F_{\psi'}'(\psi_0, \psi_0')\bar{\psi}' \quad s \in [a, b], t \geq 0, \\
&= \bar{\psi}'' + F_\psi'(\psi_0, \psi_0')\bar{\psi} + F_{\psi'}'(\psi_0, \psi_0')\bar{\psi}'
\end{aligned}$$

with homogeneous boundary condition

$$\begin{cases} K_0\bar{\psi}(t,a) + K_1\bar{\psi}'(t,a) = 0, \\ L_0\bar{\psi}(t,b) + L_1\bar{\psi}'(t,b) = 0, \quad t \geq 0 \end{cases}$$

where K_0, K_1, L_0, L_1 are obtained from B by linearization. The above equation, together with boundary condition, constitutes a linear problem. If we let $A\bar{\psi} := -\bar{\psi}'' - F_\psi'(\psi_0, \psi_0')\bar{\psi} - F_{\psi'}'(\psi_0, \psi_0')\bar{\psi}'$, the last equation can be written as $\bar{\psi}_t' + A\bar{\psi} = 0$ and A is a linear differential operator defined in some class of functions, which satisfy the boundary conditions. The domain of A, $D(A)$, may be extended to be a dense subset of some Banach space X, the norm of it is denoted, for simplicity, with $||.||$. Then $\psi_0(s)$ is an asymptotically stable stationary solution of PDE (5.3) could be simply expressed by $||\bar{\psi}|| \to 0, t \to \infty$. This can be guaranteed by the spectrum of A, if it is contained strictly in the right side of the

complex plane [97]. We transfer the equation into an eigenvalue problem with assuming that the above equation has solutions of the form:

$$\bar{\psi}(s,t) = e^{\delta t}\phi(s),$$

substituting it into the linearization gives an eigenvalue problem for ϕ:

$$\begin{cases} \delta\phi = \phi'' + F'_\psi \phi + F'_{\psi'}\phi' \\ K_0\phi(a) + K_1\phi'(a) = 0 \\ L_0\phi(b) + L_1\phi'(b) = 0. \end{cases}$$

The above equation has nontrivial solutions if and only if δ is an eigenvalue of it. If all eigenvalues have negative real parts, then $\psi_0(s)$ is P-stable, if at least one of the eigenvalues has positive real part, then $\psi_0(s)$ is P- unstable, if no real part of δ is positive, but there are some eigenvalues with zero real part, then they correspond to critical situation for equation (5.2).

Now we use this method in our model. In stability study we use the equivalent equation of (2.2):

$$\frac{d^2\Psi}{ds^2} + \lambda\sin\Psi = 0,$$

$$\Psi(0) = \pi + \gamma - \alpha, \quad \Psi'(1) = -2\gamma.$$

Compared with equation (2.2), the advantage of this equivalent equation lies in the fact that parameter λ (or p) is not involved in the boundary condition, but only involved in the differential equation, so s lies in $[0,1]$ for any p. The corresponding PDE (5.3) is now:

$$\begin{aligned} \frac{\partial\Psi}{\partial t} - \frac{\partial^2\Psi}{\partial s^2} &= \lambda\sin\Psi, \quad s \in [0,1], t > 0, \\ \Psi(0,t) &= \pi + \gamma - \alpha, \\ \Psi'(1,t) &= -2\gamma \quad t > 0. \end{aligned} \tag{5.6}$$

Let $\Psi = \Psi_0(s)$ be a solution of BVP (2.2), then the corresponding PDE (5.4) is:

$$\begin{aligned} \frac{\partial\Psi}{\partial t} - \frac{\partial^2\Psi}{\partial s^2} &= \lambda\sin\Psi, \quad s \in [0,1], t > 0, \\ \Psi(0,t) &= \pi + \gamma - \alpha, \\ \Psi'(1,t) &= -2\gamma, \quad t > 0, \\ \Psi(s,0) &= \Psi_0(s) + \tilde{\Psi}(s). \end{aligned} \tag{5.7}$$

Concerning the initial-boundary condition and boundary conditions of (5.7) and (2.2), we make some assumption for the perturbation $\tilde{\Psi}(s)$: $\tilde{\Psi}(s) \in C^2[0,1], \tilde{\Psi}(0) = 0, \tilde{\Psi}'(1) = 0, ||\tilde{\Psi}(s)||$ is very small, the situation is illustrated in figure 5.4.
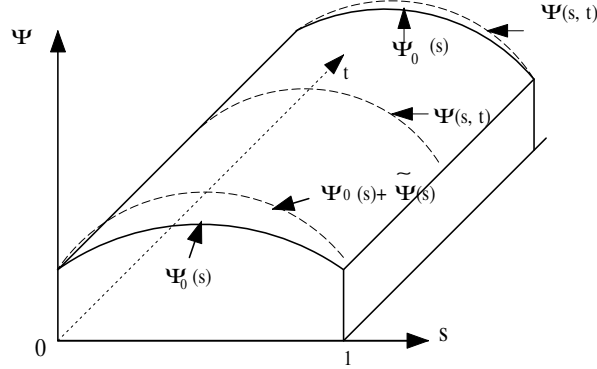
Figure 5.4: Illustration of the solutions of (5.4).

Now assume $\Psi(s,t)$ be a solution of (5.7), and $\bar{\Psi}(s,t) = \Psi(s,t) - \Psi_0(s)$, substituting this expression into (5.7) yields:

$$\frac{\partial \bar{\Psi}}{\partial t} - \frac{\partial^2 \bar{\Psi}}{\partial s^2} = \lambda \cos\left(\Psi_0(s)\right)\bar{\Psi} + O(\bar{\Psi}^2), \tag{5.8}$$

provided $||\bar{\Psi}(s,t)||$ is very small. In obtaining the last equation we used the Taylor's series of $\sin\left(\Psi_0(s) + \bar{\Psi}(s,t)\right)$ at $\Psi_0(s)$ about $\bar{\Psi}(s,t)$. Neglecting the term of high order from the last equation we get the linearized equation:

$$\frac{\partial \bar{\Psi}}{\partial t} - \frac{\partial^2 \bar{\Psi}}{\partial s^2} = \lambda \cos\left(\Psi_0(s)\right)\bar{\Psi}.$$

Using linearized equation to get the stability of the solutions of the original equation, we must check if the conditions of some criteria are satisfied. Let $A\bar{\Psi} := -\frac{\partial^2 \bar{\Psi}}{\partial s^2} - \lambda \cos\left(\Psi_0\right)\bar{\Psi}$, A is linear and continuous on $C^2[0,1]$, equation (5.8) can be written in the following form:

$$\frac{\partial \bar{\Psi}}{\partial t} + A\bar{\Psi} = f(\lambda, \Psi_0, \bar{\Psi}) \tag{5.9}$$

Then we are sure that the conditions in the Liapunov's main theorem of stability theory in Banach space [97] can be satisfied. We check this by handling with the nonlinear equation (5.4) after the transformation $\bar{\Psi}(s,t) = \Psi(s,t) - \Psi_0(s)$ and using notation $\cdot = \frac{\partial}{\partial t}$, $' = \frac{\partial}{\partial s}$,

$$\dot{\bar{\Psi}} = \Psi_0'' + \bar{\Psi}'' + \lambda \sin\left(\Psi_0 + \bar{\Psi}\right)$$

$$= \bar{\Psi}'' + \lambda(\sin\left(\Psi_0 + \bar{\Psi}\right)) - \sin\Psi_0)$$

$$= \bar{\Psi}'' + \lambda(\sin\Psi_0 \cos\bar{\Psi} + \cos\Psi_0 \sin\bar{\Psi} - \sin\Psi_0)$$

$$= \bar{\Psi}'' - \lambda \sin\Psi_0(1 - \cos\bar{\Psi}) + \lambda \cos\Psi_0 \sin\bar{\Psi}$$

$$= \bar{\Psi}'' + \lambda \cos(\Psi_0)\bar{\Psi} + \lambda \cos \Psi_0 (\sin \bar{\Psi} - \bar{\Psi}) - \lambda \sin \Psi_0 (1 - \cos \bar{\Psi}),$$

then from the last expression, for small $\bar{\Psi}$ holds

$$\dot{\bar{\Psi}} = \bar{\Psi}'' + \lambda \cos(\Psi_0)\bar{\Psi} + O(||\bar{\Psi}||^3) + O(||\bar{\Psi}||^2) = A\bar{\Psi} + O(||\bar{\Psi}||^3) + O(||\bar{\Psi}||^2). \tag{5.10}$$

Therefore the nonlinear term of the last expression has the character needed in the theorem for any defined norm. For instance we could choose a Banach space like $C^2[0,1] = \{f : [0,1] \longrightarrow I\!\!R | f'' \in C[0,1]\}$ together with the norm

$$||f|| = \sum_{i=0}^{2} \max_{0 \leq x \leq 1} |f^{(i)}(x)|, f^{(0)}(x) = f(x) \in C^2[0,1].$$

So according to the Liapunov's main theorem of stability theory in B space we know $\bar{\Psi} = 0$ is asymptotically stable if the real parts of all eigenvalues of A are negative, and it is unstable if the real part of some eigenvalue is positive. That means the stability of Ψ_0 can be determined by discussion on the eigenvalues of the linearized equation in no critical case(no eigenvalue has positive real part, but some eigenvalues have zero real part).

Now assuming $\bar{\Psi}(s,t) = e^{\delta t}\phi(s)$, substituting it into the last equation gives

$$\delta e^{\delta t}\phi(s) - e^{\delta t}\frac{\partial^2 \phi}{\partial s^2} = \lambda \cos(\Psi_0(s))e^{\delta t}\phi(s).$$

Thus

$$\frac{\partial^2 \phi}{\partial s^2} + (\lambda \cos(\Psi_0) - \delta)\phi = 0, \\ \phi(0) = 0, \quad \phi'(1) = 0. \tag{5.11}$$

This is an eigenvalue problem of elliptic equation, normally this problem has more than one eigenvalues [17], [12]. As $A\phi = \frac{\partial^2 \phi}{\partial s^2} + \lambda \cos(\Psi_0)\phi$ is a self-adjoint linear operator, then the eigenvalues of (5.11) are all real numbers[73]. The principal (largest) eigenvalue of (5.11) has the following expression:

$$\delta_m = \sup_{\phi \in M} \frac{(\phi, \frac{\partial^2 \phi}{\partial s^2}) + (\phi, \lambda \cos(\Psi_0(s))\phi)}{(\phi, \phi)}, \tag{5.12}$$

where $M = \{\phi(s)|\phi \in C^2[0,1], \phi \not\equiv 0, \phi(0) = 0, \phi'(1) = 0\}$ and (ϕ, ϕ) is the inner product defined in M by $(\phi, \psi) = \int_0^1 \phi(s)\psi(s)ds$.

Therefore the stability of $\Psi_0(s)$ depends on the sign of δ_m determined by (5.12). On the theory and calculation of eigenvalues one can consult [17] and other books on partial differential equations and functional analysis.

As an application of this method we take the stability study of the model for $\gamma = 0, \alpha = \pi$ as an example. Now the corresponding equation (5.3) is:

$$\frac{\partial \Psi}{\partial t} - \frac{\partial^2 \Psi}{\partial s^2} = \lambda \sin \Psi,$$

$$\Psi(0) = 0, \Psi'(1) = 0.$$

We intend to discuss the stability of trivial solution $\Psi_0(s) = 0$, so the corresponding eigenvalue problem is:

$$\frac{\partial^2 \phi}{\partial s^2} + (\lambda - \delta)\phi = 0,$$

$$\phi(0) = 0, \quad \phi'(1) = 0.$$

The principal eigenvalue is

$$
\begin{aligned}
\delta_m &= \sup_{\phi \in M} \frac{(\phi, \frac{\partial^2 \phi}{\partial s^2}) + (\phi, \lambda \cos(0)\phi)}{(\phi, \phi)} \\
&= \sup_{\phi \in M} \frac{\int_0^1 \phi(s)\phi''(s)ds + \lambda \int_0^1 \phi^2(s)ds}{\int_0^1 \phi^2(s)ds} \\
&= \sup_{\phi \in M} \frac{-\int_0^1 \phi'^2(s)ds + \lambda \int_0^1 \phi^2(s)ds}{\int_0^1 \phi^2(s)ds} \\
&= \lambda - \min_{\phi \in M} \frac{\int_0^1 \phi'^2(s)ds}{\int_0^1 \phi^2(s)ds}.
\end{aligned}
\tag{5.13}
$$

According to [12],

$$\min_{\phi \in M} \frac{\int_0^1 \phi'^2(s)ds}{\int_0^1 \phi^2(s)ds} = \frac{\pi^2}{4},$$

therefore we have the result: if $\lambda > \frac{\pi^2}{4}$, then $\Psi_0 = 0$ is P-unstable, if $\lambda < \frac{\pi^2}{4}, \Psi_0 = 0$ is P-stable, $\lambda = \frac{\pi^2}{4}$ is therefore a critical value for stability.

From expression (5.12) we have the following conclusion:

1. If a solution Ψ_0 of (2.2) lies totally in the area where $\cos(\Psi_0) \leq 0$, that is $\Psi_0(s)$ lies totally in one of the intervals: $(\frac{-3\pi}{2}, -\frac{\pi}{2}), (\frac{\pi}{2}, \frac{3\pi}{2})$ and $(\frac{5\pi}{2}, 3\pi)$, then this solution is P-stable, because the corresponding δ is negative. For instance, the normal solution of (2.2) for $\gamma = 0, \alpha = 0.25\pi, p = 25$ is P-stable, because it lies in $0.5\pi < \Psi < \pi$ for $s \in [0, 1]$, see figure 5.15.

2. If $p < \frac{\pi^2}{4}$, then for any γ and α the solution of (2.2) is P-stable. This comes from the fact that:

$$\min_{\phi \in M} \frac{\int_0^1 \phi'^2 ds}{\int_0^1 \phi^2 ds} \geq \frac{\pi^2}{4},$$

and equality holds if and only if ϕ is proportional to the first eigenfunction of $\frac{d^2\Psi}{ds^2} + \lambda\Psi = 0, \Psi(0) = 0, \Psi'(1) = 0$ [12].

From 2. we know in our model, the loss of stability occurs the most easily for Euler's rod. In order to get some stability behavior of other solutions which are not mentioned in last conclusion, we intend to quote a result on eigenvalue from [49]: Let a second-order self-joint linear operator be of the form

$$L\Psi = -(p(x)\Psi')' - q(x)\Psi, \Psi(0) = \Psi'(1) = 0, \tag{5.14}$$

where p', q are continuous functions on the interval $[0,1]$. Then the eigenvalue problem $L\Psi = \mu\Psi$ has the following characters:

- All eigenvalues are simple, they form a countable infinite sequence $\{\mu_n\}, \mu_n \to \infty$.

- There is a least eigenvalue.

- The number of negative eigenvalues of (5.14) is the same as the number of interior zeros of the solution to the equation

$$L\Psi = 0, \Psi(1) = 1, \Psi'(1) = 0. \tag{5.15}$$

Comparing with this eigenvalue problem, in our model $p(x) = 1, q(x) = \cos\Psi_0(s), \mu = -\lambda = -p$, we try to use this result in our model. According to the above discussion and Liapunov's theorem if the solution of $L\Psi = 0$ with boundary condition has at least one zero, then Ψ_0 is P-unstable, but if the solution has no zero we could not directly get the result on stability, because 0 is possibly an eigenvalue of $L\Psi = \mu\Psi$, in this case the corresponding solution is called neutrally stable. We try to deal with the stability of $\bar\Psi = 0$ or Ψ_0 along the following way: using the manifold method and numerical calculation to get the approximate expression of Ψ_0 whose stability is to be studied, then solving the equation (5.15) to determine if it has zero point. We take some cases for example.

Case 1. $\gamma = 0, \alpha = \pi$, along the two solutions born from the trivial one after the first bifurcation, the solutions of (5.15) have no zero, according to [49], they are P-stable and except these two solutions all other solutions for $p > \frac{\pi^2}{4}$ correspond to a solution of (5.15) having at least one zero (see, for example, figure 5.5 and 5.6), then at least one δ in our model is positive, so Ψ_0 is P-unstable.

Case 2. As in the study of bifurcation, we give a special attention to the cases that correspond to γ, α near $0, \pi$. From the results obtained in bifurcation discussion, we know when γ, α are slightly different from $0, \pi$, the bifurcations for $\gamma = 0, \alpha = \pi$ will change
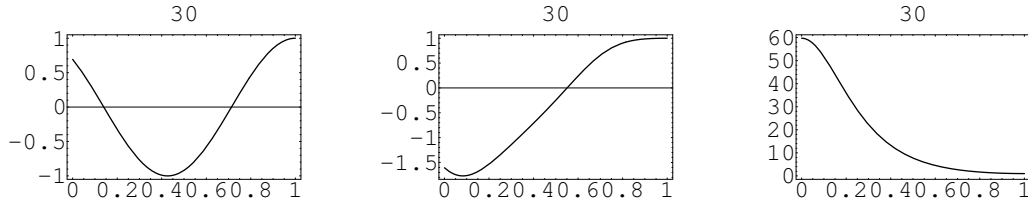
Figure 5.5: Solution curves of (5.15) for $\gamma = 0, \alpha = \pi, p = 30$ and different $\omega_0 = 0 < \omega_0^1 < \omega_0^2$ (from left to right).
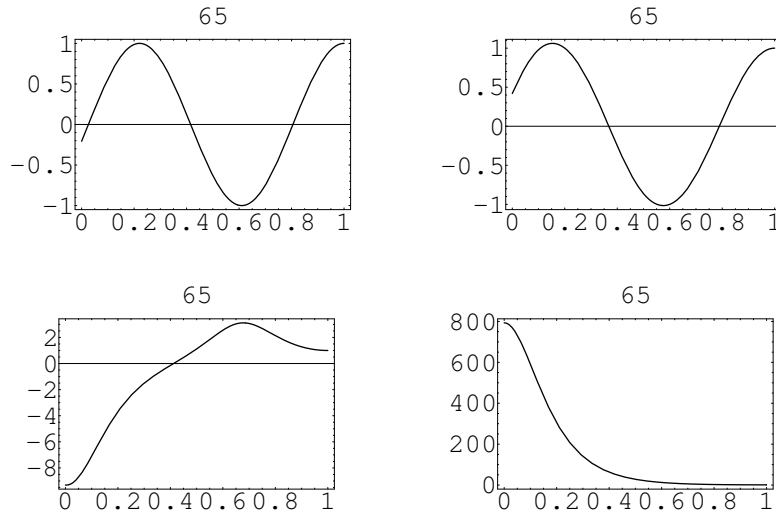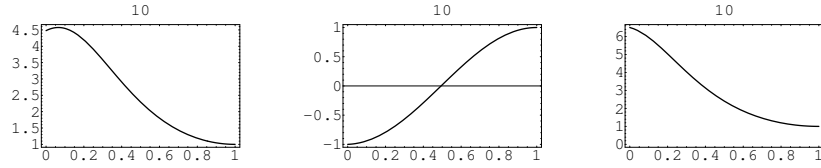

Figure 5.6: Solution curves of (5.15) for $\gamma = 0, \alpha = \pi, p = 65$ and different $\omega_0 = 0 < \omega_0^1 < \omega_0^2 < \omega_0^3$ along (1,1)-(1,2)-(2,1)-(2,2).

to turning points (see figure 4.25 and 4.31). The first turning points are formed from different branches of bifurcation diagram for $\gamma = 0, \alpha = \pi$. For discussion on the solutions of (5.15) corresponding to the $\omega_0' s$ on these new branches in bifurcation diagrams, we take one example, namely $\gamma = 0, \alpha = 0.9\pi$. From the solution curves (see figures 5.7 and 5.8) of (5.15), we know the first turning point can be a changing point for P-stability, but the second turning point is not a changing point for P-stability.

Case 3. For discussion on the cases that have turning points and bifurcation points let us take $\gamma = 0.5\pi, \alpha = -0.296851\pi$ as an example and discuss the corresponding solutions of (5.15) (see figure 5.9). These solutions show that the bifurcation point in this case is not changing point for P-stability, but the first bifurcation, that is turning point, may work as this kind of point.
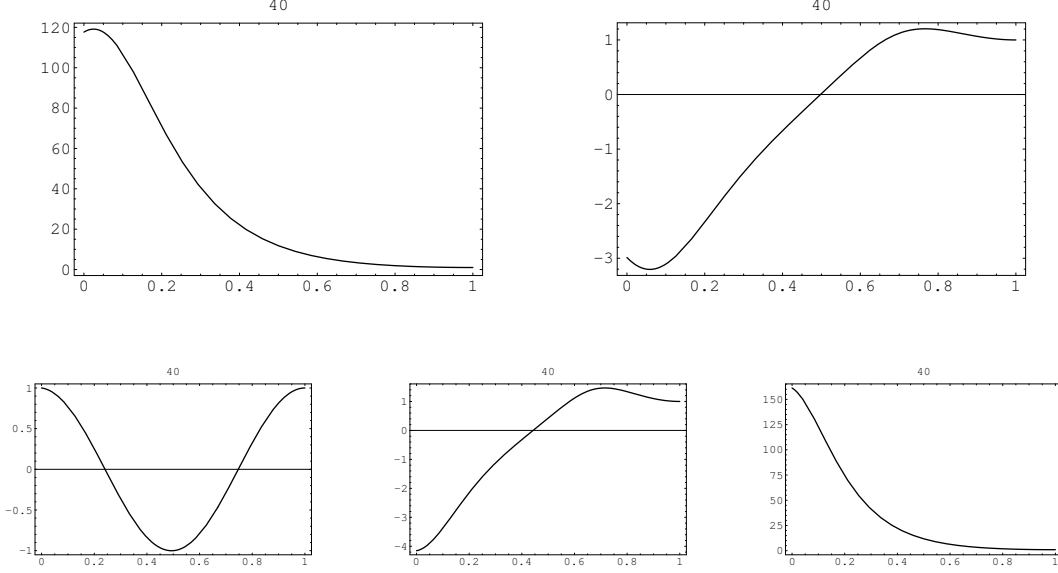
Figure 5.7: Solution curves of (5.15) for $\gamma = 0, \alpha = 0.9\pi, p = 10$ and different $\omega_0^1 < \omega_0^2 < \omega_0^3$ from left to right.

If we recall the case for bifurcation of $X-$ type (for instance the case $\gamma = 0.5\pi, \alpha = 0.84975\pi$) we know it may be changing point of P-stability (see figure 5.10). The phase curves and configurations of the two cases were given in figure 4.33 and 4.34.

For stability study on the solutions of (2.2) corresponding to the $\omega_0's$ located near the first bifurcations in bifurcation diagrams. we have another idea, which is based on the stability study of another ODE constructed from (5.4).

We build an ordinary differential equation in the following way, our pendulum equation has the form

$$
\begin{cases}
\psi'' = F(\psi, \lambda) \\
\psi(a) = \psi_a \\
\psi'(b) = \psi_b',
\end{cases}
\tag{5.16}
$$

where F is a smooth function. First we consider the corresponding initial value problem

$$
\begin{cases}
\psi'' = F(\psi, \lambda) \\
\psi(a) = \psi_a \\
\psi'(a) = \psi_a'.
\end{cases}
\tag{5.17}
$$

For each given ψ_a', (5.17) has a unique solution, but it is not guaranteed to be solution of (5.16). Let $\psi(s, \psi_a, \psi_a', \lambda)$ be a solution of (5.17), if it is also a solution of (5.16), it must satisfy the following condition

$$
\psi'(b, \psi_a, \psi_a', \lambda) = \psi_b'.
$$

We call this conditional equation a bifurcation equation, it is no doubt that each ψ_a' satisfying bifurcation equation corresponds to one solution of (5.16), therefore our task now is transferred to the study of the relations between the solution of (5.16) and the zero of bifurcation equation.

Note: Just as what we mentioned in constructing mathematical model, we could also take points (ψ_b, ψ_b') under consideration first, try to find the solution $\psi = \psi(s, \psi_b, \psi_b', \lambda)$ of the
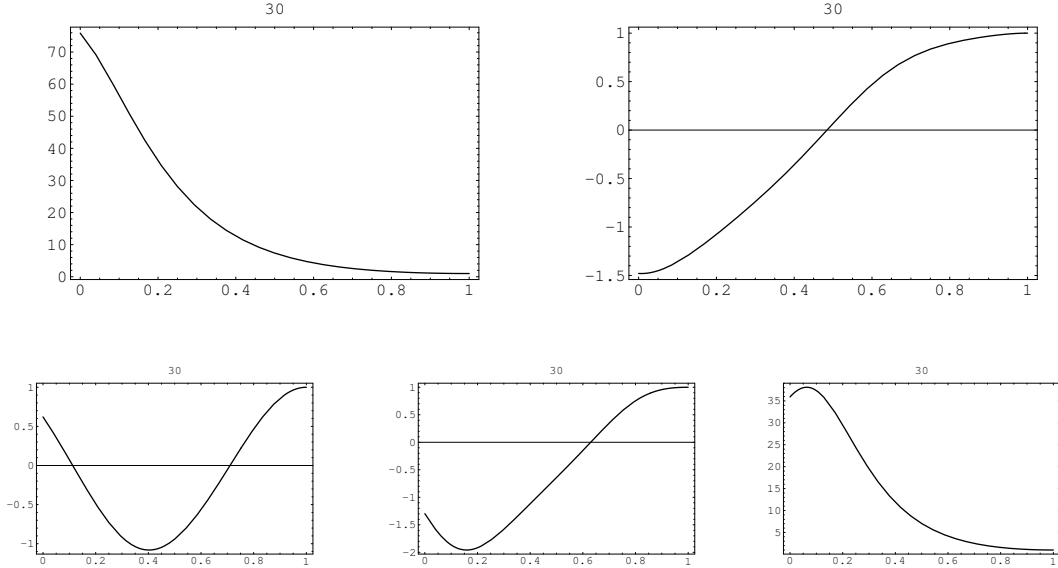
Figure 5.8: Solution curves of (5.15) for $\gamma = 0, \alpha = 0.9\pi, p = 40$ and different $\omega_0^1 < \omega_0^2 < \omega_0^3 < \omega_0^4 < \omega_0^5$ along first row and then second row from left to right.

BVP problem $\psi'' = F(\psi, \lambda), \psi(b) = \psi_b, \psi'(b) = \psi_b'$, and the task is therefore the handing of the equation

$$\psi(a, \psi_b, \psi_b', \lambda) = \psi_a.$$

Here we emphasize especially that following this correspondence between root $\psi_a' := \omega_0$ of bifurcation equation and solution of (5.16), from now on, we would take the solution of (5.16) as a root of bifurcation equation. And small perturbation to ψ_0 could be thought as small perturbation to ω_0. With this consideration, through the related partial differential equation, the stability study of the solution of (5.16) is turned to the stability study of the equilibrium of bifurcation equation, the study can be carried out to the equation

$$\frac{d\psi_a'}{dt} = \psi'(b, \psi_a, \psi_a', \lambda) - \psi_b'. \qquad (*)$$

For a solution of (5.4) starting from a small neighborhood of ψ_0, we get a solution of (*) starting from a small neighborhood of ω_0 in the following way: first $\psi_0(s) \longleftrightarrow \omega_0$ is one-to-one. For $\psi(s, 0) = \psi_0(s) + \tilde{\psi}(s)$, from a solution $\psi(s, t)$ of (5.4), we let $\omega(t) := \psi_s'(0, t)$, if $t = t_0, \omega(t_0) = \omega_0$, then $\psi_0(s) = \psi(s, t_0)$. If for arbitrary $\tilde{\psi}$ holds $t \to \infty, \omega(t) \to \omega_0$, then "$\psi(s, \infty)$" $= \psi_0(s)$, the static solution ψ_0 is P-stable, otherwise it is P-unstable. And this stability could be determined by (*) with ψ_a' substituted by $\omega_0(t)$. Some methods of the

Figure 5.9: Solution curves of (5.15) for $\gamma = 0, \alpha = -0.296851\pi, p = 30$ and different $\omega_0^1 < \omega_0^2 < \omega_0^3 < \omega_0^4 < \omega_0^5$ along first row and then second row from left to right.

stability study for singular point of ODE's could be used here for (*). If a singularity of equation(*) is stable (unstable), then the corresponding solution of (5.16) is thought to be P-stable (unstable).

Remark 1: The bifurcation equation could be obtained theoretically or numerically in different ways, so the right side of (*) could be of different forms, but they are strongly equivalent [6].

Definition 5.7 *Two smooth functions $F(s, \lambda)$ and $G(s, \lambda)$ are said to be strongly equivalent near (s_0, λ_0), if there exist two functions $R(s, \lambda)$ and $T(s, \lambda)$ with*

$$T(s_0, \lambda_0) = s_0, \left(\frac{\partial T}{\partial s}\right)_{(s_0, \lambda_0)} > 0, R(s, \lambda) > 0,$$

such that

$$F(s, \lambda) = R(s, \lambda)G(T(s, \lambda), \lambda).$$

The geometrical explanation of this definition is: $T(s, \lambda)$ can be thought as a state transformation, it is not singular with respect to s at (s_0, λ_0) and offers an one-to-one mapping from (s, λ) to $T(s, \lambda)$ for fixed λ as $\left(\frac{\partial T}{\partial s}\right)_{(s_0, \lambda_0)} > 0$, while $R(s, \lambda)$ can be considered as a transformation to $G(s, \lambda)$, which could be an amplification or reduction on $G(s, \lambda)$, F, G have same zero point as $R(s, \lambda) > 0$. Based on this ground, the equilibriums of $F = 0$ and
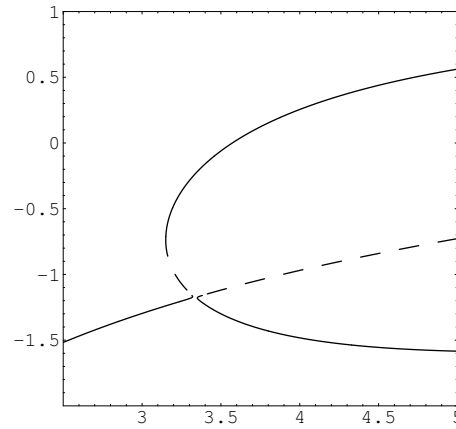
Figure 5.10: A typical sample of stability diagram for $\gamma = 0.5\pi, \alpha = 0.84975\pi$, dashed (solid) curves correspond to P-unstable (neutrally stable) solutions of (2.2).

$G = 0$ have the same qualitative structure.

Remark 2: This method is only used locally near the first bifurcations in the bifurcation diagrams.

Overview of the idea:

1. For the BVP of ordinary differential equation:

$$\psi'' + F(\psi, \psi', \lambda) = 0, B(\psi(a), \psi(b), \psi'(a), \psi'(b)) = 0, \qquad (5.18)$$

   construct the corresponding BVP of the partial differential equation of parabolic type:

$$\frac{\partial\psi}{\partial t} - \frac{\partial^2\psi}{\partial s^2} = F(\psi, \psi', \lambda), B(\psi(t, a), \psi(t, b), \psi'(t, a), \psi'(t, b)) = 0;$$
$$(5.19)$$

2. For the first critical value λ_0 of λ, using methods available to get the bifurcation equation $f(x, \lambda)$=0 of (5.18), a solution $\psi = \psi_0(s)$ of (5.18) corresponds to a root $x = x_0$ of bifurcation equation;

3. In a small neighborhood of (x_0, λ_0) find a simple function $\bar{f}(x, \lambda)$, which is normally a polynomial function and strongly equivalent to $f(x, \lambda)$;

4. The stability of $\psi = \psi_0(s)$ is the same as that of $x = x_0$, which can be determined via $\frac{dx}{dt} = \bar{f}(x, \lambda_0)$ (or $\frac{dx}{dt} = -\bar{f}(x, \lambda_0)$) with practical meaning of the solutions under consideration and the sign does not affect the critical value for stability.

Now we use this method to the stability study of our model for $\gamma = 0, \alpha = \pi$ (Euler's rod), in the discussion we use the equivalent equation of (2.2),

$$\begin{cases} \Psi'' + \lambda \sin \Psi = 0 \\ \Psi(0) = 0, \Psi'(1) = 0, \end{cases} \tag{5.20}$$

with $\lambda = p$. The corresponding partial differential equation is

$$\begin{cases} \frac{\partial \Psi}{\partial t} - \Psi'' - \lambda \sin \Psi = 0 \\ \Psi(t, 0) = 0, \Psi'(t, 1) = 0 \end{cases} \tag{5.21}$$

Now we try to get the bifurcation equation with Liapunov-Schmidt method (see appendix 1). Let

$$f(\Psi, \lambda) = \Psi'' + \lambda \sin \Psi,$$

here f can be thought as an operator acting in $\bar{Y}$ (defined below). Concerning the boundary condition of (5.20), we have $f(0, \lambda) = 0$ for any λ, that is $\Psi = 0$ is a solution of $f(\Psi, \lambda) = 0$ for any λ.

Now we compose two sets of functions

$$\bar{Y} = \{y | y \in C^2[0, 1]; y(0) = y'(1) = 0\};$$

$$\bar{Z} = \{z | z \in C^0[0, 1]\},$$

in these two sets, norm is defined as follows

$$||z|| = \sup[|z(\sigma)|, 0 \le \sigma \le 1],$$

$||y|| = \max\{\sup[|y^i(\sigma)| : 0 \le \sigma \le 1], i = 0, 1, 2$, where y^i represents the derivative of y of order $i\}$.

The linear part of f is

$$B(\lambda)\Psi = \Psi'' + \lambda\Psi, \quad \Psi \in \bar{Y}.$$

$B(\lambda, \Psi) = 0$ gives

$$\lambda_n = (n\pi + \frac{\pi}{2})^2, \Psi = c_n \sin (n\pi + \frac{\pi}{2})\sigma, n = 0, 1, 2....$$

For the smallest eigenvalue

$$n = 0, \lambda = \lambda_0 = \frac{\pi^2}{4}, \Psi = c \sin \frac{\pi}{2}\sigma,$$

so $\sin\frac{\pi}{2}\sigma$ can be chosen as a basis for $Kern(B(\frac{\pi^2}{4}))$, that gives

$$Kern(B(\frac{\pi^2}{4})) = Span[\sin\frac{\pi}{2}\sigma]$$

$$\bar{Y} = Span[\sin\frac{\pi}{2}\sigma] \oplus M,$$

where

$$M = Kern(B(\frac{\pi^2}{4}))^{\perp} = \{\Psi \in \bar{Y} :< \Psi, q >= 0, q \in Kern(B(\frac{\pi^2}{4}))\},$$

because $B(\frac{\pi^2}{4}) = \frac{d^2}{d\sigma^2} + \frac{\pi^2}{4}$ is Fredholm operator of zero index (see appendix 1), so

$$CodimRange(B(\frac{\pi^2}{4})) = 1 = DimKern(B(\frac{\pi^2}{2})).$$

As $B(\frac{\pi^2}{4}) = B^*(\frac{\pi^2}{4})$, so $B^*(\frac{\pi^2}{4})w = 0$ offers $w = d\sin\frac{\pi}{2}\sigma$, which can be taken as a basis of $\bar{N}$, thus

$$\bar{N} = Kern(B^*(\frac{\pi^2}{4})) = Span[\sin\frac{\pi}{2}\sigma]$$

$$\bar{Z} = Span[\sin\frac{\pi}{2}\sigma] \oplus Range[B(\frac{\pi^2}{4})].$$

Decomposing Ψ as $\Psi_0 + r$ with $\Psi_0 \in Kern(B(\frac{\pi^2}{4}))$ and $r \in M$, we have

$$\Psi = ac\sin\frac{\pi}{2}\sigma + \bar{r}(ac\sin\frac{\pi}{2}\sigma, \triangle\lambda),$$

where $\triangle\lambda = \lambda - \frac{\pi^2}{4}$ is very small. The order of a included in $\bar{r}$ is at least 2, but $f(\Psi, \lambda) = -f(-\Psi, \lambda)$ indicates that the order is not less than 3 [6].

In $\bar{Y}$ and $\bar{Z}$ we define the inner product as follows

$$< \Psi_1, \Psi_2 >:= \int_0^1 \Psi_1(\sigma)\Psi_2(\sigma)d\sigma.$$

With the help of Liapunov-Schmidt method, we have bifurcation function

$$F(a, \triangle\lambda) = \int_0^1 f(ac\sin\frac{\pi}{2}\sigma + \bar{r}(ac\sin\frac{\pi}{2}\sigma, \triangle\lambda), \frac{\pi^2}{4} + \triangle\lambda)d\sin\frac{\pi}{2}\sigma d\sigma.$$

Expanding $f(\Psi, \lambda)$ as the Taylor series of Ψ at $\Psi = 0$,

$$f(\Psi, \frac{\pi^2}{4} + \triangle\lambda) = \Psi'' + (\frac{\pi^2}{4} + \triangle\lambda)(\Psi - \frac{1}{6}\Psi^3 + 0(\Psi^5)),$$

substituting $\Psi = ac\sin\frac{\pi}{2}\sigma + \bar{r}(ac\sin\frac{\pi}{2}\sigma, \triangle\lambda)$ into this expression and then into F gives

$$f(ac\sin\frac{\pi}{2}\sigma + \bar{r}(ac\sin\frac{\pi}{2}\sigma, \triangle\lambda), \frac{\pi^2}{4} + \triangle\lambda)$$

$$= \bar{r}'' + \frac{\pi^2}{4}\bar{r} + ac\triangle\lambda\sin\frac{\pi}{2}\sigma - \frac{\pi^2}{4}\frac{1}{6}ac\sin\frac{\pi}{2}\sigma^3 + 0(|\triangle\lambda|a^3, a^5)$$

and

$$F(a, \triangle\lambda) = \int_0^1 (\bar{r}'' + \frac{\pi^2}{4}\bar{r}$$

$$+ac\triangle\lambda\sin\frac{\pi}{2}\sigma - \frac{\pi^2}{24}ac\sin\frac{\pi}{2}\sigma^3 + 0(|\triangle\lambda|a^3, a^5))d\sin\frac{\pi}{2}\sigma\, d\sigma,$$

because

$$\bar{r}'' + \frac{\pi^2}{4}\bar{r} \in Rang(B(\frac{\pi^2}{4}))$$

and

$$\sin\frac{\pi}{2}\sigma \in Kern(B^*(\frac{\pi^2}{4})) = \bar{N} = Range(B(\frac{\pi^2}{4}))^\perp,$$

we have

$$\int_0^1 (\bar{r}'' + \frac{\pi^2}{4}\bar{r})\sin\frac{\pi}{2}\sigma\, d\sigma = 0,$$

so

$$F(a, \triangle\lambda) = c_1 a\triangle\lambda - c_3 a^3 + 0(|\triangle\lambda|a^3, a^5)$$

with

$$c_1 = cd\int_0^1 \sin^2\frac{\pi}{2}\sigma d\sigma = \frac{1}{2}cd,$$

$$c_3 = \frac{\pi^2}{24}c^3 d\int_0^1 \sin^4\frac{\pi}{2}\sigma\, d\sigma = \frac{\pi^2}{64}c^3 d,$$

here c, d are arbitrary constants, take $c, d > 0$, then $c_1, c_3 > 0$, so near $(\frac{\pi^2}{4}, 0)$ the bifurcation function is strongly equivalent to

$$\bar{F} = c_1 a\triangle\lambda - c_3 a^3,$$

therefore in a sufficiently small neighborhood of $(\frac{\pi^2}{4}, 0)$, the equilibriums of bifurcation equation $F = 0$ are near the equilibriums of $\bar{F} = 0$ and have the same stability behavior, which can be determined via

$$\frac{da}{dt} = c_1 a\triangle\lambda - c_3 a^3. \tag{5.22}$$

The singular points of last equation satisfy

$$c_1 a\triangle\lambda - c_3 a^3 = 0,$$

According to the stability behavior of equilibrium of ODE with separable variables [43], if $\triangle\lambda < 0$, $a = 0$ is the only singular point, it is stable, the corresponding solution of (2.2) is P-stable. If $\triangle\lambda > 0$, there are three singular points: $a_0 = 0, a_{1,2} = \pm\sqrt{\frac{c_1}{c_3}\triangle\lambda}$, satisfying

$a_1 < a_0 < a_2$, that means $\triangle\lambda = 0$ is a critical value for bifurcation equation. With the same discussion as before, we know, $a_0 = 0$ is unstable, while the other two are stable, so the correspond solutions of (2.2) are P-unstable and P-stable respectively.

Here we should indicate that a in our discussion acts as ω_0 and $\triangle\lambda$ corresponds the perturbation of p in our model, so we have the result

Theorem 5.2 *For pendulum equation (2.2) with $\alpha = \pi, \gamma = 0$, there exists a critical value p_c of p, such that $(0,0)$ is P-stable for $p < p_c$, P-unstable for $p > p_c$ and furthermore the numerical value of p_c is $\frac{\pi^2}{4}$.*

Note: For the original model of straight elastic rod, this critical value of p corresponds to $\frac{\pi^2 EI}{4L^2}$ of the acting force.

Using ω_0, λ to replace $a, \triangle\lambda$ we show our stability result near $(\pi^2, 0)$ in figure 5.11,
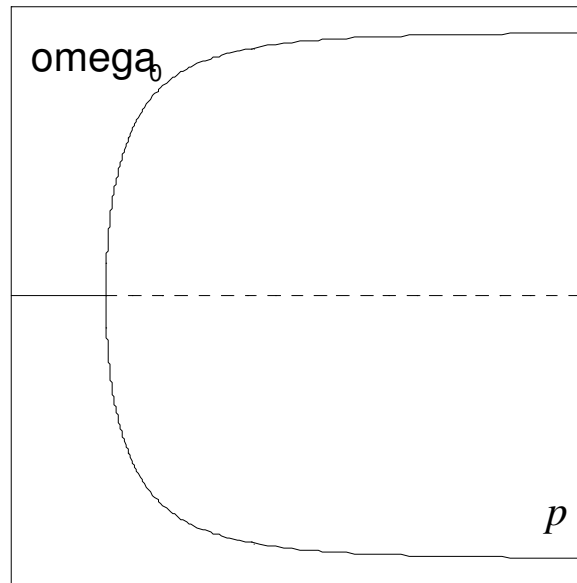
Figure 5.11: The stability diagram of (5.20) near the first bifurcation point.

in figure 5.11 equilibriums on the solid branches are P-stable and those on dashed branch are P-unstable as discussed above. A sample of corresponding configurations of (2.3) in this case can be seen in figure 4.7.

Note: In choosing constants, say c, d, we have considered the practical background of our model, for instance, we know the straight form (or zero solution) of the elastic rod is stable for sufficiently small p according to its mechanical meaning, which corresponds to $\triangle\lambda < 0$, so we choose $c, d > 0$.

Now we use this method to stability study of a deformed straight rod, whose left end is fixed and the right end can move horizontally along its axis, the acting force on it points to the left(see figure 5.12)[60]. The deflection of the rod follows the differential equation
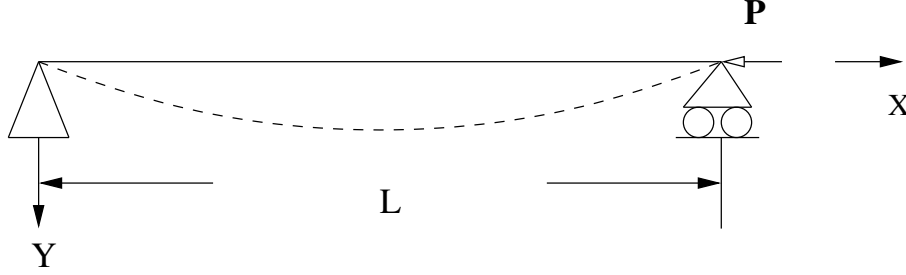
Figure 5.12: The originally straight elastic rod with an axial acting force.

$$EI\frac{d^2Y}{dX^2} + PY[1 - (\frac{dY}{dX})^2]^{\frac{1}{2}} = 0, \qquad (5.23)$$

with boundary value condition

$$Y(0) = 0, Y(L) = 0.$$

Introducing the following transformation

$$\lambda = \frac{PL^2}{EI}, \sigma = \frac{S}{L}, y = \frac{Y}{L}$$

gives

$$\begin{cases} \ddot{y} + \lambda(1 - \dot{y}^2)^{\frac{1}{2}}y = 0 \\ y(0) = 0, y(1) = 0, \end{cases} \qquad (5.24)$$

where ˙ represents the derivative with respect to σ. The corresponding partial differential equation is

$$\begin{cases} \frac{\partial y}{\partial t} - \ddot{y} - \lambda(1 - \dot{y}^2)^{\frac{1}{2}}y = 0 \\ y(t, 0) = 0, y(t, 1) = 0 \end{cases} \qquad (5.25)$$

Now we use Liapunov-Schmidt method again to get the bifurcation equation. Let

$$f(y, \lambda) = \ddot{y} + \lambda(1 - \dot{y}^2)^{\frac{1}{2}}y,$$

concerning the boundary condition of (5.24), we have $f(0, \lambda) = 0$ for any λ, that means $y = 0$ is a solution of $f(y, \lambda) = 0$ for any λ.

The two sets of functions defined in last model are now

$$\bar{Y} = \{y | y \in C^2[0, 1]; y(0) = y(1) = 0\},$$

$$\bar{Z} = \{z|z \in C^0[0,1]\},$$

in these two sets, norm is defined as in last model. The linear part of f is

$$B(\lambda)y = \ddot{y} + \lambda y.$$

From $B(\lambda)y = 0$ we have

$$\lambda_n = n^2\pi^2, y_n = c_n \sin n\pi\sigma, n = 1, 2, ...$$

For the smallest eigenvalue $\lambda = \lambda_1 = \pi^2, y = c\sin\pi\sigma$ and

$$Kern(B(\pi^2)) = Span[\sin\pi\sigma]$$

$$\bar{Y} = Span[\sin\pi\sigma] \oplus M,$$

where

$$M = Kern(B(\pi^2))^\perp = \{y \in \bar{Y} :< y, q >= 0, q \in Kern(B(\pi^2))\}.$$

Using the procedure as in last example, we get the bifurcation function

$$F(\omega_0, \lambda) = \bar{c}_1\lambda\omega_0 - \bar{c}_3\omega_0{}^3 + 0(|\lambda|\omega_0{}^3, \omega_0{}^4)$$

with

$$\bar{c}_1 = cd \int_0^1 \sin^2\pi\sigma d\sigma = \frac{1}{2}cd,$$

$$\bar{c}_3 = \frac{1}{2}c^3d\pi^4 \int_0^1 \sin^2\pi\sigma\cos^2\pi\sigma d\sigma = \frac{\pi^4}{16}c^3d,$$

here c, d are arbitrary constant, take $c, d > 0$, then $\bar{c}_1, \bar{c}_3 > 0$, so near $(\pi^2, 0)$ the bifurcation function is strongly equivalent to

$$\bar{F} = \bar{c}_1\lambda\omega_0 - \bar{c}_3\omega_0{}^3,$$

therefore with the same discussion as in last model, we know, near $(\pi^2, 0)$, the stability of this model can be also presented with figure 5.11.

Now we try to discuss a typical case, for example $\gamma = 0.25\pi, \alpha = 0$, having turning point at the first bifurcation (see figure 8.1). In this case, according to the concept of strong equivalence and some results from [32], [41], we could make the assumption that in a sufficiently small neighborhood of the first bifurcation, the bifurcation function is strongly equivalent to

$$\bar{F}(\omega_0, \lambda) = -\omega_0(\omega_0{}^2 - \lambda\omega_0 + c), \quad \lambda = p, c > 0,$$

The negative sign in the function is determined according to the fact that when p is small the unique solution of equation (2.2) is P-stable. If $\lambda^2 - 4c < 0$, $\bar{F}(\omega_0, \lambda) = 0$ has only one equilibrium $\omega_0 = 0$, it is P-stable. If $\lambda^2 - 4c > 0$, then there are two more equilibriums:

$$\omega_0^{1,2} = \frac{1}{2}(\lambda \pm \sqrt{\lambda^2 - 4c}), 0 < \omega_0^1 < \omega_0^2,$$

so $\omega_0^1(\omega_0^2)$ in P-unstable (stable). The stability diagram is shown in 5.13 (left).
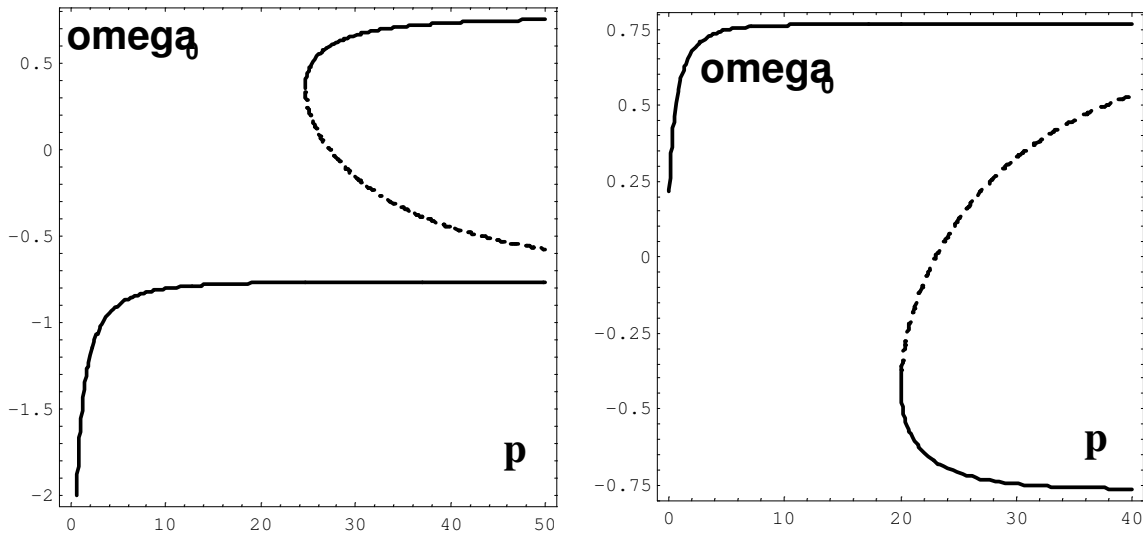
Figure 5.13: The stability diagram of the equilibrium of (2.2) for $\gamma = 0.25\pi, \alpha = 0$ (left) and $\gamma = 0, \alpha = 0.25\pi$ (right).

Some corresponding phase curves of equation (2.2) and configurations of equation (2.3) are shown in figure 5.14.

The same discussion on the case of $\gamma = 0, \alpha = 0.25\pi$ gives the stability behavior shown in figure 5.13(right) and some correspond phase curves of (2.2) and configurations of (2.3) are shown in figure 5.15.

Referring bifurcation diagrams and above examples, the P-stability of solutions of pendulum equation (2.2) could possibly be lost or gained at the first turning point, bifurcation point of pitchfork type or X-type.
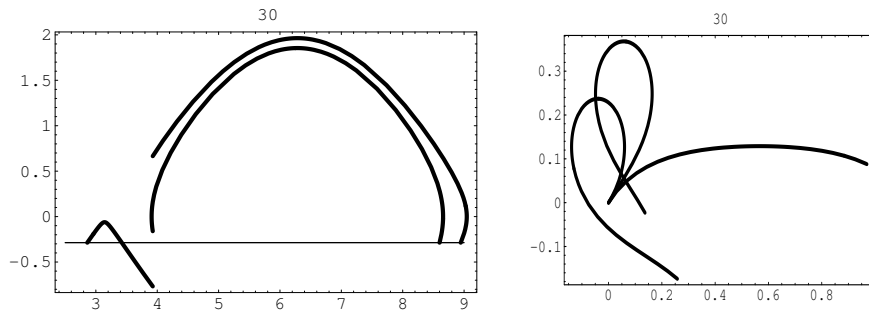
Figure 5.14: The phase curves of (2.2) (left) and configurations of (2.3) for $\gamma = 0.25\pi, \alpha = 0$ and $p = 30$ (right).
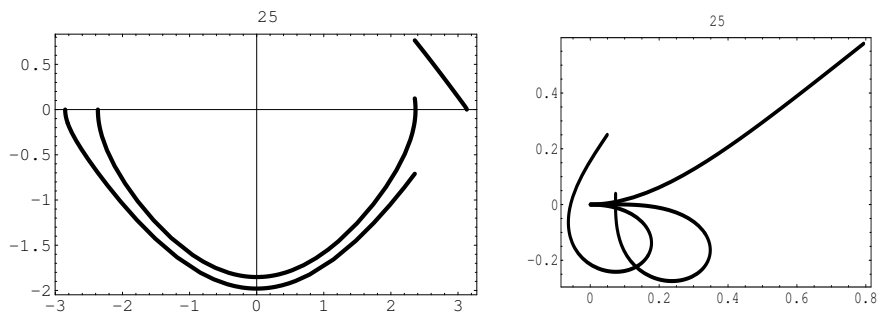
Figure 5.15: The phase curves of (2.2) (left) and configurations of (2.3) (right) for $\gamma = 0, \alpha = 0.25\pi$ and $p = 25$.

Chapter 6

Characteristics as nonlinear springs and gripper elements

6.1 Spring characteristics
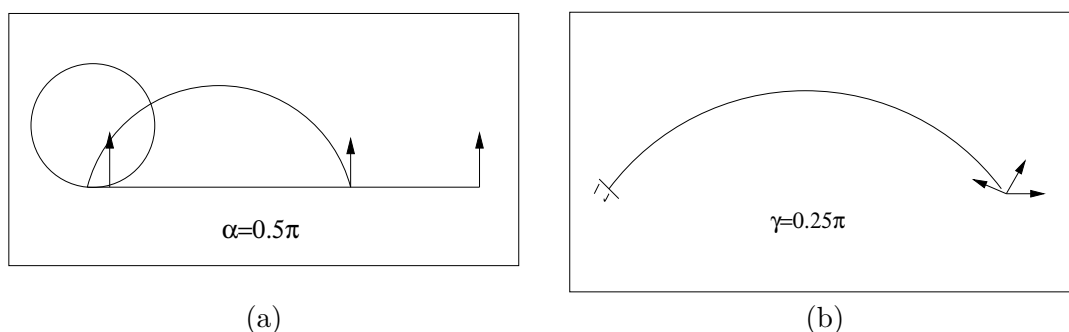
Figure 6.1: The undeformed elastic circular arcs with a fixed direction of force $\alpha = \frac{\pi}{2}$ (a) and a arc $\gamma = \frac{\pi}{4}$ with different directions of force(b).

Using ω_0 obtained with the methods given in section **4**, we can get the implicit solution of equations (2.2) and (2.3). Taking the elastic circular rod as a nonlinear spring, we should discuss the displacement of the free end of the rod, particularly $y(1) = h(\gamma, \alpha, p)$. The aim is to make it clear how h changes with the parameters. Figure 6.2(a) shows a sample relation between h and p for fixed α (say $\frac{\pi}{2}$) and different γ ($\gamma = 0(\frac{\pi}{8})\pi$, the corresponding undefromed arcs are shown in figure 6.1), or in other words, this figure shows the half openings of different arcs with fixed direction of acting force. The result says that, for
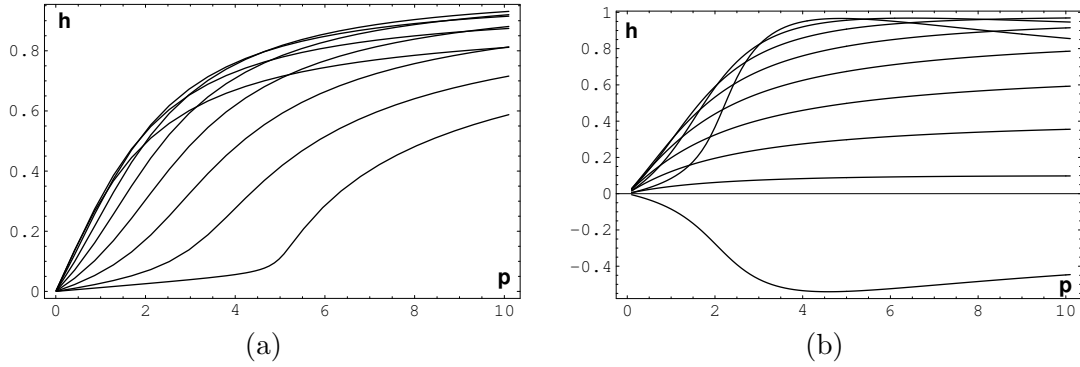
Figure 6.2: (a): h *vs.* p for $\alpha = \frac{\pi}{2}$ and $\gamma = 0(\frac{\pi}{8})\pi$ (on the left from top to the bottom). (b): h *vs.* p for $\gamma = \frac{\pi}{4}$, $\alpha = 0(\frac{\pi}{8})\frac{7\pi}{8}$ (in the middle from the curve above the p axis to the top) and π (under the p axis).
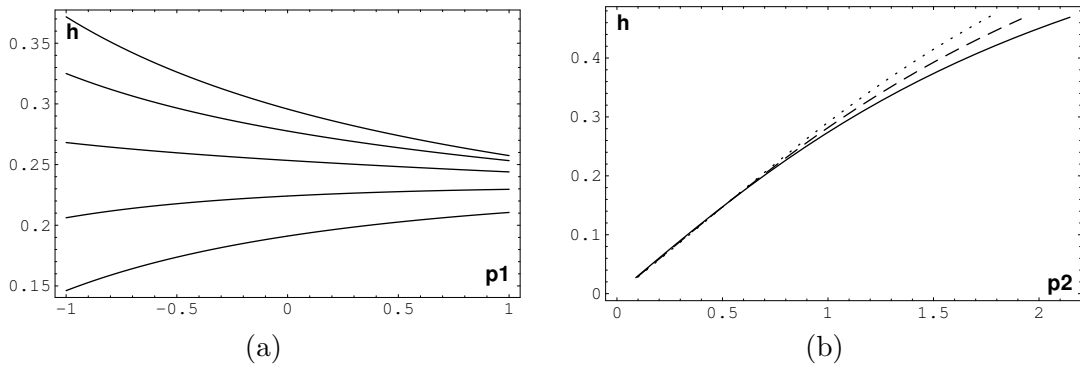
Figure 6.3: (a): h *vs.* p_1 for $\gamma = \frac{\pi}{4}(\frac{\pi}{16})\frac{\pi}{2}$ (from bottom to the top), $p_2 = 1$. (b): p_2 *vs.* h for $\gamma = \frac{\pi}{4}, \mu = 0.1$ (dotted line), 0.3 (dashed line), 0.5 (solid line).

fixed γ, h increases with p (not too big). That means: for each original rod of fixed form, the bigger the acting force is, the larger the half opening h will be. But for fixed and smaller p, $h(., \frac{\pi}{2}, p)$ decreases with γ, and for relatively bigger p, h increases with γ first, reaches a maximal value for some γ and then decreases with γ. It means that it is easier (harder) to deform the rod with smaller (bigger) curvature, when p is relatively small. Figure 6.2(b) shows a sample result for fixed γ (say $\frac{\pi}{4}$) and different α (the corresponding undeformed rod is shown in figure 6.1), or the half opening of one special rod with different direction of acting force. The result states that for each $\alpha < \frac{7\pi}{8}$, $h(\frac{\pi}{4}, \alpha, .)$ increases with p (not too big), while $h(\frac{\pi}{4}, \alpha, .)$ has a maximal value for $\alpha \geq \frac{7\pi}{8}$. When p is fixed, $h(\frac{\pi}{4}, ., p)$ has a maximal value for some value of α. In order to determine the influence of the weight grasped on the

(a)   (b)
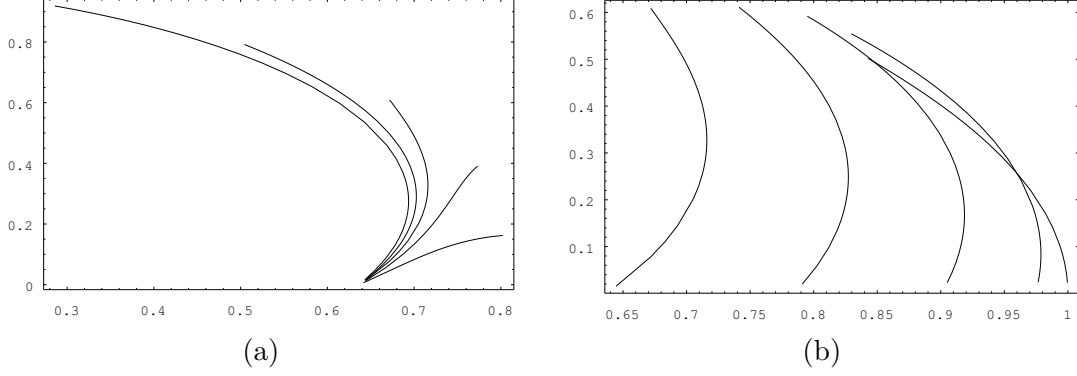
Figure 6.4: (a): The tracks of the end points of the solutions of (2.3) for $\gamma = \frac{\pi}{2}, p \in$ $(0.1, 10)$ and $\alpha = 0(\frac{\pi}{8})\frac{\pi}{2}$ from right to the left. (b): The tracks of the end points of the solutions of (2.3) for $\alpha = \frac{\pi}{4}, p \in (0.1, 10)$ and $\gamma = 0(\frac{\pi}{8})\frac{\pi}{2}$ from right to the left).

half opening, we discussed also the dependence of h on p_1 for fixed p_2 (see figure 6.3(a)), here p_1, p_2 represents the horizontal, vertical components of the acting force. The result shows that when $\gamma \leq \frac{5\pi}{16}$, h increases with p_1, it decreases with p_1 when $\frac{3\pi}{8} \leq \alpha \leq \frac{\pi}{2}$. The result about the relation between h and p_2 for different $\mu = 0.1(0.2)0.5$ (μ denotes the friction coefficient at rest) is described in figure 6.3(b). Figure 6.4 shows the track of the end points of the deformed arcs.$\gamma = \frac{\pi}{2}$ Figure 6.4(a) shows the result for the half ring with different directions of force, the result states that for half ring, when $p \in [0, 10]$, the maximal half opening increase as α increases in $[0, \frac{\pi}{2}]$. Figure 6.4(b) shows the result for different arcs with a fixed direction of force $\alpha = \frac{\pi}{4}$. One can get the information how the free ends of the deformed elastic rods move under the acting force and how they are affected by parameters.

6.2 Gripper characteristics

The use of the double symmetric circular rods as a gripper relies on Coulomb's law in equilibrium: $|p_1| \leq \mu p_2$, practically μ ranges from 0.1 to 0.7. The peculiarity of this gripper type is: no external force needed for clamping the object, but needed for to loosen it. $G = 2|p_1|$ is the normed weight to be grasped. The maximal value of G (*i.e.*, $p_1 = \pm \mu p_2, \tan \alpha = \pm\frac{1}{\mu}$) is determined for given half opening h of the rods. For fixed μ, taking $\alpha = \arctan \frac{1}{\mu}$ or $\alpha = \pi - \arctan \frac{1}{\mu}$, through (2.2) and (2.3), h can be considered as a function of p ($0 \leq p \leq p_{max}$), here p_{max} is the value of p, under the action of which the tangent of the rod at its free end is parallel to the x axis. The reason for choosing this value is: in
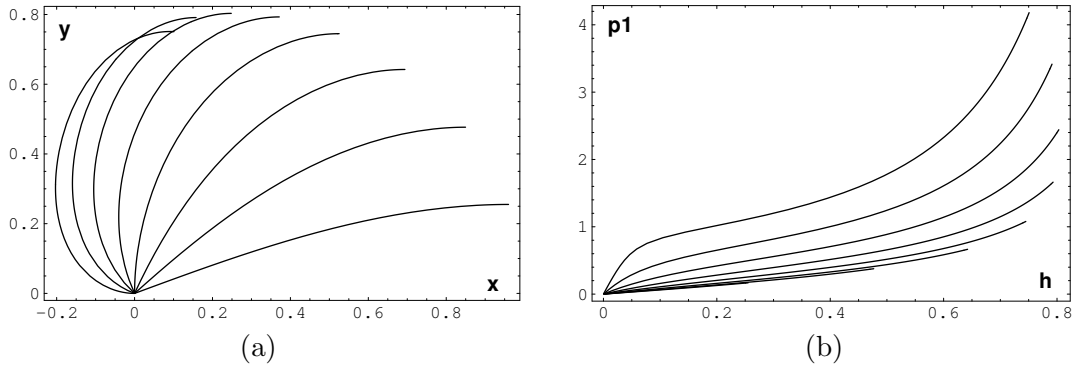
Figure 6.5: (a): Deformed rod with its tangent at the free end parallel to x axis for $\mu = 0.2$, $\gamma = \frac{\pi}{8}(\frac{\pi}{8})\pi$ (from right to left) and $p = p_{max}$. (b): p_1 *vs.* h for $\mu = 0.2$, and $\gamma = \frac{\pi}{8}(\frac{\pi}{8})\pi$(from bottom to the top).

practice, the gripper device composed of two circular rods holds a body, which is in touch with only the two free ends of circular rods, the case corresponds to $0 < p \le p_{max}$. When $p > p_{max}$, the free ends of the deformed circular rods are no more in touch with the object, provided the device and the body held are as shown in 2.1, but other part could touch the body. Figure 6.5(a) shows the configurations for $\mu = 0.2$ and $\gamma = \frac{\pi}{8}(\frac{\pi}{8})\pi$ with $p = p_{max}$. In the following discussion, the configurations are confined from the original undeformed form to the one corresponding to p_{max}. As $p_1 = p\cos\alpha$, then p_1 *vs.* h can be constructed. The result for $\mu = 0.2$ is taken as an example (see 6.5(b)). For any h the ordinate p_1 in figure 6.5(b) is half of the maximal weight G to be held. The results show that G is an increasing function of h. As α ranges from 0 to π, p_1 can be positive or negative and for some h there are more than one interesting and practical results. In order to compare the results for both cases, we considered also the relation between maximal p_1 (acting along positive x axis ($\alpha = \arctan\frac{1}{\mu}$) and negative x axis ($\alpha = \pi - \arctan\frac{1}{\mu}$)) and h. The results are shown in figure 6.6 and 6.7 (note: in these two figures p might be greater than p_{max}). From figure 6.5(b) we know that for the same half opening h, the weight grasped (described by p_1) increases as γ grows. So the device composed of two symmetric circular rods with large curvature is better than that composed of two circular rods with small curvature.
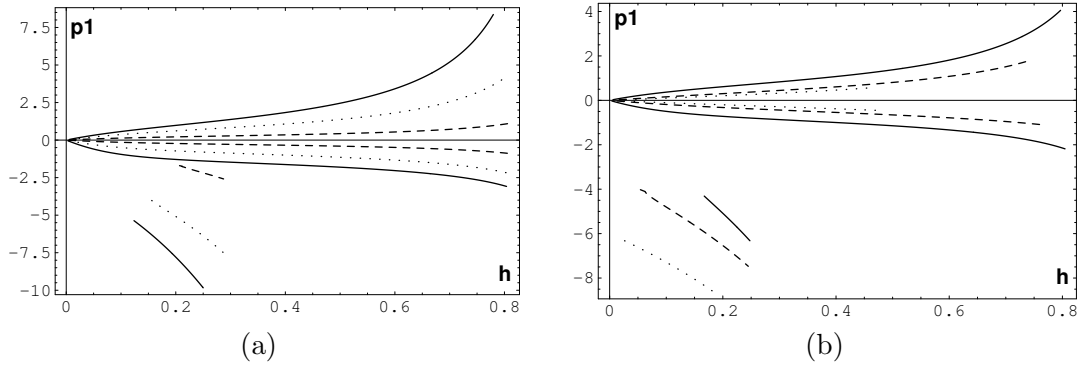
Figure 6.6: (a): Maximal p_1 *vs.* h for $\gamma = 0.75\pi$, μ=0.1 (dashed line), 0.3 (dotted line) and 0.5 (solid line). (b): Maximal p_1 *vs.* h for $\mu = 0.3$, and $\gamma = \frac{\pi}{4}$ (dotted line), $\frac{\pi}{2}$ (dashed line) and $\frac{3\pi}{4}$ (solid line).
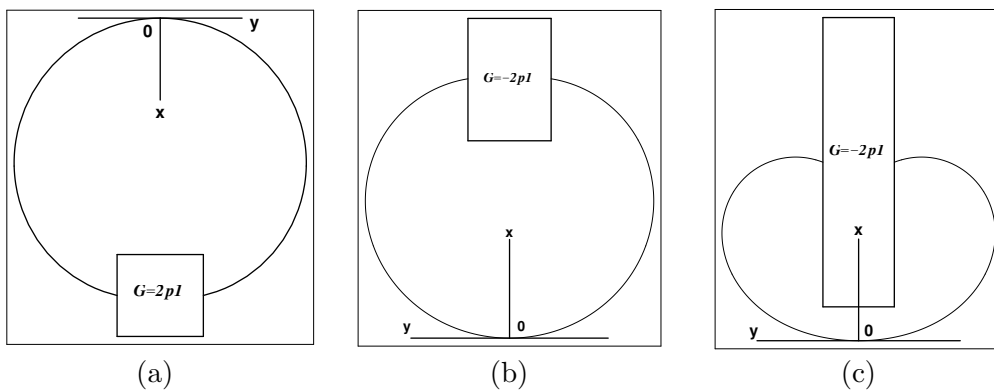

Figure 6.7: $\gamma = \frac{\pi}{2}, \mu = 0.5, h = 0.1054$, $p_1 = 0.266188$ (a), $p_1 = -0.343999$ (b), $p_1 = -2.23605$ (c).

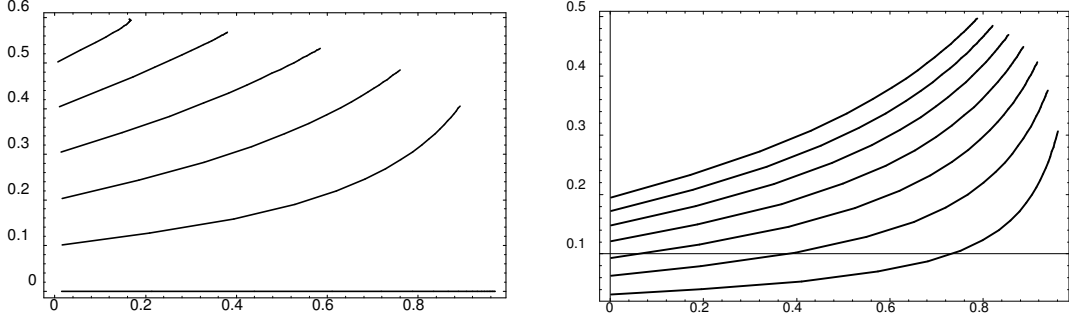## 6.3   Maximum point of the bending moment for $\gamma = \pi/2$

Figure 6.8: $\overline{\sigma}$ vs. h for $\alpha = 0(\frac{\pi}{10})\frac{\pi}{2}$ from bottom to the top (left), $\overline{\sigma}$ vs. h for $\mu = 0.1(0.1)0.7$ from bottom to the top (right).

In this section we intend to discuss the bend of the deformed elastic half ring, one of the typical characters of the deformation is the curvature of the deformed configuration, therefore we are interested in the maximum of the curvature, this is in turn connected with the bending moment of the half ring. The bending moment is a function of arc length s:

$$\mathcal{M}(s) = EI(\theta'(s) - \kappa). \tag{6.1}$$

Thus, using (2.1)

$$\mathcal{M}'(s) = EI\left\{\frac{1}{EI}[P_1 \sin\theta(s) - P_2 \cos\theta(s)]\right\} = P \sin[\theta(s) - \alpha]. \tag{6.2}$$

If $\bar{s}$ is an extreme point of the bending moment, then $\bar{s}$ must be a root of the equation

$$\theta(s) - \alpha = n\pi,$$

here n takes some certain different integers for different α and p. The above equation is also identical to $\Psi(t) = (n+1)\pi$. So we have:

$$\mathcal{M}''(\bar{t}) = -P\Psi'(\bar{t})\cos\Psi(\bar{t})$$

with $\bar{t} = \sqrt{p}\,\overline{\sigma}, \bar{s} = L\overline{\sigma}$.

From the above listed equations we can determine the values of $\bar{t}$, then $\overline{\sigma}$ and finally $\bar{s}$, which are the maximum points of $|\mathcal{M}|$. It is obvious that both $\overline{\sigma}$ and h are functions of

α and p. So we can take $\overline{\sigma}$ as a function of h. Its diagrams for $\alpha = 0(\frac{\pi}{10})\frac{\pi}{2}$ are shown in figure 6.8 (left).

From this result one can numerically determine at which point on the halfring the bending moment reaches its maximum value for a given half opening h.

For practical use, we have also investigated the same problem for $\mu = 0.1(0.1)0.7$ and p from 0.01 to 25 ($\tan \alpha = \frac{1}{\mu}$, *i.e.*, under maximal grasped weight acting to the right). The result is shown in figure 6.8 (right).

Chapter 7

Conclusion

In this dissertation the discussions were concentrated on large deformations of elastic clamped-free circular arcs under force load acting at their free ends. The topic of the research originated from practical problem in mechanics and engineering, it is of practical significance in connection with gripping devices and spring elements. The mathematical treatment is based on qualitative analysis of phase curves and numerical calculations of a pendulum equation with three parameters, which represent the concentrated force acting at the free end and the original shape of undeformed arc. For different values of these parameters the multiplicity and bifurcation of the pendulum equation were studied with manifold method introduced in this dissertation. For $p \leq 50$ the result was represented by bifurcation diagram, which showed the number of solutions, the value of parameters for multiplicity and change tendency of phase curves and configurations of (2.2) and (2.3). For $p \leq 50$, (2.2) has at most 7 solutions, its bifurcation diagrams include turning point, hysteresis point, bifurcation point of pitchfork and $X-$ type, they are the only points at which the stability behavior of motion and structural stability may change, the set of parameters corresponding to these points divides the parameter plane (one of the three parameters γ, α and p is fixed) into several zones, in each of them equation (2.2) and (2.3) have the same number of solutions. In stability study of nontrivial equilibriums the concept of P-stability was introduced. The methods introduced and used in this work were explained in general form and could be of importance in investigation on bifurcation and stability of boundary value problems of ordinary differential equations. In application the load-displacement characteristics (spring behavior) were given a particularly consideration, exploiting this, for a gripper that consists of two such arcs in symmetric configuration, the grasping forces at given opening width and friction coefficient were found, the principle for gripper is: opening the gripper by mens of auxiliary force, then holding a body by elasticity

and friction. At the same time the maximal bending moment was also studied.

Chapter 8

Appendix

8.1 Liapunov -Schmidt reduction

Liapunov-Schmidt reduction method is a very useful tool in the study of bifurcation for autonomous differential equation. Here we give a brief introduction to this method, the detailed description can be found in [6] and [16].

Let Y and Z be two completely normed linear spaces, in our applications, they are function spaces, satisfying certain regularity conditions. And $y \in Y$ satisfies some boundary condition. Let

$$F : Y \times I\!R \longrightarrow Z$$

and without loss of generality, we assume that

$$F(0, \lambda) = 0.$$

Her F is a non-linear operator, λ is a parameter. We intend to discuss the problem

$$F(y, \lambda) = 0$$

under the boundary condition

$$R(y(\xi), \lambda) = 0, \xi \in [0, 1].$$

Our task is to find the solution of the bifurcation problem

$$\begin{cases} F(y(\xi), \lambda) = 0, & \xi \in (a, b) \\ R(y(\xi), \lambda) = 0, & \xi \in \{a, b\}, \end{cases} \tag{8.1}$$

Without loss of generality, we suppose that $a = 0, b = 1$, $F(y(\xi), \lambda)$ is differentiable at point $(0, \lambda)$. Denote the Frechét derivative of F at $(0, \lambda)$ with $B(\lambda)$, that is

$$\lim_{||h||_Y \to 0} \frac{||F(y + h, \lambda) - F(y, \lambda) - B(\lambda)h||_Z}{||h||_Y} = 0,$$

here $||.||_Y, ||.||_Z$ are norms on Y, Z separately, and later we will use $||.||$ to replace both of them. Suppose further that $B(\lambda)$ be compact linear operator and the above formula be analytic, first let $y = 0$ in the above formula, and then for convenience denote h with y instead, we have

$$F(y, \lambda) = B(\lambda)y + T(y, \lambda)$$

with

$$\lim_{||y|| \to 0} \frac{T(y, \lambda)}{||y||} = 0.$$

If $B(\lambda) = L_0 + \lambda$, the already known result states that a necessary condition for $(0, \lambda_0)$ to be a solution of $F(y, \lambda)$ is that λ_0 is an eigenvalue of L_0.

Now at $\lambda = \lambda_0$ define

$$Kern(B(\lambda_0)) = \{y | y \in Y, B(\lambda_0)y = 0\}$$

and

$$Range(B(\lambda_0)) = \{z | z \in Z, \exists y \in Y \text{ such that } B(\lambda_o)y = z\}.$$

Since B is compact linear operator, $Kern(B)$ is finite dimensional and $codim Range(B(\lambda_0))$ is also of a finite dimension. Under the assumption that the Fredholm index of B

$$i(B) = dim Kern(B) - codim Range(B) = 0,$$

Y, Z could be decomposed as

$$Y = Kern(B(\lambda_0)) \oplus M, Z = N \oplus Range(B(\lambda_0))$$

with

$$M = Kern(B(\lambda_0))^{\perp} = \{y | y \in Y, < y, q >_Y = 0, \text{for all } q \in Kern(B(\lambda_0))\},$$

$$N = Range((B(\lambda_0)))^{\perp} = \{z | z \in Z, < z, w >_Z = 0, \text{for all } w \in Range(B(\lambda_0))\},$$

provided that inner products $< ., . >_Y, < ., . >_Z$ can be defined in Y, Z respectively (later we use $< ., . >$ to replace them). Let $\hat{P}$ be continuous projection defined on Z satisfying

$$Range(\hat{P}) = Range(B(\lambda_0)).$$

We try to find the solution (y, λ) of (8.1) near $(0, \lambda_0)$ with $||y||$ small and $\lambda = \lambda_0 + \triangle\lambda$ ($\triangle\lambda$ small), since $F(y, \lambda) \in Z$ and $\hat{P}$ has the same range as $B(\lambda_0)$, therefore the solution of (8.1) near $(0, \lambda_0)$ is the solution of the equations

$$\begin{cases} \hat{P}F(y, \lambda_0 + \triangle\lambda) = 0 \\ (I - \hat{P})F(y, \lambda_0 + \triangle\lambda) = 0, \end{cases} \tag{8.2}$$

where $||y||, ||\triangle\lambda||$ are very small. Decomposing y as $y = y_0 + r$ with $y_0 \in Kern(B(\lambda_0)), r \in M$ and substituting it into (8.2) give

$$\begin{cases} \hat{P}(B(\lambda_0 + \triangle\lambda)(y_0 + r) + T(y_0 + r, \lambda_0 + \triangle\lambda)) = 0, \\ (I - \hat{P})(B(\lambda_0 + \triangle\lambda)(y_0 + r) + T(y_0 + r, \lambda_0 + \triangle\lambda)) = 0. \end{cases} \tag{8.3}$$

As $B(\lambda_0)y_0 = 0, \hat{P}y_0 = 0$ since $y_0 \notin Range(B(\lambda_0))$ and $\hat{P}Br = Br$ since $B(\lambda_0)r \in Range(B(\lambda_0))$, the first equation of (8.3) is now

$$B(\lambda_0 + \triangle\lambda)r + \hat{P}T(y_0 + r, \lambda_0 + \triangle\lambda) = 0,$$

denoting the inverse of $B(\lambda_0)$ restricted to M with B^{-1}, the last equation can be solved for r,

$$r = \hat{r}(y_0, \lambda_0 + \triangle\lambda)$$

with $\hat{r} = 0(||y||^2)$ when $y \to 0$ since $\hat{r}(0, \lambda_0) = 0$ and $D_{y_0}\hat{r}(0, \lambda_0 + \triangle\lambda) = 0$. Substituting it into the second equation of (8.3), as $B(\lambda)\hat{r} = 0$ and $B(\lambda_0)y_0 = 0$, we get

$$\begin{aligned} f(y_0, \triangle\lambda) &= (I - \hat{P})F(y_0 + \hat{r}(y_0, \lambda_0 + \triangle\lambda), \lambda_0 + \triangle\lambda) \\ &= (I - \hat{P})(B(\lambda_0 + \triangle\lambda)(y_0 + \hat{r}) + T(y_0 + \hat{r}, \lambda_0 + \triangle\lambda)) \\ &= (I - \hat{P})(L_0 + \lambda_0 + \triangle\lambda)y_0 + (I - \hat{P})T(y_0 + \hat{r}, \lambda_0 + \triangle\lambda) \\ &= (I - \hat{P})((L_0 + \lambda_0)y_0 + \triangle\lambda y_0) + (I - \hat{P})T(y_0 + \hat{r}, \lambda_0 + \triangle\lambda) \\ &= \triangle\lambda y_0 + (I - \hat{P})T(y_0 + \hat{r}, \lambda_0 + \triangle\lambda) = 0. \end{aligned} \tag{8.4}$$

This function f is called the bifurcation function and equation (8.4) is called the bifurcation equation of bifurcation problem (8.1).

Now choosing a basis $\{y_i\}, i = 1, 2, ...$ for $Kern(B(\lambda_0))$ and a basis $\{w_i\}, i = 1, 2, ...$ for N, these bases contain the same number base vectors. Sometimes the basis for N could be chosen as the eigenvectors of $B^*(\lambda_0)$(here $B^*(\lambda_0)$ is the adjoint of B) owing to $N = Range(B(\lambda_0))^{\perp} = B^*(\lambda_0)$. Now

$$y_0 = \sum_{i=1}^{n} a_i y_i, ai \in \mathbb{R},$$

substituting it into the bifurcation equation, we get

$$f_i(a_i, \lambda_0) = < w_i, F(\sum_{i=1}^{n} a_i y_i + \hat{r}(\sum_{i=1}^{n} a_i y_i, \lambda_0 + \triangle\lambda)) >= 0, i = 1, 2, ...$$

From these equations we could get $a_i, i = 1, 2, ...$, then y_0 and at last $y = y_0 + r$.

This is the so called Liapunov-Schmidt method, we divided it into the following steps:

- Decompose

$$Y = Kern(B(\lambda_0)) \oplus M,$$

$$Z = N \oplus Range(B(\lambda_0));$$

- Write the original bifurcation problem in the form of (8.2);

- Let $y = y_0 + r$ with $y_0 \in Kern(B(\lambda_0)), r \in M$, solve the fist equation of (8.3) to get $r = \hat{r}(y_0, \lambda_0 + \triangle\lambda)$;

- Build bifurcation equation (8.4);

- Choose basis $\{y_i\}, i = 1, 2, ...$ for $Kern(B(\lambda_0))$ and basis $\{w_i\}, i = 1, 2, ...$ for $N = Range(B(\lambda_0))^{\perp} = B^*(\lambda_0)$, then solve

$$f_i(a_i, \lambda_0) = < w_i, F(\sum_{i=1}^{n} a_i y_i + \hat{r}(\sum_{i=1}^{n} a_i y_i, \lambda_0 + \triangle\lambda)) >= 0, i = 1, 2, ...$$

  to get $a_i, i = 1, 2, ...$

8.2 Structural stability

Here we intend to give a description to structural stability (see [2], [45]) as a complement to the definition in section 5.

We consider the differential equation

$$x' = f(x), x \in M,$$

we say that this equation defines a dynamic system and denote it as (M, v).

Definition 8.1 *Two systems* $(M_1, v_1), (M_2, v_2)$ *are said to be diffeomorphic if there exists a diffeomorphism* $h : M_1 \to M_2$ *transferring the vector field* v_1 *into* v_2.

This kind of equivalence is somewhat too fine, because if a diffeomorphism converts a singularity of v_1 into a singularity of v_2, then the linearization of these two systems at singularity have same eigenvalues. Under this kind of equivalence, the following two systems $x' = 2x, x' = 3x$ are not diffeomorphic at $x = 0$, but the qualitative structures of these two systems have no big difference. The following is a less strong equivalence by replacing diffeomorphism with homeomorphism.

Definition 8.2 *Two systems $(M_1, v_1), (M_2, v_2)$ are topologically equivalent if there exists a homeomorphism of the phase space of the system (M_1, v_1) onto the phase space of (M_2, v_2), which converts the phase flow of (M_1, v_1) into the phase flow of (M_2, v_2).*

Under this definition $x' = 2x, x' = 3x$ are obviously topologically equivalent. If we take the orientation of the flow into consideration, we have the following definition of topologically orbitally equivalent.

Definition 8.3 *Two systems $(M_1, v_1), (M_2, v_2)$ are topologically orbitally equivalent if there exists a homeomorphism of the phase space of the system (M_1, v_1) onto the phase space of (M_2, v_2), which converts the oriented phase curves of (M_1, v_1) into the phase curves of (M_2, v_2), no coordination of the motion on corresponding phase curves is required.*

According to this definition, $x' = 2x, x' = 3x$ are topologically orbitally equivalent., Finally we give the definition of structural stability.

Definition 8.4 *Let M be a compact manifold of class C^{r-1} $(r \geq 1)$, v be a vector field of class C^r. The system (M, v) is said to be structurally stable if there exists a neighborhood of v in the space C^1 such that every vector field in this neighborhood defines a system topologically orbitally equivalent to (M, v), and the homeomorphism realizing the equivalence is close to the identity homeomorphism.*

From this definition we see $x' = 2x$ is structurally stable, in the neighborhood of this equation, we define $y' = (2 + \epsilon)y$ and denote $x_0(t) = e^{2t}, y_0(t) = e^{(2+\epsilon)t}$, choose a mapping $x \to y$ with $x(t) = cx_0(t) \to y(t) = cy_0(t) = cx_0(t)^{(1+\frac{\epsilon}{2})}$, then this mapping is the homeomorphism needed in the definition.

8.3   Bifurcation diagrams of (2.2)

In this section we put most of the bifurcation diagrams obtained in section 4 together.
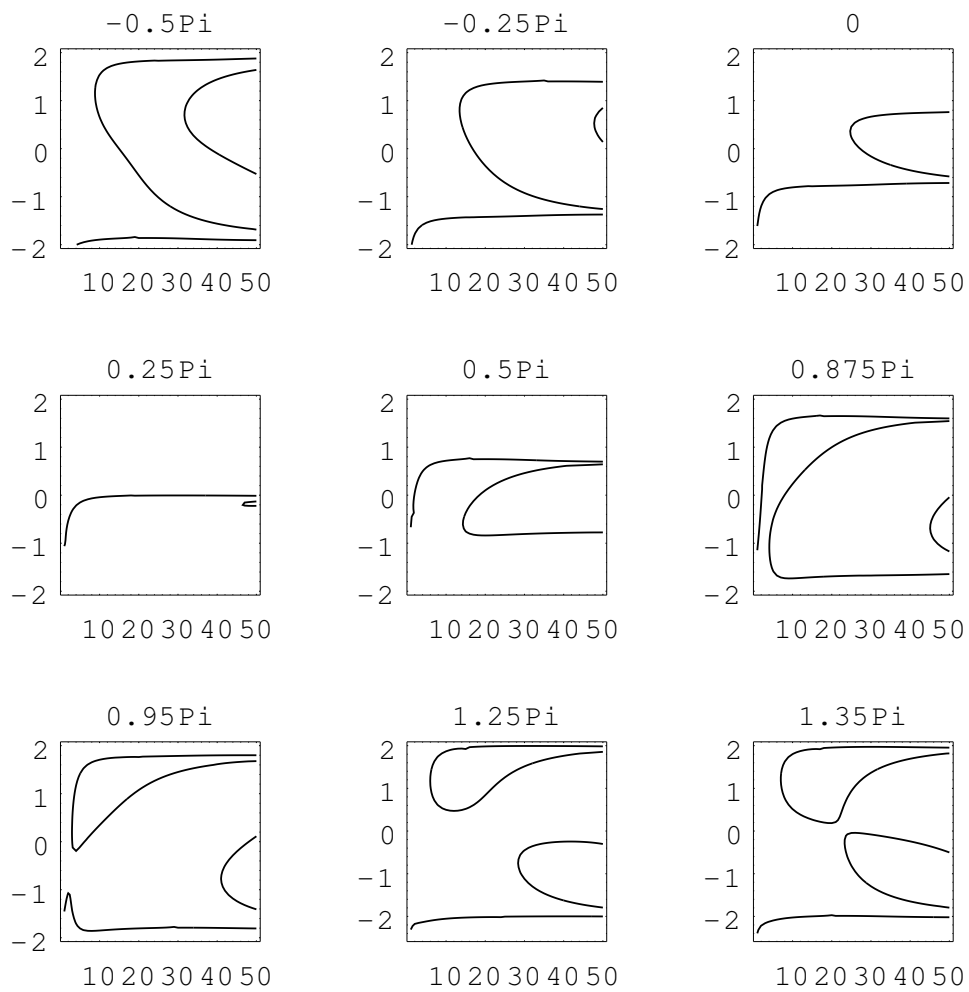
8.3.1   The bifurcation diagrams for fixed γ

Figure 8.1: Bifurcation diagram $\{(p, \alpha, \omega_0) | \alpha$ fixed, $p \in [0, 50]\}$ for $\gamma = 0.25\pi$, (α values above diagrams).
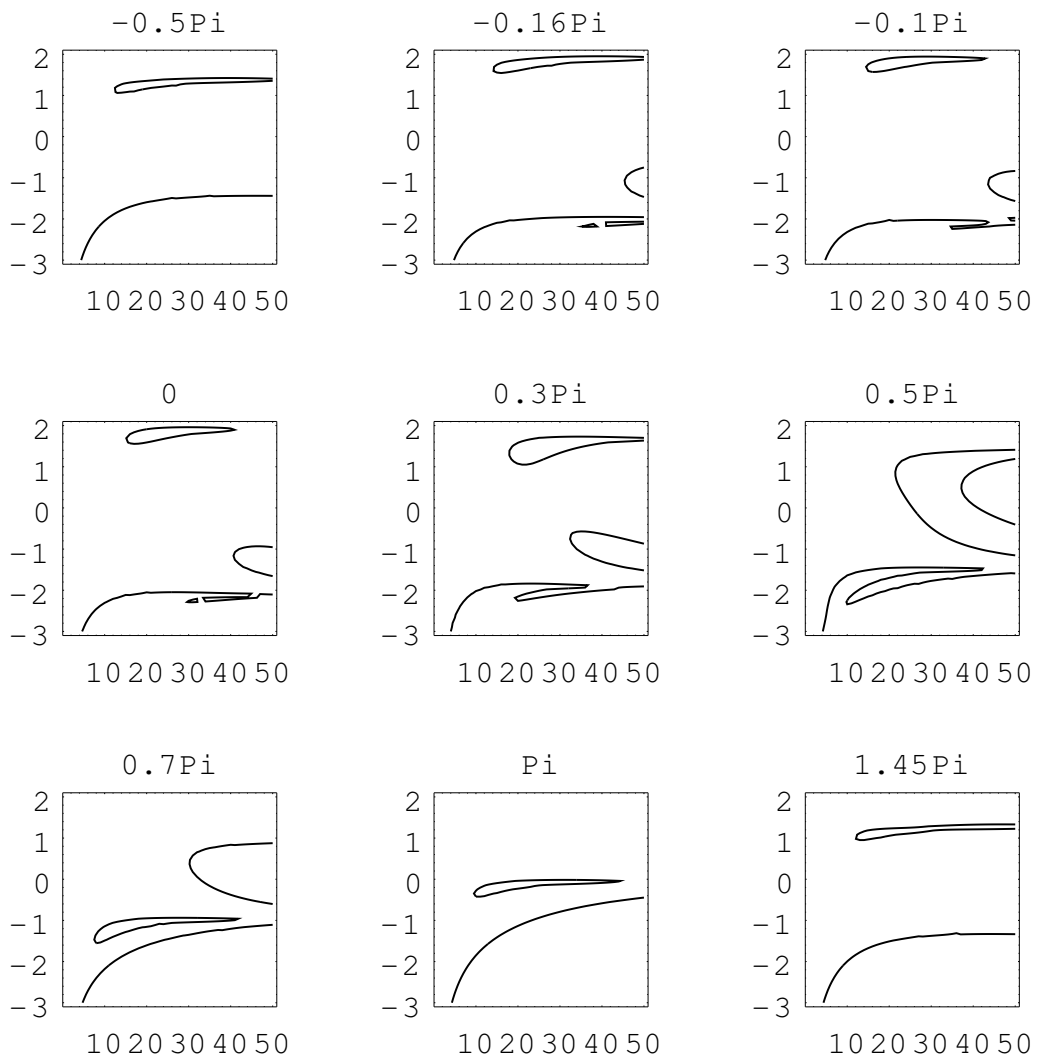
Figure 8.2: Bifurcation diagram $\{(p, \alpha, \omega_0) | \alpha$ fixed, $p \in [0, 50]\}$ for $\gamma = \pi$, (α values above diagrams).
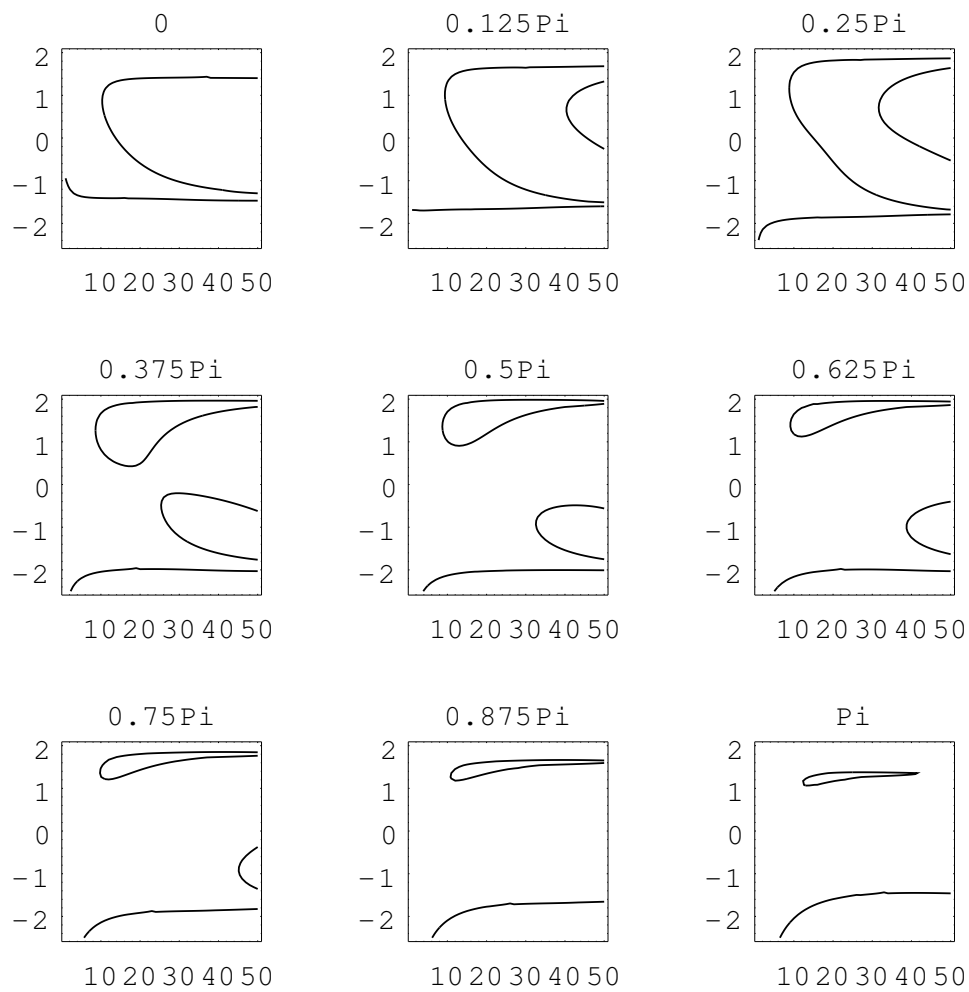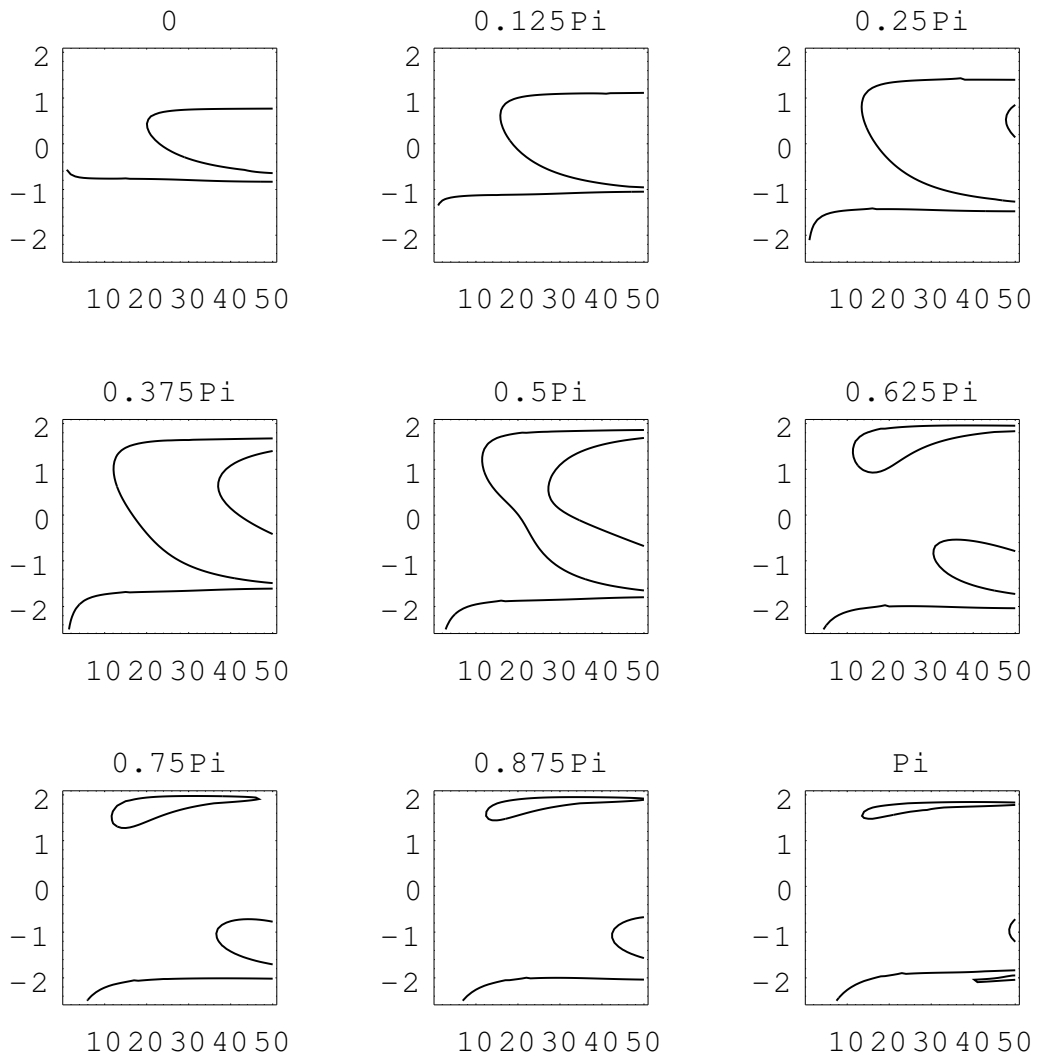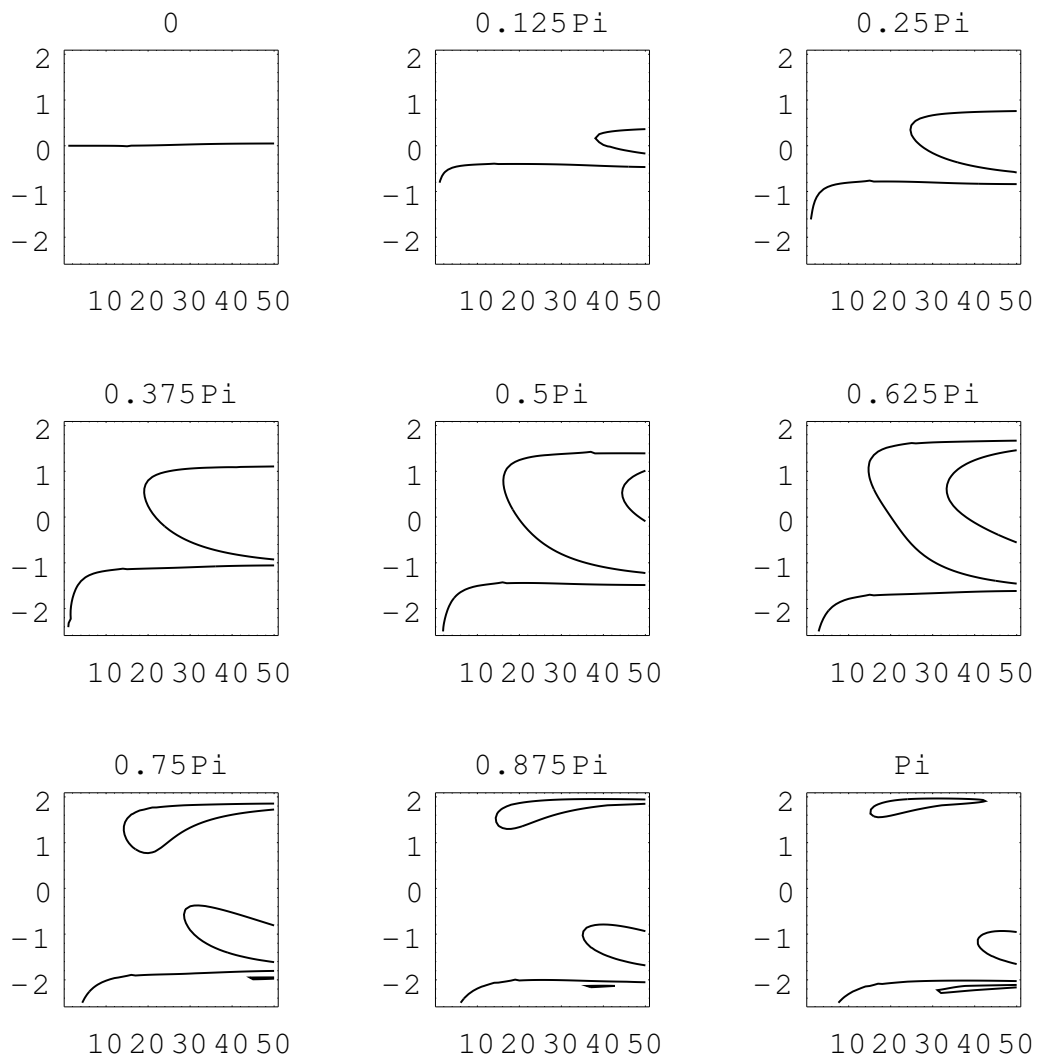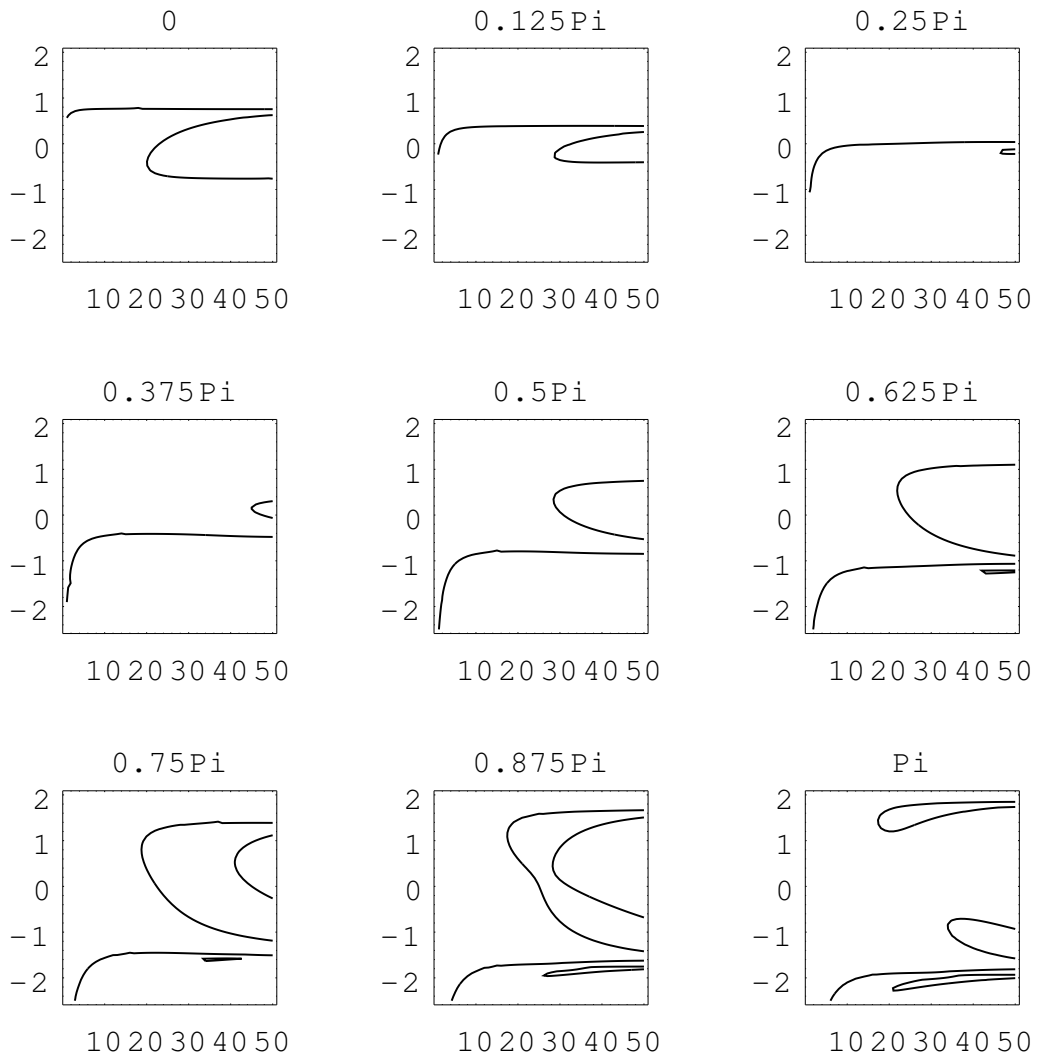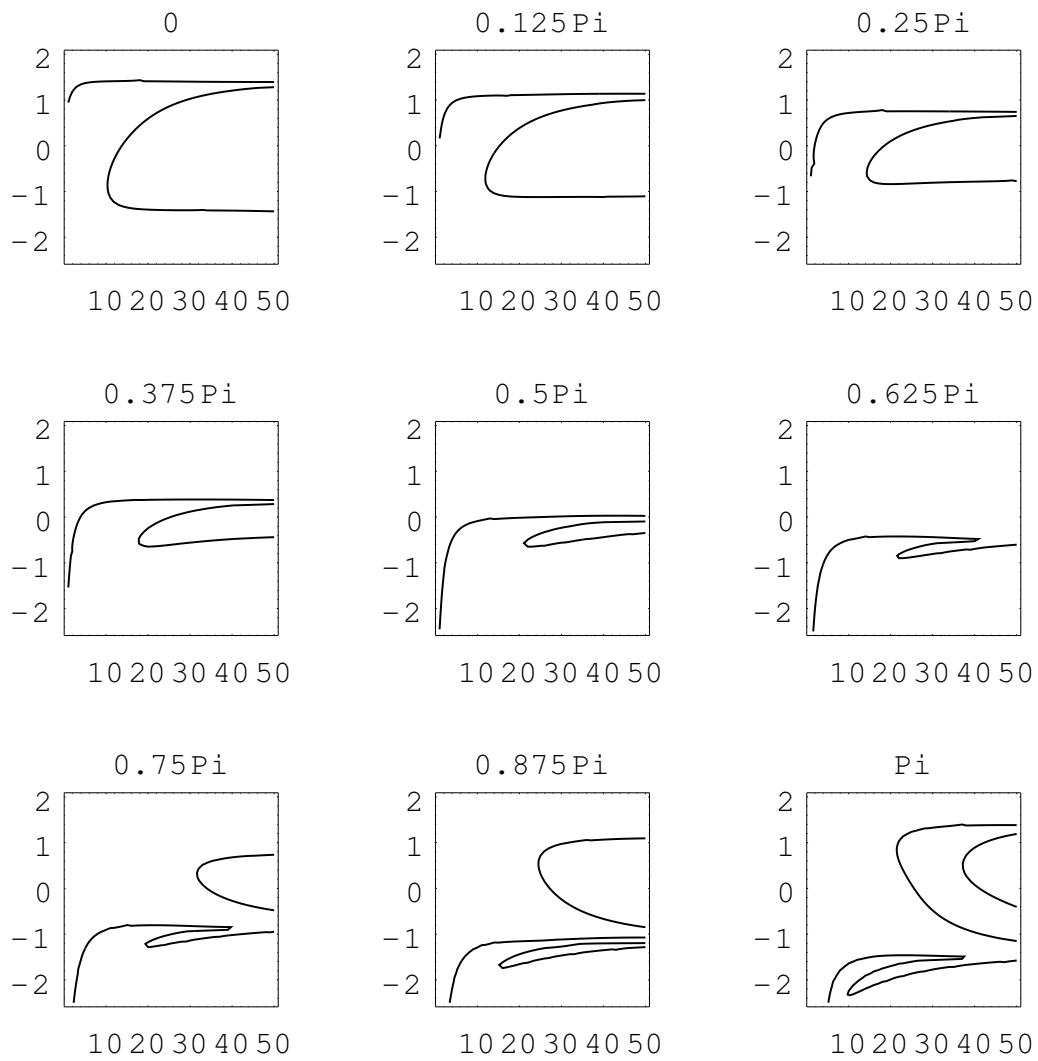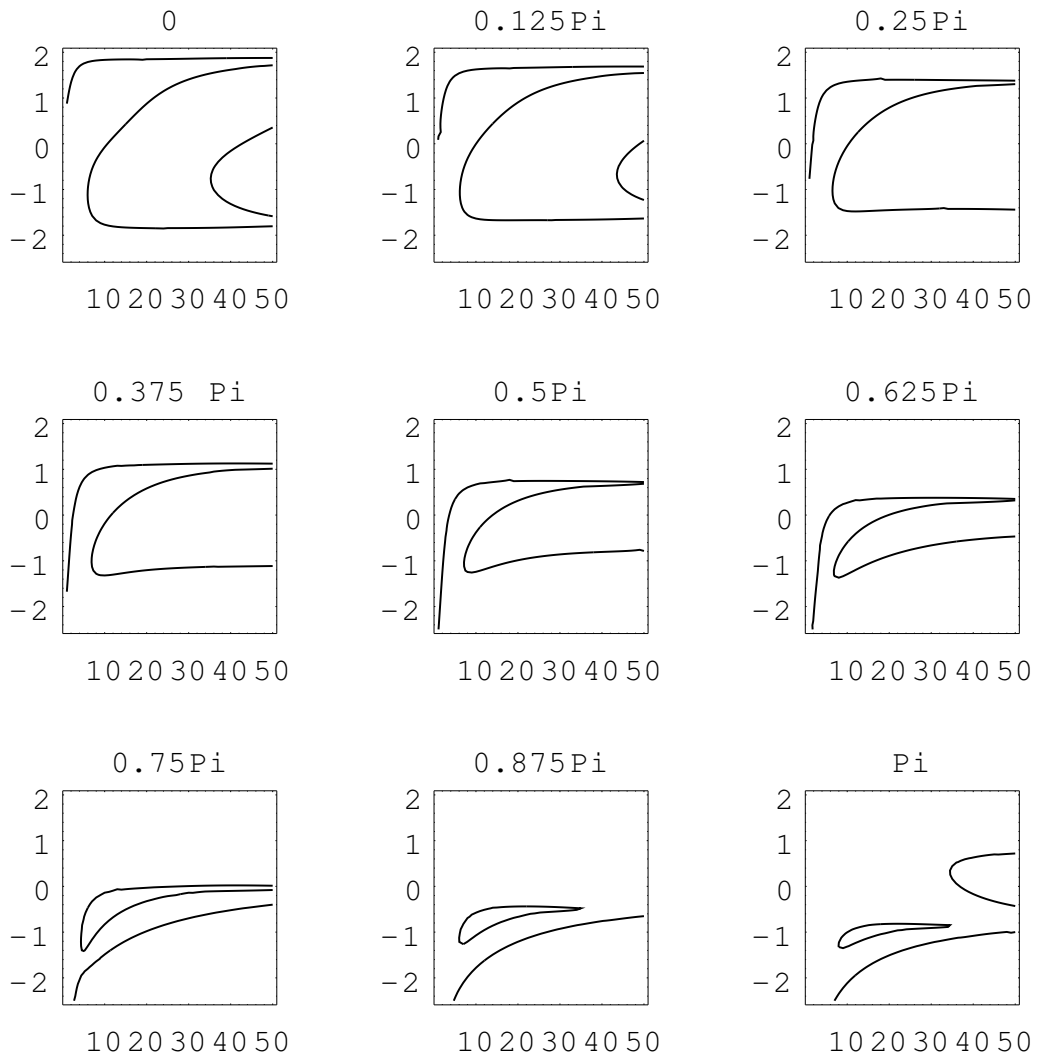
8.3.2   The bifurcation diagrams for fixed α

Figure 8.3: Bifurcation diagram $\{(p,\alpha,\omega_0)|\gamma \text{ fixed}, p \in [0,50]\}$ for $\alpha = -0.5\pi$, (γ values above diagrams).

Figure 8.4: Bifurcation diagram $\{(p, \alpha, \omega_0)|\gamma \text{ fixed}, p \in [0, 50]\}$ for $\alpha = -0.25\pi$, (γ values above diagrams).
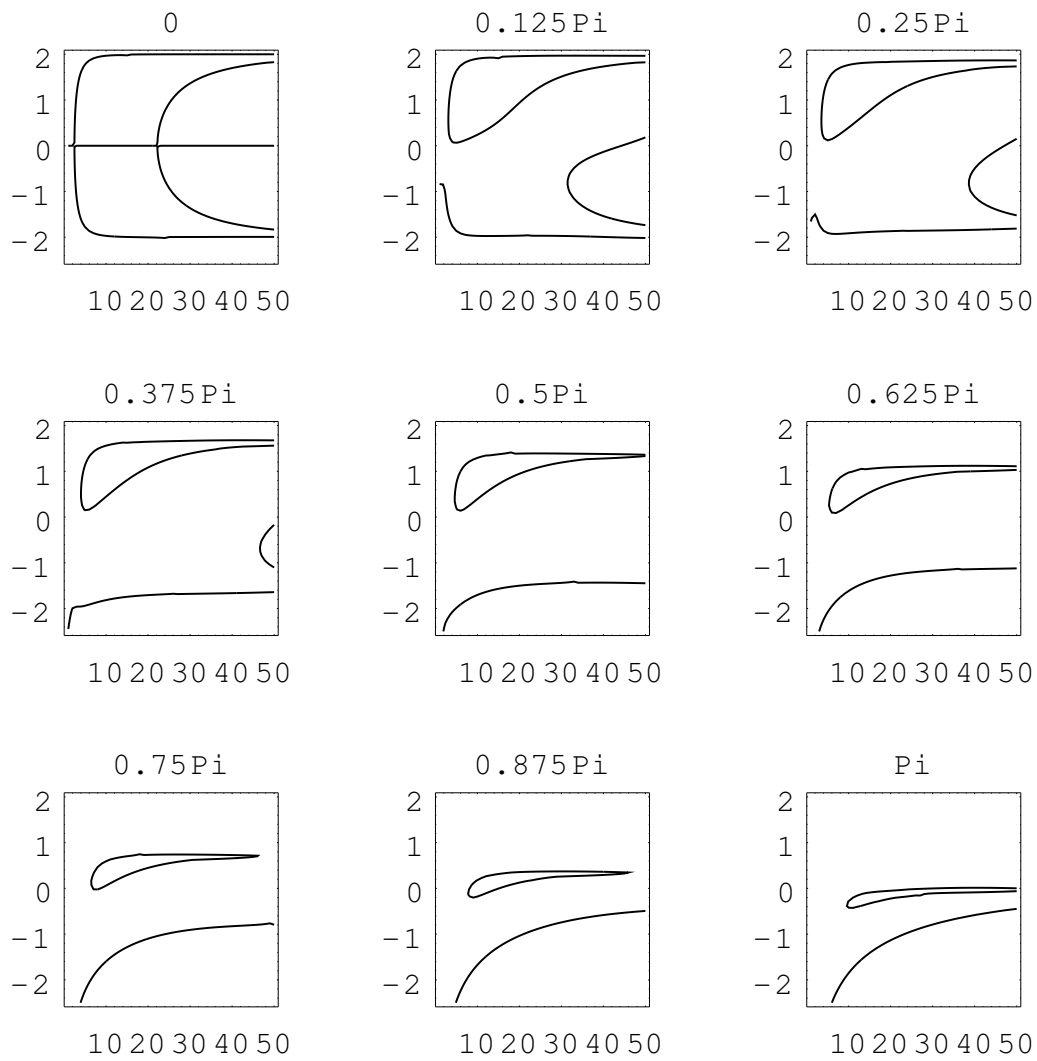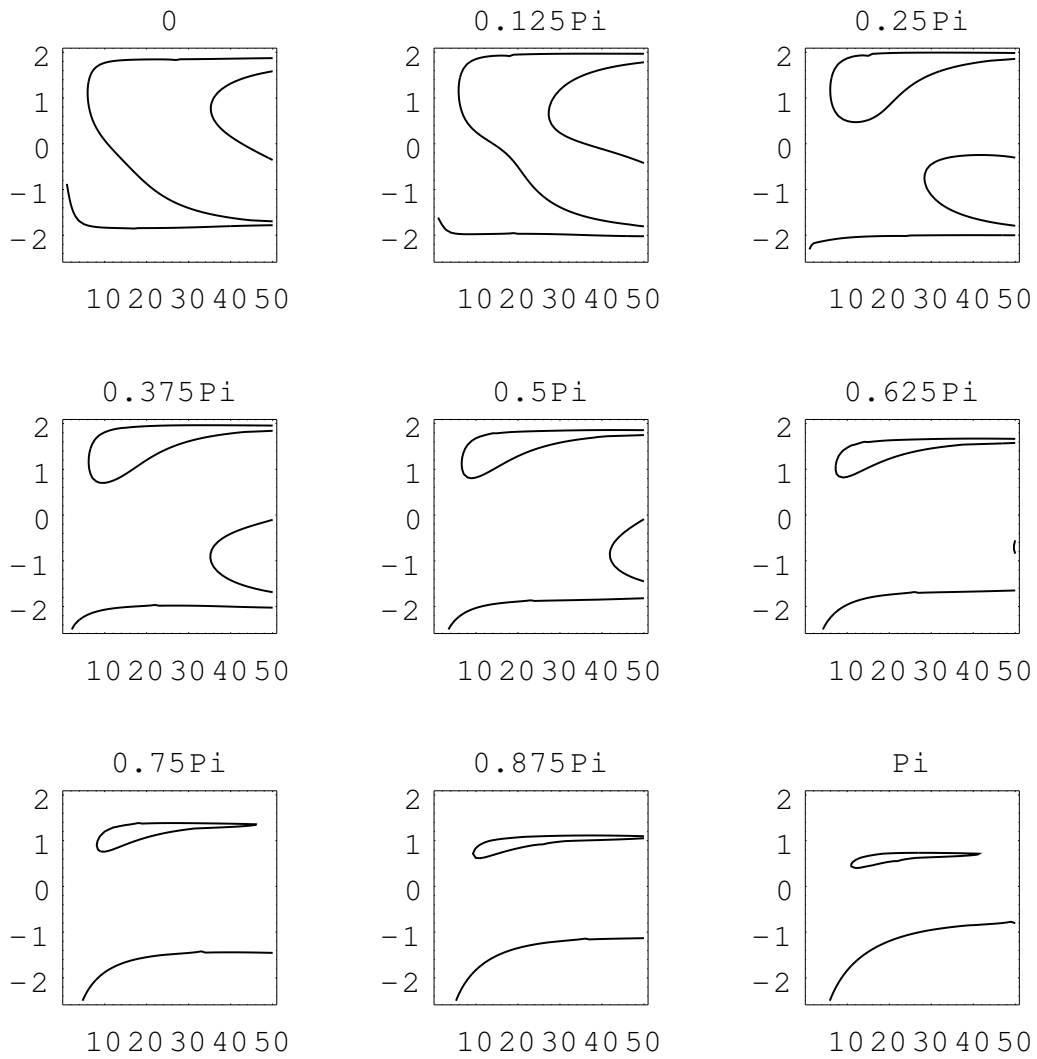
Figure 8.5: Bifurcation diagram $\{(p,\alpha,\omega_0)|\gamma \text{ fixed}, p \in [0,50]\}$ for $\alpha = -0\pi$, (γ values above diagrams).

Figure 8.6: Bifurcation diagram $\{(p, \alpha, \omega_0)|\gamma \text{ fixed}, p \in [0, 50]\}$ for $\alpha = 0.25\pi$, (γ values above diagrams).

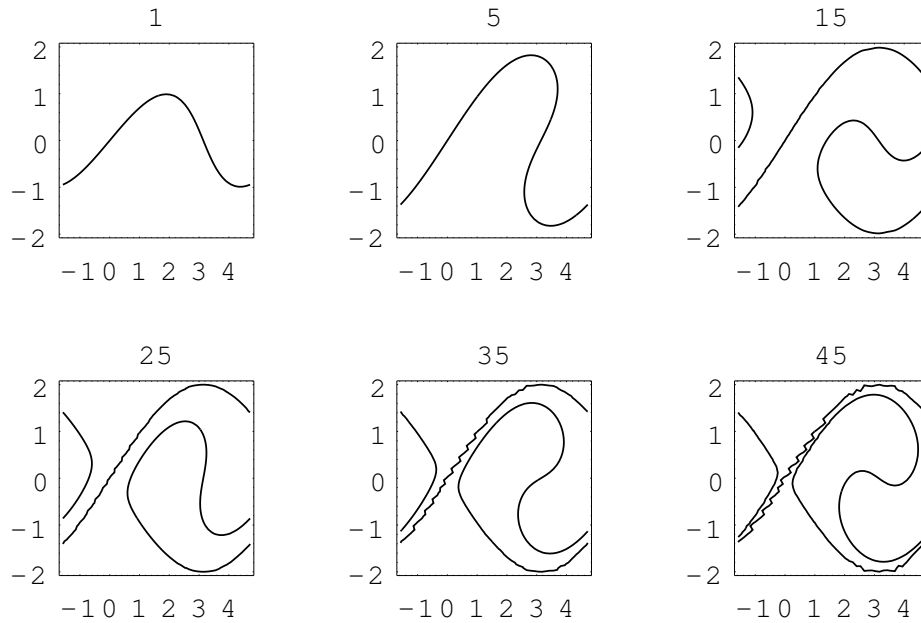Figure 8.7: Bifurcation diagram $\{(p, \alpha, \omega_0)|\gamma$ fixed, $p \in [0, 50]\}$ for $\alpha = 0.5\pi$, (γ values above diagrams).

Figure 8.8: Bifurcation diagram $\{(p, \alpha, \omega_0) | \gamma$ fixed, $p \in [0, 50]\}$ for $\alpha = 0.75\pi$, (γ values above diagrams).

Figure 8.9: Bifurcation diagram $\{(p, \alpha, \omega_0) | \gamma \text{ fixed}, p \in [0, 50]\}$ for $\alpha = \pi$, (γ values above diagrams).

Figure 8.10: Bifurcation diagram $\{(p, \alpha, \omega_0)|\gamma \text{ fixed}, p \in [0, 50]\}$ for $\alpha = 1.25\pi$, (γ values above diagrams).

8.3.3 The bifurcation diagrams for fixed p

Figure 8.11: Bifurcation diagram $\{(p, \alpha, \omega_0)|p$ fixed, $\alpha \in [-0.5\pi, 1.5\pi]\}$ for $\gamma = 0$, $(p$ values above diagrams).
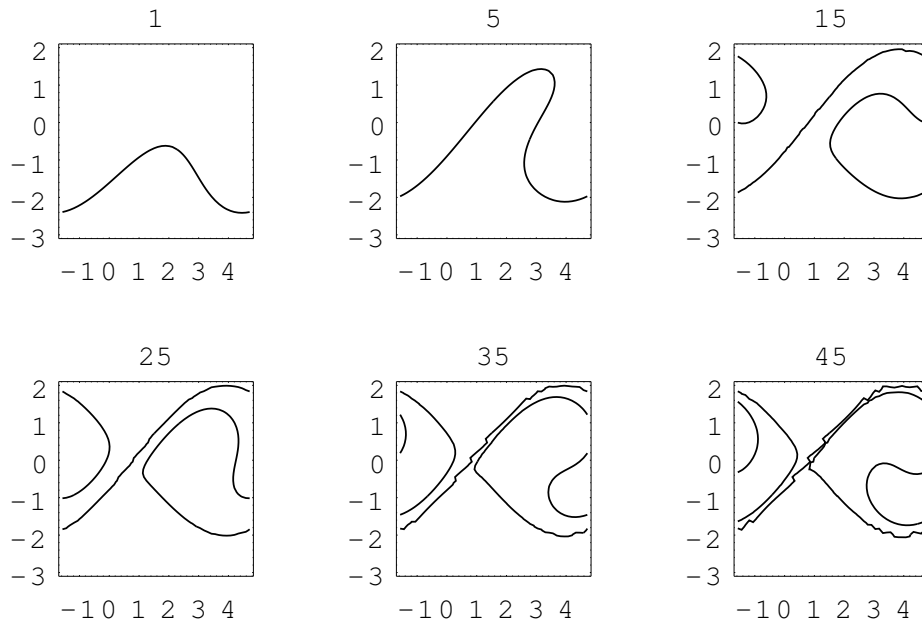
Figure 8.12: Bifurcation diagram $\{(p, \alpha, \omega_0)|p$ fixed, $\alpha \in [-0.5\pi, 1.5\pi]\}$ for $\gamma = 0.25\pi$, (p values above diagrams).
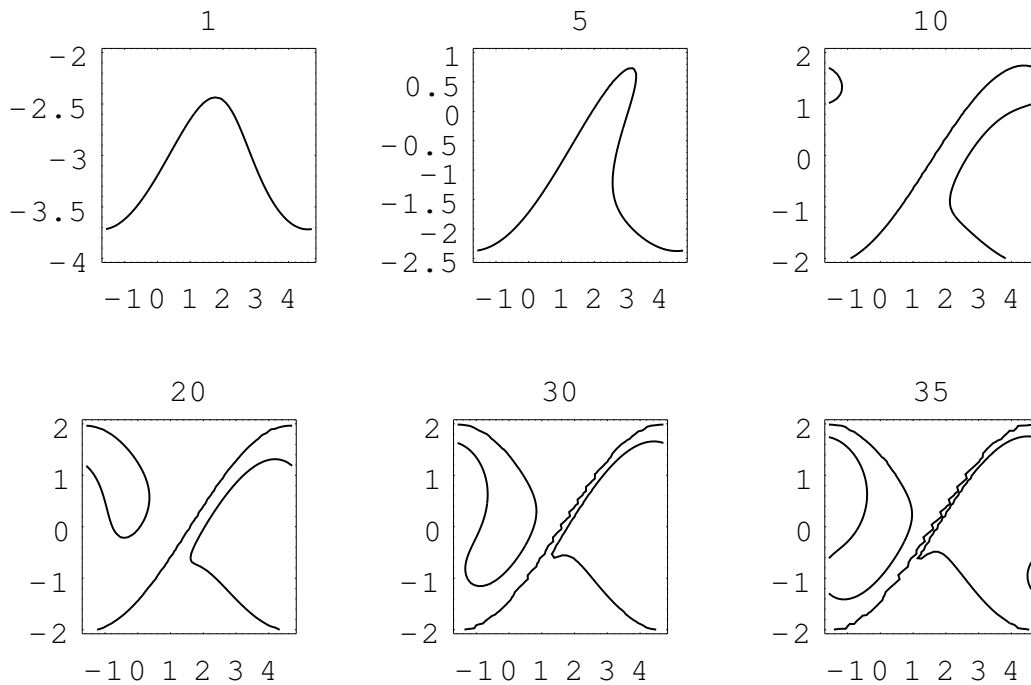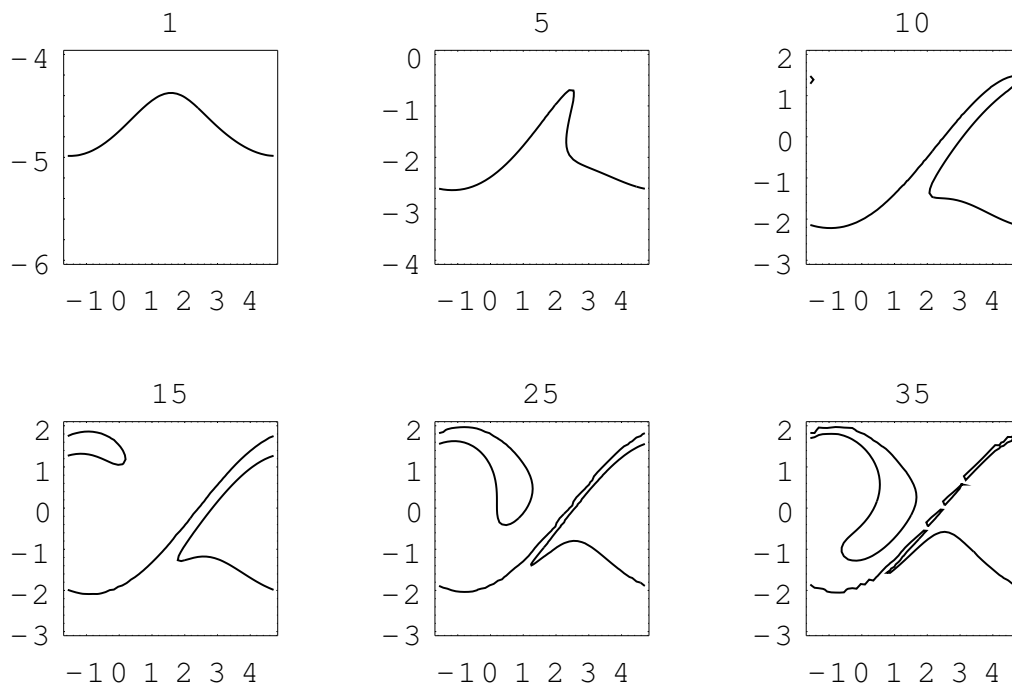

Figure 8.13: Bifurcation diagram $\{(p, \alpha, \omega_0)|p$ fixed, $\alpha \in [-0.5\pi, 1.5\pi]\}$ for $\gamma = 0.5\pi$, (p values above diagrams).

Figure 8.14: Bifurcation diagram $\{(p, \alpha, \omega_0)|p$ fixed, $\alpha \in [-0.5\pi, 1.5\pi]\}$ for $\gamma = 0.75\pi$, (p values above diagrams).
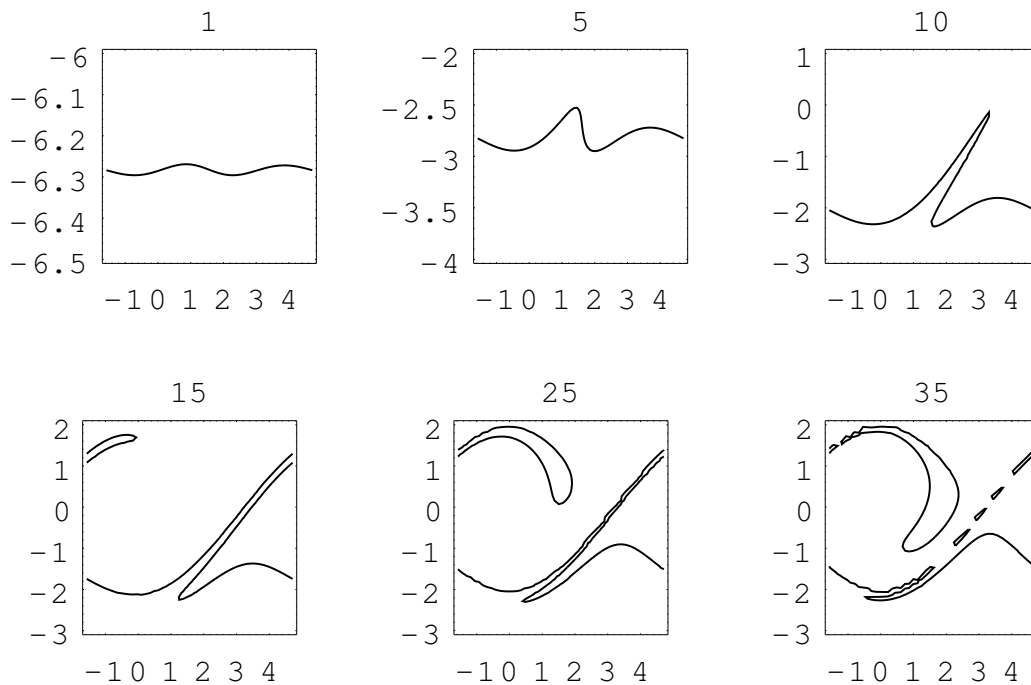

Figure 8.15: Bifurcation diagram $\{(p, \alpha, \omega_0)|p$ fixed, $\alpha \in [-0.5\pi, 1.5\pi]\}$ for $\gamma = \pi$, (p values above diagrams).

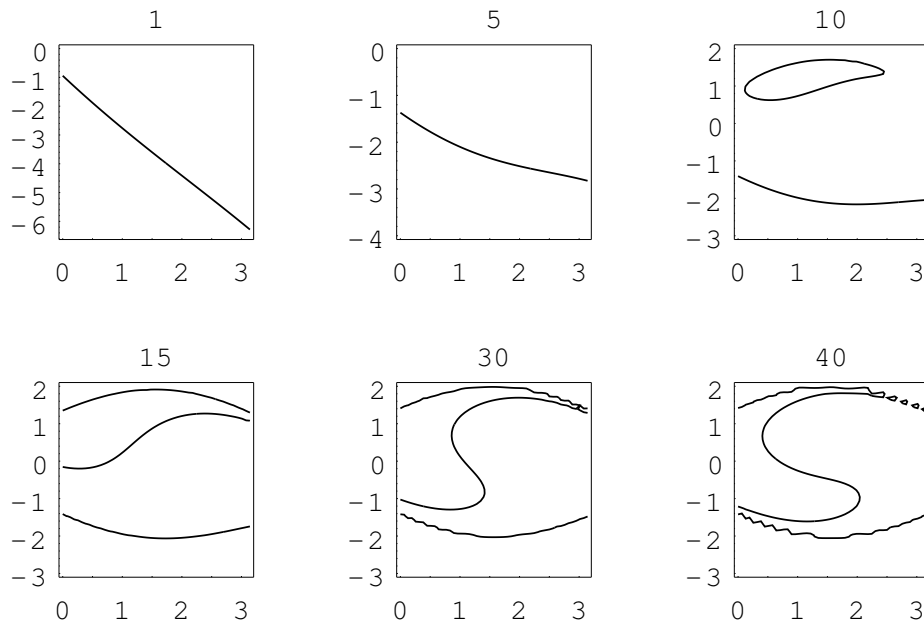Figure 8.16: Bifurcation diagram $\{(p,\alpha,\omega_0)|p$ fixed, $\gamma \in [0,\pi]\}$ for $\alpha = -0.5\pi$, $(p$ values above diagrams).

Figure 8.17: Bifurcation diagram $\{(p,\alpha,\omega_0)|p$ fixed, $\gamma \in [0,\pi]\}$ for $\alpha = -0.25\pi$, $(p$ values above diagrams).

Figure 8.18: Bifurcation diagram $\{(p, \alpha, \omega_0)|p$ fixed, $\gamma \in [0, \pi]\}$ for $\alpha = 0$, (p values above diagrams).

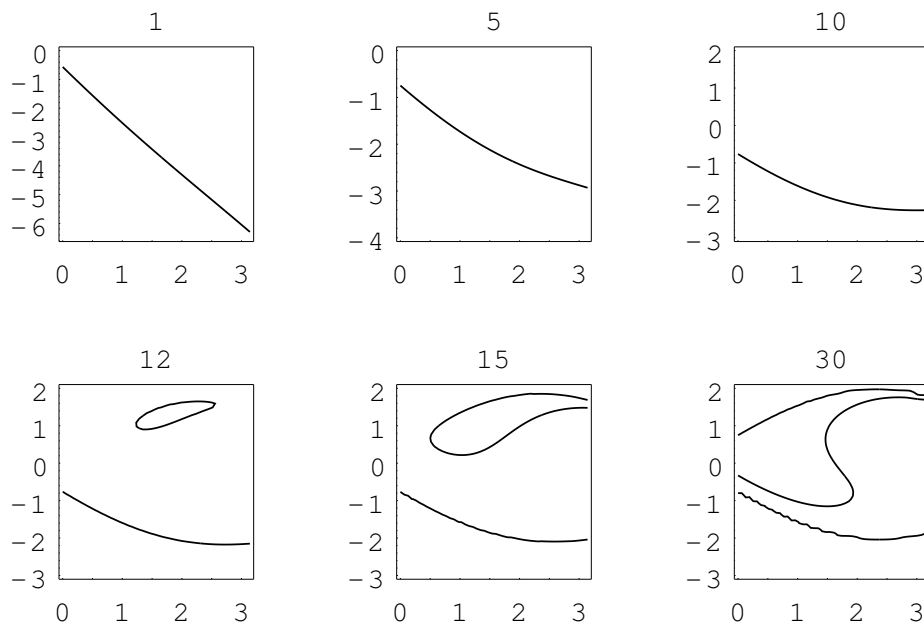
Figure 8.19: Bifurcation diagram $\{(p, \alpha, \omega_0)|p$ fixed, $\gamma \in [0, \pi]\}$ for $\alpha = 0.25\pi$, (p values above diagrams).

Figure 8.20: Bifurcation diagram $\{(p, \alpha, \omega_0)|p$ fixed, $\gamma \in [0, \pi]\}$ for $\alpha = 0.5\pi$, $(p$ values above diagrams).

Figure 8.21: Bifurcation diagram $\{(p, \alpha, \omega_0)|p$ fixed, $\gamma \in [0, \pi]\}$ for $\alpha = 0.75\pi$, $(p$ values above diagrams).
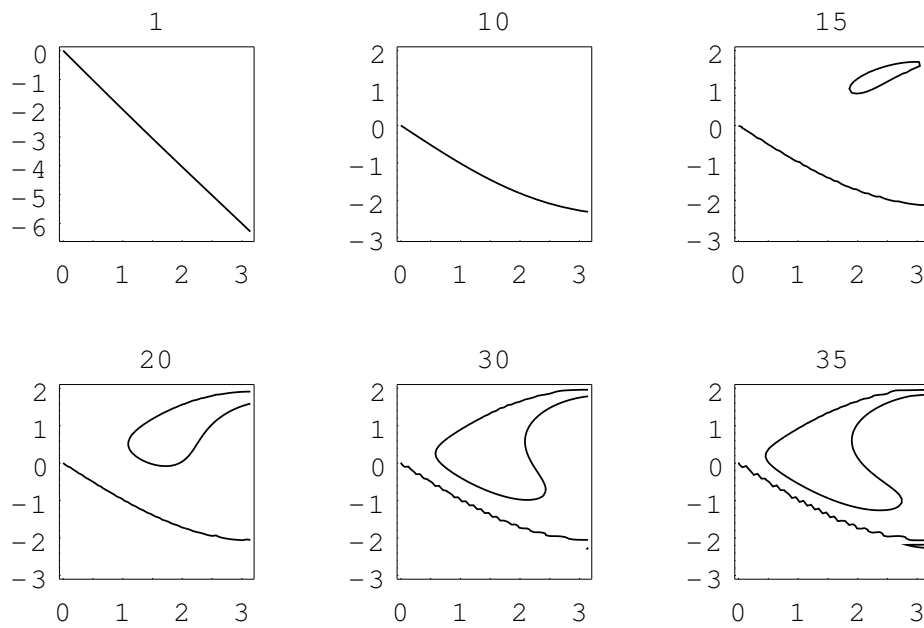
Figure 8.22: Bifurcation diagram $\{(p, \alpha, \omega_0)|p$ fixed, $\gamma \in [0, \pi]\}$ for $\alpha = \pi$, (p values above diagrams).
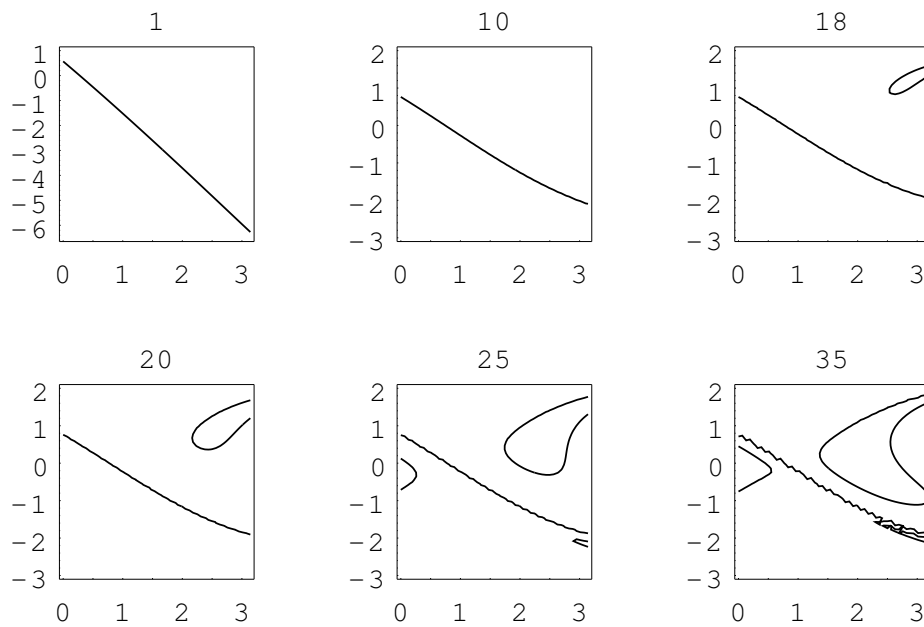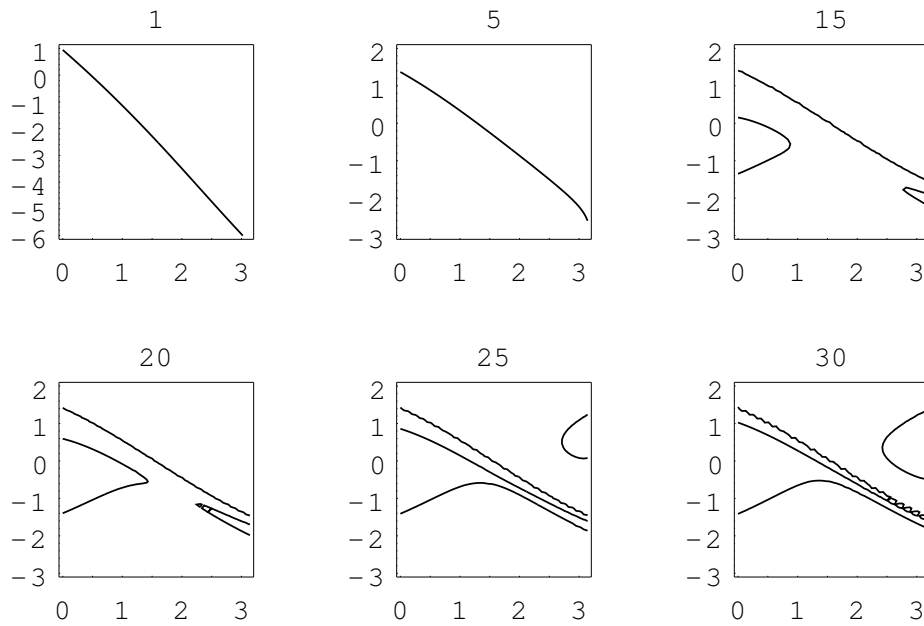

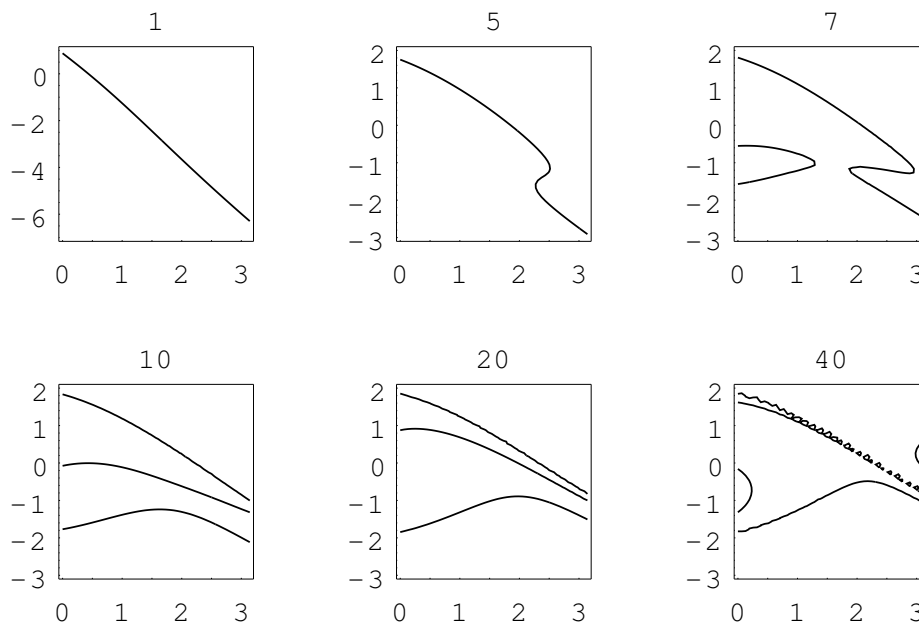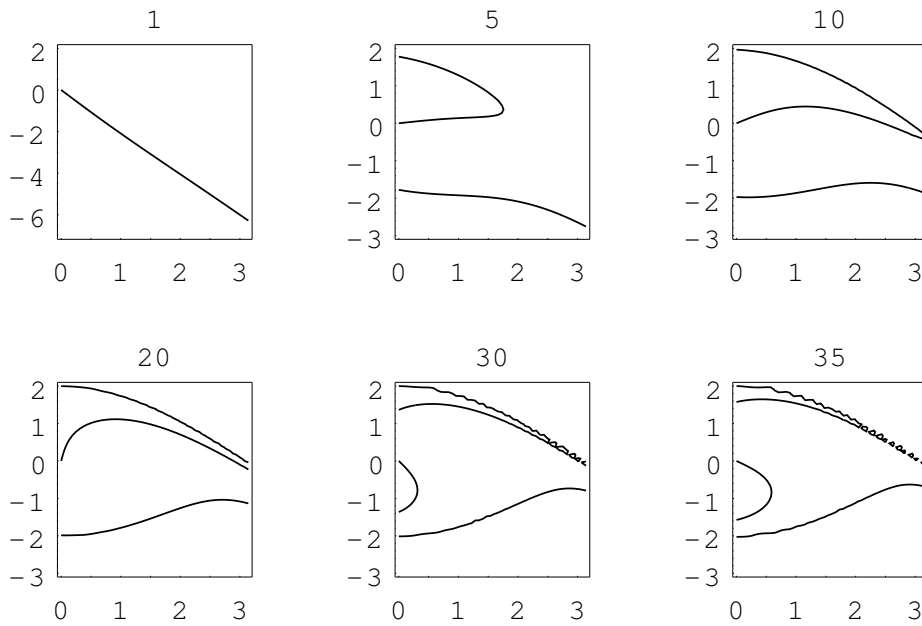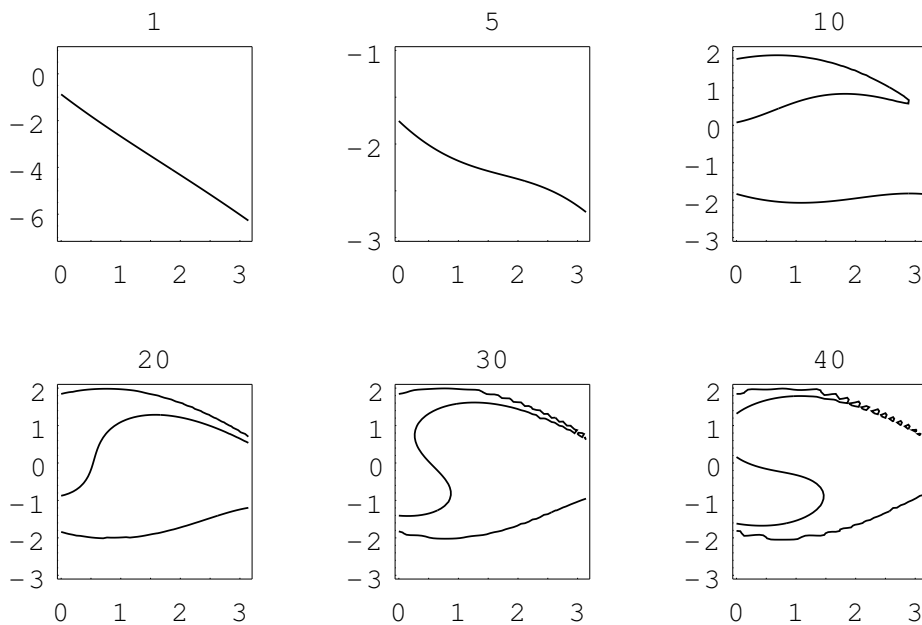Figure 8.23: Bifurcation diagram $\{(p, \alpha, \omega_0)|p$ fixed, $\gamma \in [0, \pi]\}$ for $\alpha = 1.25\pi$, (p values above diagrams).

Bibliography

[1] F. F. Afagh and J. X. Lee, *Vibration of rods with a concentrated mass in the presence of non-conservative forces*, Archive of Applied Mechanics 65(1995), PP 507-521.

[2] V. I. Arnold, *Geometrical Methods in the Theory of Ordinary Equations*, Springer verlag, New York, Heidelberg, 1983.

[3] V. I. Arnold, *Catastrophy Theory*, Springer Verlag, 1992.

[4] U. Ascher and R. D. Russell, *Reformulation of boundary value problem into "standard" form*, SIAM Review, Vol. 23, No. 2, 1981, PP 238-253.

[5] T. M. Atanackovic, *Buckling of a heavy compressed column with imperfections*, Q. Jl. Mech. appl. Math., Vol. 39, Pt.3, 1986, PP 361-379.

[6] T. M. Atanackovic, *Stability Theory of Elastic Rods*, World Scientific, 1996.

[7] T. M. Atanackovic, *On the rotating rod with variable cross section*, Archive of Applied Mechanics 67(1997), PP 447-456.

[8] T. M. Atanackovic, B. B. Marctic and J. M. Milidragovic, *On the stability of an elastic column positioned on an elastic half space*, Archiv of Applied Mechanics, 69(1999), PP 94-104.

[9] J. R. Banerjee, *Explicit model analysis of an axially loaded Timoshenko beam with bending-torsion coupling*, Journal of Applied Mechanics, Vol. 67, June 2000, PP 307-312.

[10] R. Bhattacharyya, *Behavior of a rubber spring pendulum*, Journal of App. Mechanics, June 2000, Vol. 67, PP 332-337.

[11] Max Born, *Untersuchungen ueber Die Stabilität der Elastischen Linien in Ebene und Raum*, Goettingen, 1906.

[12] G. Buttazzo, M. Giaquinta and S. Hildebrandt, *One-dimensional variational problem*, Clarendon Press, Oxford, 1998.

[13] E. Buzano, *Secondary bifurcations of a thin rod under axial compression*, SIAM J. MATH. ANAL. Vol. 17, No.2, 1986, PP 312-321.

[14] G. Cederbaum, *Post-buckling behavior of poroelastic columns*, International Journal of Mechanical Science, Vol. 42, 2000, PP 771-783.

[15] Y-Z. Chen and N. Hasebe, *Fredholm integral equation for the multiple circular arc crack problem in plane elasticity*, Archive of Applied Mecfanics, 67(1997), PP 433-446.

[16] S. N. Chow and J. K. Hale, *Methods of Bifurcation Theory*, Springer- Verlag, New York, Heidelberg, Berlin, 1982.

[17] L. Collatz, *Eigenwertaufgaben mit technischen Anwendungen*, Akademische Verlagsgesellschaft Geest Potig K.-G., Leipzig, 1949.

[18] N. Cònsul and J. Solà-Morales, *Stability of local minima and stable nonconstant equilibria*, Journal of differential equations, 157(1999), PP 61-81.

[19] M. G. Crandall, *Applications of bifurcation theory*, Editor P. H. Rabinowitz, Academic Press Inc. New York, 1977.

[20] M. Degiovanni and F. Schuricht, *Buckling of nonliearly elastic rods in the pressure of obstacles treated by nonsmooth critical point theory*, Math. Ann. 311, 1998, PP 675-728.

[21] Z. Q. Deng, *Boundary Value Problem of Ordinary Diffrential Equations and Sturm Comparison Theory*, Publishing House of Central China Pedagogical University, Wuhan, 1990.

[22] M. Drawshi and J. Betten, *Investigation of the deformation and the stability of geometrically nonliear beams*, Archiv of Applied Mechanics, 62(1992), PP 394-403.

[23] J. Dugundji, *Topology*, Allyn and Bacon Inc. Boston, London, Sydney, 1975.

[24] L. C. Evans, *Partial Differential Equations*, American Mathematical Society, Providence, Rhode Island, 1998.

[25] K. Feng and Z. Shi, *Mathematical Theory of Elastic Structures*, Springer and Science Press Beijing, 1996.

[26] A. Friedman, *Partial Differential Equation of Parabolic Type*, Prentice-Hall, Inc. 1964.

[27] C. Foias, *Inertial manifolds for nonlinear evolution equations*, Journal of differential equations, 73(1988), PP 309-353.

[28] C. Foias, M. S. Jolly, I. G. Kevrekidis, G. R. Sell and E. S. Titi, *On the computation of inertial manifolds*, Physics Letter, Vol. 131, No. 7,8, 1988, PP 433-436.

[29] C.-E. Fröberg, *Numerical Mathematics*, The Benjamin/Cummings Publishing Company, Inc., Menlo Park, California,*etc*, 1985.

[30] S. Fuĉik, *Solvability of Nonlinear Equation and Boundary Value Problems*, D. Reidel Publishing Company, Dordrecht, Boston, London, 1980.

[31] R. Gardner and C. K. R. T. Jones, *A stability index for steady state solutions of boundary value problems for parabolic systems*, Journal of Differential Equations, Vol. 91, 1991, PP 181-203.

[32] M. Golubitsky and D. Schaeffer, *A theory for imperfect bifurcation via singularity theory,* Commun. Pure. Appl. Math. Vol. XXXII, PP 21-98, 1979.

[33] J. Hale,*Ordinary differential equations*, Wiley-Interscience, New York, 1969.

[34] J. Hale and H. Kocak, *Dynamics and Bifurcations*, Springer Verlag, New York, 1991.

[35] N. Hasebe, K. Yoshikawa, M. Uedand T. Nakamura, *Plane elastic solution for the second mixed boundary value problem and its application*, Archive of Applied Mechanics, 64(1994), PP 295-306.

[36] R. F. Heinmann and A. B. Poore, *Multiplicity, stability, and oscillatory dynamics of the tubular reactor*, Chemical Engineering Science, Vol. 36, 1981, PP 1411-1419.

[37] M. A. Horn, *Stabilization of the dynamic system of elasticity by nonlinear boundary freeback*, International Series of Numerical Mathematics, Vol. 133, Birkhäuser Verlag Basel, 1999, PP 201-210.

[38] A. Inannelli and G. Prouse, *Analysis of a nonlinear model of the vibrating rod*, Nonlinear Differential Equation and Applications, 4(1997), PP 233-248.

[39] K. F. Jensen and W. Harmon Ray, *The bifurcation behavior of tubular reactors*, Chemical Engineering Science, Vol. 37, N0. 2, 1982, PP 199-222.

[40] A. D. Jepson and A. Spence, *Singular points and their computation*, International Series of Numerical Mathematics, Vol. 70, Birkhäuser Verlag Basel, 1984, PP 195-209.

[41] A. D. Jepson and A. Spence, *The numerical solution of nonliear equations having several parameters I: scalar equations*, SIAM. J. NUMER. ANAL. Vol. 22, No. 4, Aug. 1985, PP 736-759.

[42] N. M. Kinkaid, O. M. O'Reilly and J. S. Turcotte, *On the study of a rotating elastic rod*, Journal of Applied Mechanics, Vol. 68, Sep. 2001, PP 766-771.

[43] J. Knobloch and J. Steigenberger, *Gewöhnliche Differentialgleichungen*, Skriptum, Instut. für Math., Technical University of Ilmenau, 1996.

[44] F. K. Labisch, *Qualitative and quantitative behavior of nonlinear elastic Rings under hydrostatic pressure*, International Series of Numerical Mathematics, Vol. 97, Birkhäuse Verlag Basel, 1991, PP 243-247.

[45] K. K. Lee, *Lectures on Dynamic Systems, structural stability and their Applications*, World Scientific, Singapore, New Jersey, london, Hong Kong, 1992.

[46] H. Leipholz, *Stabilitätstheorie*, B. G. Teubner, Stuttgart, 1968.

[47] Q. Y. Li, *Numerical Method of Ordinary Differential Equations*, Publishing House of High Education, Beijing, 1992.

[48] D. Luo, X. Wang, D. Zhu and M. Han, *Bifurcation Theory and Methods of Dynamical Systems*, World Scientific, 1997.

[49] J. H. Maddocks, *Stability of nonlinear elastic rods,* Arch. Rational Mech. Anal. 85. 1984.

[50] J. E. Marsden and T. J. R. Hughes, *Mathematical Foundations of Elasticity,* Dover Publications, Inc. 1994.

[51] A. A. Martynyuk, *Stability Analysis: Nonlinear Mechanics Equations*, Gordon and Breach Publishers, 1995.

[52] G. Moore, *The numerical buckling of a visco-elastic rod*, International Series of Numerical Mathematics, Vol. 70, Birkhäuser Verlag Basel, 1984, PP 335-343.

[53] Y. Nishiura and H. Fujii, *Stability of singulary perturbed solutions to systems of reaction-diffusion equations*, SIAM J. MATH. ANAL, Vol. 18, N0. 6, 1987, PP 1726-1770.

[54] D. O'Regan, *Existence Theory for Nonlear Ordinary Differential Equations*, Kluwer Academic Publishers, Dordrecht, Boston, London, 1997.

[55] E. Ossa, *Topologie*, Vieweg, Braunschweig/Wiesbaden, 1992.

[56] Ya. G. Panovko and I. I. Gubanova, *Stability and Oscillation of Elastic Systems: Modern Concepts, Paradoxes and Errors*, National Aeronautics and Space Administration, Washington, D. C, Nov. 1973.

[57] G. H. Peng and G. L. Wang, *Basis of Elastic Mechanics* (in Chinese), Publishing House of Industry, Beijing, 1994.

[58] L. Perko, *Differential Equation and Dynamical Systems*, Springer, 1996.

[59] J. F. Pierce, *Sigularity Theory, Rod Theory, and Symmetry-Breaking Loads*, Springer-Verlag, Berlin, Heidelberg, New York, London, Paris, Tokyo, 1989.

[60] M. Pignataro, N. Rizzi and A. Luongo, *Stability, Bifurcation and Postcritical Behavior of Elastic Structure*, Elsevier, Amsterdam-London-New York-Tokyo.

[61] G. Pönisch, *On computing coupled turning points of parameter dependent nonlinear equations*, International Series of Numerical Mathematics, Vol. 97, Birkhäuser Verlag Basel, 1991, PP 289-295.

[62] Y. X. Qin, L. Wang and M. Q. Wang, *Theory and Application of Motion Stability* (in Chinese), Science Publishing House, Beijing, 1981.

[63] L. S. Ramachandra and D. Roy, *A New method for nonlear two point boundary value problems in solid mechanics*, Journal of Applied Mecanics, Vol. 68, Sep. 2001, PP 776-785.

[64] L. Saalschütz, *Der belastete Stab*, B.G.Teubner, 1880.

[65] R. Z. Sagdeev, D. A. Usikov and G. M. Zaslavsky, *Nonlinear Physics, from the Pendulum to Turbulence and Chaos*, Harwood Academic Publishers, 1992.

[66] R. Schaaf, *Global Solution Branches of Two Point Boundary Value Problem*, Springer-Verlag, Berlin, Heidelberg, New York, 1990.

[67] R. Seydel, *Numerical computation of branching points in ordinary differential equations*, Numer. Math. 32(1979), PP 51-68.

[68] R. Seydel, *Numerical computation of branching points in nonlinear equations*, Numer. Math. 33(1979), PP 339-352.

[69] R. Seydel, *Branching switching in bifurcation problems for ordinary differential equations*, Numer. Math. 41(1983), PP 93-116.

[70] J. Sijbrand, *Studies in non-linear stability and bifurcation theory*, Te Zaandam, Juli, 1954.

[71] R. Sinclair, *Numerical sinmulation of an elastica pendulum*, Computational Mechanics 26(2000), PP 419-429.

[72] J. Smoller and A. Wassermann, *Global bifurcation of steady-state solutions*, Journal of Differential Equations, 39(1981), PP 269-290.

[73] J. Smoller,*Shock Waves and Reaction -Diffusion Equations*, Springer-Verlag, New York, 1983.

[74] S. V. Sorokin and A. V. Terentiev, *On the optimal design of the shape of a buckling elastic beam*, Struct Multidisc Optim, 21(2001), PP 60-68.

[75] A. Spence and A. D. Jepson, *The numerical calculation of cusps, bifurcation points and isola formation points in two parameter problems*, International Series of Numerical Mathematics, Vol. 70, Birkhäuser Veralg Basel, 1984, PP 502-513.

[76] J. Steigenberger, *Technische Mechanik*, Technische Hochschule Ilmenau, 1967.

[77] J. Steigenberger, K. Zimmermann, S.Petkun, *Modelle der Elastomechanik und ihre Anwendung in der Mikrotechnik*, Proc. Int. Wiss. Kolloq. Tech. Uni. Ilmenau, 1996.

[78] J. Steigenberger, K. Zimmermann, U. Schulte, *On large deformations of elastic rings via phase-plane discussion,* Archive of Applied Mechanics, 70(2000), PP 489-507.

[79] G. Suire and G. Cederbaum,*Elastica type dynamics stability analysis of viscoelastic columns*, Archive of Applied Mechanics, 64(1994), PP 307-316.

[80] M. E. Taylor, *Partial Differential equations III. Nonliear equations*, Springer, New York, 1996.

[81] J. M. T. Thompson and H. B. Stewart, *Nonlinear Dynamics and Chaos,* John Wiley and Sons, 1994.

[82] S. P. Timoshenko, J. M. Gere, *Theory of Elastic Stability*, McGraw-Hill Book Com., Inc, 1961.

[83] S. P. Timoshenko, J. M. Gere, *Mechanics of Materials*, Nostrand Peinhold Company, 1972.

[84] D. A. Tones and E. S. Titi, *Determining finite volume element for the 2D Navier-Stokes equations*, Physica D, 60(1992), PP 185-174.

[85] H. Troger, *Application of bifurcation theory to the solution of nonlinear stability problem in mechanical engineering*, International Series of Numerical mathematics, Vol. 70, Birkhäuser Verlag Basel, 1984, PP 525-546.

[86] V. Tvergaard, *Studies of elastic-plastic instabilities*, Journal of Applied Mechanics, Vol. 66, Mar. 1999, PP 3-9.

[87] F. Verhulst, *Nonlinear Differential Equations and Dynamical Systems*, Springer, Beilin, 1996.

[88] C. Y. Wang, *On the bifurcation solutions of an axially rotating rod*, Q. Jl. Mech. appl. Math., Vol. XXXV, Pt.3(1982), PP 391-402.

[89] C. Y. Wang, *Asymptotic formular for the flexible bar*, Mechanism and Machine Theory, PP 645-655, 34(1999)

[90] B. Werner, *Test functions for bifurcation points and hopf points in problems with symmetries*, International Series of Numerical Mathematics, Vol. 104, Birkhäuser Verlag Basel, 1992, PP 317-327.

[91] S. Wiggins, *Global Bifurcations and Chaos, Analytical Methods*, Springer Verlag, New York, Berlin, Heidelberg, Paris, Tokyo, 1988.

[92] J. Wloka, *Partielle Differentialgleichungen*, B. G. Teubner Stuttgart, 1982.

[93] P. Wolfe, *Bifurcation theory of an elastic conducting rod in a magnetic field*, Q. Jl. Mech. appl. Math., Vol.41, Pt. 2(1988), PP 265-279.

[94] P. Wolfe, *Deformation of rods with small bending stiffness*, Q. Jl. Mech. appl. Math., Vol. 46, Pt. 2, 1993, PP 311-329.

[95] B. Wu, *Secondary buckling of an elastic column with spring-supports at clamped ends*, Archive of Applied Mechanics, 68(1998), PP 342-351.

[96] Z. C. Xie, *Material Mechanics*, Publishing House of Qinghua University, Beijing, 1993.

[97] E. Zeidler, *Nonlear Functional analysis and its application(IV), Application to mathematical physics*, Springer-Verlag, 1998.

[98] Z. F. Zhang, T. R. Deng, W. Z. Huang, Z. X. Dong, *Qualitative Theory of Differential Equations*, Science Press, Beijing, 1985.

[99] K. Zimmermann, J. Grabow, *Ansaetze zur Modellierung von Antriebssystemen nach biologischem Vorbild*, Workshop "Mechanisch aktive Mikrosysteme", TU Ilmenau, 4,15. Juli 1996, Tagungsband, S. 76-84.